Year : 2018

Epigenetic therapy a good BET for glioblastoma? A systems biology approach to identify a rational combination therapy.

Gusyatiner Olga

UNIL | Université de Lausanne

Faculté de biologie et de médecine

Département des Neurosciences Cliniques
Service de Neurochirurgie, CHUV

Epigenetic therapy a good BET for glioblastoma?
A systems biology approach to identify a rational combination therapy.

Thèse de doctorat ès sciences de la vie (PhD)

présentée à la

Faculté de biologie et de médecine
de l'Université de Lausanne

par

Olga Gusyatiner

Master en Sciences de l'Université de Oulu, Oulu, Finlande

Jury

Prof. Jacqueline Pouw Schoumans, Présidente
Prof. Monika Hegi, Directrice de thèse
Dr. Mauro Delorenzi, Co-directeur
Prof. Tatiana Petrova, Experte et représentante du comité de doctorat
Dr. Francesco Bertoni, Expert

Lausanne 2018

UNIL | Université de Lausanne

Faculté de biologie et de médecine

**Département des Neurosciences Cliniques
Service de Neurochirurgie, CHUV**

**Epigenetic therapy a good BET for glioblastoma?
A systems biology approach to identify a rational combination
therapy.**

Thèse de doctorat ès sciences de la vie (PhD)

présentée à la

Faculté de biologie et de médecine
de l'Université de Lausanne

par

Olga Gusyatiner

Master en Sciences de l'Université de Oulu, Oulu, Finlande

Jury

Prof. Jacqueline Pouw Schoumans, Présidente
Prof. Monika Hegi, Directrice de thèse
Dr. Mauro Delorenzi, Co-directeur
Prof. Tatiana Petrova, Experte et représentante du comité de doctorat
Dr. Francesco Bertoni, Expert

Lausanne 2018

Imprimatur

Vu le rapport présenté par le jury d'examen, composé de

Président·e	Madame	Prof.	Jacqueline **Schoumans Pouw**
Directeur·trice de thèse	Madame	Prof.	Monika **Hegi**
Co-directeur·trice	Monsieur	Dr	Mauro **Delorenzi**
Expert·e·s	Madame	Prof.	Tatiana **Petrova**
	Monsieur	Prof.	Francesco **Bertoni**

le Conseil de Faculté autorise l'impression de la thèse de

Madame Olga Gusyatiner

Master in Science University of Oulu, Finlande

intitulée

**EPIGENETIC THERAPY A GOOD BET FOR GLIOBLASTOMA?
A SYSTEMS BIOLOGY APPROACH TO IDENTIFY
A RATIONAL COMBINATION THERAPY**

Lausanne, le 27 avril 2018

pour le Doyen
de la Faculté de biologie et de médecine

Prof. Jacqueline Schoumans Pouw

Acknowledgements

First of all, I would like to express my gratitude and appreciation to Prof. Monika Hegi, who supervised me during these 4.5 years for her support, patience, motivation and immense knowledge of the field.

Besides my advisor, I acknowledge the people, who directly contributed to this work. Dr. Pierre Bady did the alignment and PCO of the RNA-seq data, and validated G12 cluster structure in TCGA. Master and Bachelor students Minh Pham Diêu Thanh, Yvonne Lei, and Jungyeon Park contributed to some of the experiments presented here. Thi Tham Nguyen assisted intracranial injections. Janine Horlbeck performed macrodissection of frozen tissue blocks for the experiments with xenografts. I thank Dr. Mauro Delorenzi for his input to the biostatistical analysis of the data.

I also acknowledge with a deep sense of reverence, my gratitude towards my parents Dr. Mikhail Gusyatiner and Dr. Elvira Voroshilova, who raised and educated me to be able to obtain PhD title. Lastly, I would like to thank my fiancé Dr. Giorgio Tamò for continuously encouraging me throughout my PhD years. This accomplishment would not have been possible without my family and friends.

Any omission in this brief acknowledgement does not mean lack of gratitude.

Merci!

Спасибо!

Abstract

Glioblastoma (GBM) is the most aggressive primary brain tumour in adults with a median overall survival of only 15 months. Despite multiple attempts, single agent therapies have failed in clinical trials and new strategies for combination treatments are urgently needed.

Here, our aim was to predict rational combination therapies with BET inhibitors (BETi) that target bromodomain and extra-terminal tail (BET) proteins. BET proteins are readers of lysine acetylation on histone tails, therefore promoting gene transcription. BETi are currently being evaluated as anti-cancer drugs.

First, we have assessed the biological activity of the tool drug JQ1, a small molecule inhibitor of BET, using glioblastoma derived sphere lines (GS-lines). The results suggested intermediate sensitivity of GS-lines to JQ1. Importantly, we observed that JQ1 impaired the self-renewal capacity of all 4 tested GS-lines.

With the view to identify BETi-induced vulnerabilities in cancer relevant pathways that may be targeted with a second drug, we obtained differential expression profiles of glioma sphere lines treated with the BETi JQ1. Gene set enrichment analysis using MSigDB collections revealed several significantly disturbed pathways. They included IFN-α response genes and signatures of response to histone deacetylase inhibitors (HDACi).

In order to validate the observed down regulation of the interferon response genes, we primed our GS-lines with IFN-α and confirmed that interferon-stimulated genes (ISGs), such as *MX1, OAS1*, and *CD274* are down regulated after a 4-hour exposure to JQ1. Importantly, the levels of pSTAT1 in the nucleus remained unchanged upon JQ1 treatment, suggesting that JQ1 was acting directly on the transcriptional level of ISGs and not on the IFN-induced JAK-STAT signalling. Similar results were obtained in adherent GBM cell lines that constitutively express ISGs. Moreover, in U87MG orthotopic xenografts in mice, a single i.p. injection of JQ1 down regulated *OAS1* and *CD274* expression.

Finally, we showed that HDACi and JQ1 synergize to reduce cell viability of GS-lines *in vitro*. Further experiments are necessary to test HDACi and BETi drug combinations in mouse orthotopic xenografts of GS-lines.

Résumé

Le glioblastome (GBM) est la tumeur cérébrale la plus agressive avec une survie globale médiane de seulement 15 mois. Malgré de multiples tentatives, les traitements en monothérapie ont échoué dans les essais cliniques et de nouvelles stratégies pour les traitements combinés sont nécessaires.

Notre objectif était de prédire les combinaisons thérapeutiques rationnelles avec les inhibiteurs BET (BETi) qui ciblent la bromodomaine et les protéines de la queue extra-terminale (BET), et qui sont actuellement évaluées comme médicaments anticancéreux. Premièrement, nous avons évalué l'activité biologique du médicament JQ1, une petite molécule inhibant BET, en utilisant des lignées de sphères dérivées du glioblastome (lignées-GS). Nos résultats suggèrent une sensibilité intermédiaire des lignées-GS à JQ1. Fait important, nous avons observé que JQ1 a réduit la capacité d'auto-renouvellement des quatre lignées-GS testées.

Afin d'identifier les vulnérabilités induites par JQ1 dans les voies pathologiques cancéreuses susceptibles d'être ciblées par un second médicament, nous avons obtenu des profils d'expression différentielle des lignées-GS traitées avec JQ1. L'analyse de l'enrichissement des ensembles de gènes a révélé plusieurs voies significativement perturbées qui comprenaient des gènes de réponse à IFN-α et des signatures de réponse aux inhibiteurs de l'histone désacétylase (HDACi).

Afin de valider la régulation négative observée de la signature du gène de réponse à l'interféron, nous avons exposés les lignées-GS à IFN-α et confirmé que l'expression des gènes stimulés par interféron (ISGs), tels que MX1, OAS1 et CD274, est réduite par JQ1. Notamment, les niveaux de pSTAT1 dans le noyau sont inchangés lors du traitement JQ1, suggérant que JQ1 agissait directement au niveau transcriptionnel des ISG et non sur la voie JAK-STAT. Des résultats similaires ont été obtenus dans des lignées cellulaires GBM adhérentes qui expriment constitutivement des ISG. De plus, dans les xénogreffes orthotopiques U87MG chez la souris, une seule injection i.p. de JQ1 a diminué l'expression OAS1 et CD274.

Enfin, nous avons montré que HDACi et JQ1 synergisent pour réduire la viabilité cellulaire des lignées-GS *in vitro*. D'autres expériences sont nécessaires pour tester les combinaisons de médicaments HDACi et BETi dans des xénogreffes orthotopiques murines des lignées-GS.

List of abbreviations

2HG: 2-hydroxyglutarate

5-Aza: 5-Azacytidine

5-hmC: 5-Hydroxymethylcytosine

5-mC: 5-methylcytosine

α-KG : α-Ketoglutaric acid

β-Gal : β-Galactosidase

7-AAD: 7-aminoactinomycin D

AML: Acute myeloid leukemia

ANOVA: Analysis of variance

BET: Bromodomain and Extra-Terminal Domain proteins

BETi: Bromodomain and Extra-Terminal Domain protein inhibitors

BRD4: Bromodomain Containing 4 protein

BrdU: 5-bromo-2'-deoxyuridine

C-MYC: MYC Proto-Oncogene, BHLH Transcription Factor

C-PARP: cleaved Poly (ADP-ribose) polymerase

CD274: Gene coding for PD-L1 protein

ChIP: Chromatin immunoprecipitation

CIMP: CpG island methylator phenotype

CML: Chronic myelogenous leukemia

CTCF: CCCTC-Binding Factor - Binding Factor

DAPI: 4',6-Diamidino-2-Phenylindole

DMSO: Dimethyl sulfoxide

DNA: Deoxyribonucleic acid

DNMT: DNA methyltransferase

DNMTi: DNA methyltransferase inhibitors

EGF: Epidermal growth factor

EGFR: Epidermal growth factor receptor

EGFRviii: Epidermal Growth Factor Receptor Variant III

EZH2: Enhancer of Zeste 2 Polycomb Repressive Complex 2 Subunit

EZH2i: Enhancer of Zeste 2 Polycomb Repressive Complex 2 Subunit inhibitors

FACS: Fluorescence-activated cell sorting

FBS: Fetal bovine serum

FC: Fold change

FDR: False Discovery Rate

FGF: Fibroblast growth factor

G-CIMP: Glioma CpG Island Methylator Phenotype

GAPDH: Glyceraldehyde 3-phosphate dehydrogenase

GBM: Glioblastoma

GS: Glioma sphere

GSEA: Gene Set Enrichment Analysis

H&E: Hematoxylin and eosin stain

H3: Histone H3

H3K27: Histone H3 Lysine 27

HAT: Histone acetyltransferase

HBSS: Hanks' Balanced Salt Solution

HDAC: Histone deacetylase

HDACi: Histone deacetylase inhibitors

HEXIM1: Hexamethylene Bisacetamide Inducible 1

IC50: Concentration of a drug that gives half-maximal inhibition

IDH1/2: Isocitrate dehydrogenase 1/2

IFN: Interferon

i.p.: Intraperitoneal

IRF: Interferon regulatory factor

ISG: Interferon-stimulated gene

ISRE: Interferon-sensitive response element

JAK: Janus kinase

KDM: Histone lysine demethylase

LGG: Lower Grade Glioma

MGMT: O-6-Methylguanine-DNA Methyltransferase

mRNA: Messenger RNA

mt: mutant

MX1: MX Dynamin like GTPase 1

nd: not defined

N-MYC: MYCN Proto-Oncogene, BHLH Transcription Factor

NF1: Neurofibromin 1

ns: not significant

NSG: NOD scid gamma

NUT: Nuclear Protein in Testis

OAS1: 2'-5'-Oligoadenylate Synthetase 1

P16/ARF: Cyclin Dependent Kinase Inhibitor 2A

PARP: Poly (ADP-ribose) polymerase

PBS: Phosphate-buffered saline

PD-1: Programmed cell death-1

PD-L1: Programmed death-ligand 1

pSTAT1: phosphorylated Signal Transducer And Activator Of Transcription 1

PTEN: Phosphatase And Tensin Homolog

RMA: Robust Multi-array Average

RT: radiotherapy

sc: Subcutaneous injections

SD: Standard Deviation

SDS-PAGE: Sodium dodecyl sulfate polyacrylamide gel electrophoresis

STAT1: Signal Transducer And Activator Of Transcription 1

TCGA: The Cancer Genome Atlas

TMZ: Temozolomide

TP53: Tumour Protein P53

TSA: Trichostatin A

TSS: Transcription start site

TUBB3: Neuron-specific Class III β-tubulin gene

TUJ1: Neuron-specific Class III β-tubulin protein

WHO: World Health Organization

wt: wild-type

Table of contents

List of Figures

List of Tables

Chapter 1   Introduction

1.1   Classification of glioma in adults.

Glioma is the most common primary brain tumour in adults accounting for more than 70% of brain tumours. For almost 100 years glioma classification was based on the histological examination, it was updated in 2016 by WHO (Louis et al., 2016a) (Fig. 1:1). Gliomas remain to be graded histologically from I to IV according to their malignancy. This way, grade I lesions have a low proliferative index and can be treated with surgical resection only. Whereas grade IV designation is applied to malignant, proliferating, often necrotic lesions that progress under the standard of care and lead to death. Patients with WHO grade II tumours typically survive over 5 years, with grade III tumours survive 2-3 years, whereas the majority of patients diagnosed with grade IV tumour (glioblastoma, GBM) die within one year.

Gliomas are stratified by the presence of IDH mutation (a point mutation in the Isocitrate dehydrogenase 1 or 2 gene). This way, grade IV glioma can be either IDH-wild type (90% of the cases) or IDH-mutant. The latter associates with better survival. For the low grade gliomas (grade II-III) IDH wild-type tumours are either diffuse astrocytoma or a rare case of oligodendroglioma. IDH mutant low grade gliomas are further classified based on the chromosome arms 1p/19q codeleted (oligodendroglioma) and non-codeleted (astrocytoma), the later exhibits mutations in ATRX and TP53 genes (Louis et al., 2016b). In summary, IDH-mutant and IDH wild-type gliomas are thought to arise from different cells of origin and therefore represent different diseases.
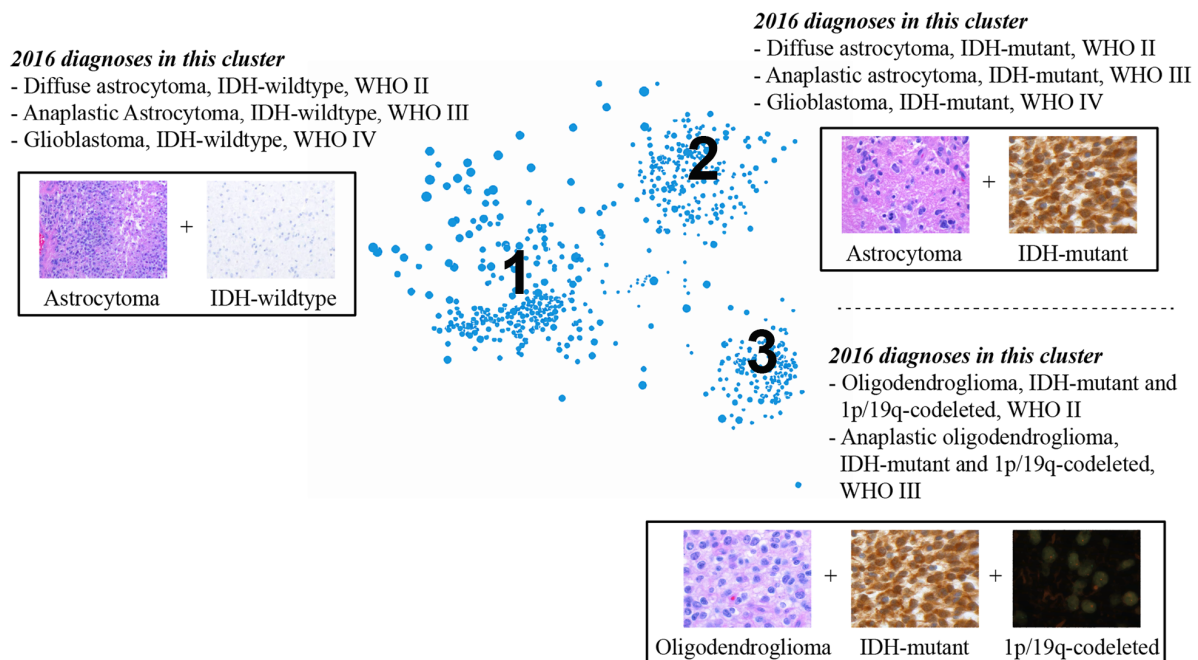
Figure 1:1. Visualization of the 2016 WHO classification of gliomas.
Multidimensional scaling demonstrates 3 major clusters of gliomas. The current WHO classification represents well these clusters and can be divided into:
1) astrocytic gliomas/glioblastomas, IDH-wildtype (WHO grades II–IV);
2) astrocytic gliomas/glioblastomas, IDH-mutant (WHO grades II–IV);
3) oligodendroglial tumours, IDH-mutant and 1p/19q-codeleted (WHO grades II–III).
Adapted from (Cimino et al., 2017).

1.2 Molecular subclassification of glioblastoma

Glioblastoma was also classified into 4 molecular subtypes comprising proneural, neural, classical, and mesenchymal, which are based on gene expression. These subtypes were characterized by abnormalities in EGFR (classical), PDGFRA/IDH1 (proneural), and NF1 (mesenchymal) (Fig.1:2). Verhaak and others proposed that the subtypes associate with different survival and may require different treatments. They showed that proneural GBM patients did not have survival advantage from RT/TMZ (combination of radiotherapy and Temozolomide) therapy, whereas mesenchymal and classical benefited from the standard of care (Verhaak et al., 2010). However, with the development of single cell RNA sequencing, it was demonstrated that different glioblastoma cells within the same tumour might belong to different molecular subtypes (Lee et al., 2017; Patel et al., 2014). Moreover, recent study showed that 63% of GBMs were classified to a different expression subtype at recurrence. Interestingly, in the same study the loss of EGFRvIII at recur-

rence was associated with a switch from classical to other expression subtypes (Wang et al., 2016). Moreover, the subtypes were recently updated to three (mesenchymal, proneural, and classical) after deconvolution of IDHwt GBM expression profiles into GBM cells and associated stroma *in silico* (Wang et al., 2017). All in all, even though the molecular subtypes are well accepted in the field, their prognostic value is rather limited.
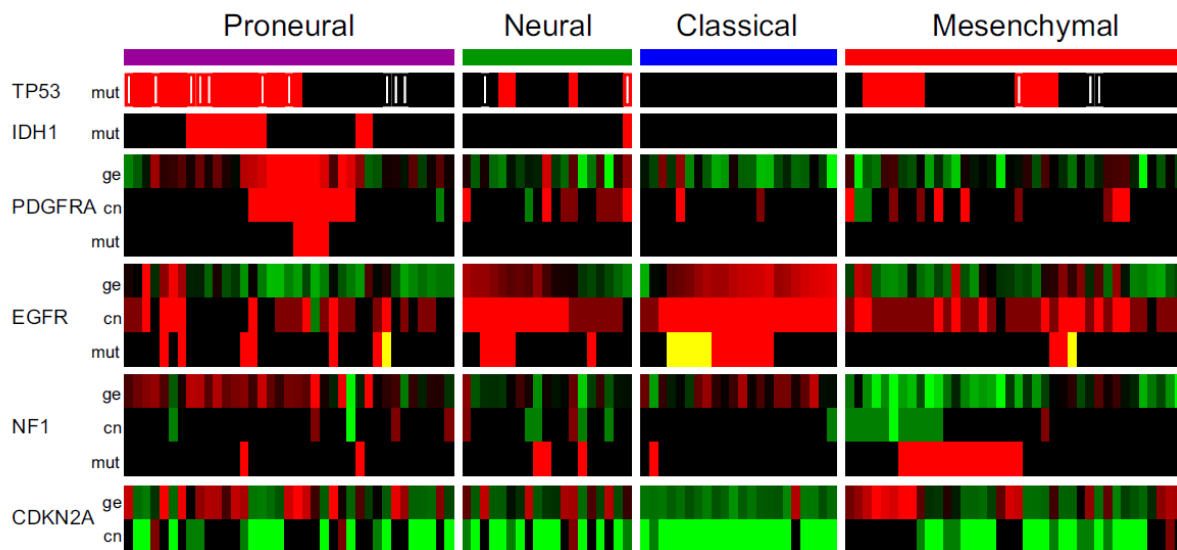
Figure 1:2. Four GBM expression subtypes proposed by (Verhaak et al., 2010)**.** Based on gene expression GBM can be divided into 4 groups, molecular subtypes that are associated with mutations in the *PDGFRA*, *EGFR*, *NF1*, *IDH1* and other genes. Adapted from https://verhaaklab.github.io/images/publpics/gbmsubtypes_header.png

1.3 Treatment of glioblastoma patients

The first step in glioblastoma management is surgical resection. The glioblastoma margins are not clear due to its invasiveness and a complete resection is often not achievable. However, the tumour resection allows for the pathological diagnosis. Radiotherapy remains a staple in glioblastoma management. From 2005, alkylating agent temozolomide is used in addition to radiation. The glioblastoma progression is often monitored by magnetic resonance imaging (MRI). The addition of temozolomide concomitant and adjuvant to RT improved median overall survival from 12.1 to 14.6 months (Stupp et al., 2009). Temozolomide mainly benefits patients with a methylated O-6-methylguanine-DNA methyltransferase (MGMT) gene promoter (Hegi et al., 2005), and unmethylated patients should be directed to clinical trials to test novel agents (Hegi and Stupp, 2015). In the United States Bevacizumab (anti-

VEGF (Vascular endothelial growth factor) monoclonal antibody) is approved for recurrent GBM, however clinical trials demonstrated that Bevacizumab does not significantly improve survival of patients with recurrent GBM. Whereas, in Europe Bevacizumab is used off-label mainly to reduce edema of the brain (Hottinger et al., 2014).

After the failure of more than a dozen of clinical trials adding targeted drugs to the standard of care (Prados et al., 2015), Tumour Treating Fields (TTFields, trademark Optune, Novocure) were reported to give 2 months overall survival benefit for GBM patients (Fig. 1:3). TTFields are low-intensity alternating electric fields that were shown to block mitosis. They are delivered continuously to the brain by a medical device that is worn on the scalp at least 18 hours per day. The treatment with TTFields takes place after TMZ/RT combination and lasts for at least 4 weeks, but maximum 7 weeks after last day of radiotherapy, together with TMZ for maintenance. There is no biomarker that predicts the response to TTFields so far, and MGMT methylation status did not play a significant role in response to TTFields (Stupp et al., 2017). All in all, the standard of care is evolving, TTFields plus TMZ should become the new standard at least for those patients who are willing to undergo this therapy.
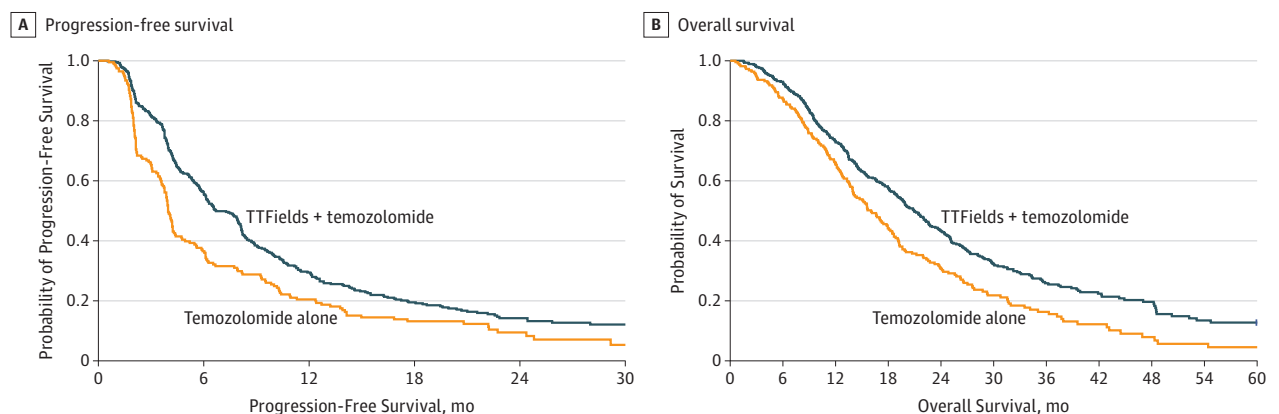
Figure 1:3. Kaplan-Meier curves for progression-free survival and overall survival for GBM patients treated with TMZ versus TTField + TMZ.
(A) Median progression-free survival from randomization for TMZ treated group was 4 months and for the TTFields + TMZ group was 6.7 months.
(B) Median overall survival from randomization was 16 months for TMZ alone group and 20.9 months for the TTFields + TMZ group. Adapted from (Stupp et al., 2017).

1.4 Glioma epigenetics: From subclassification to novel treatment options

This chapter comprises a published review in the peer-reviewed journal Seminars in Cancer Biology. My contribution included writing parts on the Histone code, Chromatin organization, Targeting the glioma epigenome; designing and drawing figures 2 and 3, as well as editing of the manuscript.

Review

Glioma epigenetics: From subclassification to novel treatment options

Olga Gusyatiner, Monika E. Hegi*

Laboratory of Brain Tumor Biology and Genetics, Neuroscience Research Center and Service of Neurosurgery, Lausanne University Hospital, 1066 Epalinges, Switzerland

ABSTRACT

Gliomas are the most common malignant primary brain tumors, of which glioblastoma is the most malignant form (WHO grade IV), and notorious for treatment resistance. Over the last decade mutations in epigenetic regulator genes have been identified as key drivers of subtypes of gliomas with distinct clinical features. Most characteristic are mutations in *IDH1* or *IDH2* in lower grade gliomas, and *histone 3* mutations in pediatric high grade gliomas that are also associated with characteristic DNA methylation patterns. Furthermore, in adult glioblastoma patients epigenetic silencing of the DNA repair gene *MGMT* by promoter methylation is predictive for benefit from alkylating agent therapy. These epigenetic alterations are used as biomarkers and play a central role for classification of gliomas (WHO 2016) and treatment decisions. Here we review the pivotal role of epigenetic alterations in the etiology and biology of gliomas. We summarize the complex interactions between "driver" mutations, DNA methylation, histone post-translational modifications, and overall chromatin organization, and how they inform current efforts of testing epigenetic compounds and combinations in preclinical and clinical studies.

1. Introduction

Gliomas are among the most common primary brain tumors in adults and account for over 70% of malignant brain tumors, of which glioblastoma is the most common and most malignant (World Health Organization [WHO] grade IV) with an incidence rate of 3.2 per 100 000 population [1]. The median survival is less than 2 years with the current standard of care of maximal safe resection, followed by combined radio-chemotherapy with the alkylating agent Temozolomide [2] that may be modestly improved with the addition of Tumor Treating Fields [3]. Glioblastomas are notorious for resistance to therapy, and despite numerous efforts, the addition of targeted agents against genetic or biological hallmarks of gliomas have largely failed [4]. Lower grade gliomas (LGG) WHO grade II and III are less common and affect younger patients. They have a better prognosis and show some sensitivity to therapy that both depend on the molecular subtype [5,6]. After resection LGG patients may first just be followed according to a "wait and see" strategy that depends on clinical and molecular risk factors, before entering treatment with different schemes of radio- or chemotherapy, or a combination thereof [6–8]. The optimal therapy is debated, however treatment related effects on cognitive function require risk-adapted (molecularly driven) treatment strategies, given that LGG patients may live more than 15 years [9].

2. Epigenetics of glioma

2.1. Epigenetic subtypes of gliomas

Insights into the molecular landscape of diffuse gliomas have revealed characteristic genetic and epigenetic profiles which have clarified their etiologic evolution [5,10–16] and allowed their classification into distinct molecular subtypes that have been integrated into the 2016 WHO classification (Fig. 1) [17]. Mutations in the epigenetic modulator genes isocitrate dehydrogenase 1 or 2 (*IDH1* or *IDH2*), and in the histone genes *H3F3A* or *HIST1H3 B* have become key biomarkers for tumor classification and emphasize the important role of epigenetic alterations as drivers in the evolution and biology of gliomas [10,12,18–20].

A point mutation in *IDH1* or *IDH2* (IDHmt) is characteristic for lower grade gliomas (WHO grade II/III), which are most prevalent in young adults. IDHmt gliomas are further subdivided into two major subtypes: oligodendrogliomas, with codeletion of chromosomal arms 1p/19q (1p/19q codel) that are usually associated with an activating mutation in the promoter of *TERT,* and astrocytomas, without 1p/19q codel. The latter are almost always associated with a mutation in *TP53,* and a mutation in *ATRX* that leads to loss of its nuclear expression, and diagnostically can be determined by immunohistochemistry [20]. Low grade gliomas without *IDH* mutation are termed IDH wild-type (IDHwt)

O. Gusyatiner, M.E. Hegi

ARTICLE IN PRESS

Fig. 1. Major genetic and epigenetic subgroups of gliomas. Characteristic epigenetic alterations are written in bold. CHR, chromosome; H3, histone 3; G-CIMP, glioma CpG island methylator phenotype.

	Glioblastoma H3K27M WHO grade IV	Glioblastoma H3G34R/V WHO grade IV	Glioblastoma IDHwt WHO grade IV	Glioblastoma IDHmt WHO grade IV	
MGMT meth	<5%	~65%	~35-50%	~90%	~100%
Age group	Children	Children, young adults	Older adults	Young adults	
Characteristic alterations	•Loss of H3-Lysine trimethylation	•DNA hypo-methylation	•Gain CHR 7 •Loss CHR10 •TERTp-mt •EGFR amp	•G-CIMP •ATRX mt •TP53mt	•G-CIMP •TERTp-mt

Above the Glioblastoma columns: Astrocytoma IDHmt WHO grade II; Oligodendroglioma IDHmt, 1p/19q$_{codel}$ WHO grade II; Astrocytoma IDHmt WHO grade III; Oligodendroglioma IDHmt, 1p/19q$_{codel}$ WHO grade III.

astrocytomas and are considered a provisional entity by the 2016 WHO classification. Upon further genetic analyses they may be classified into other entities [21]. In glioblastomas IDHmt are infrequent (< 10%) [10], and are usually observed in younger patients whose tumors may have progressed from an IDHmt non-codeleted lower grade glioma WHO grade II or III [22]. The histone mutation H3K27 M is characteristic for pediatric midline high grade glioma and the H3G34R/V mutation for hemispheric high grade glioma in children and young adults [23]. Most interestingly, these epigenetic driver mutations are associated with characteristic DNA methylation profiles, display characteristic age distributions and tumor locations that is suggestive of brain development related associations and are considered different diseases Fig. 1 [12,23].

2.2. DNA methylation

The most commonly studied epigenetic alterations in cancer comprise changes in DNA methylation, in particular methylation at the 5th position of cytosines at CpG sites, resulting in 5-methylcytosine, also known as the "fifth base" of DNA. There are several DNA methyltransferases involved in DNA methylation, of which all use S-adenosyl-L-methionine as source of methyl groups. DNMT1 preferentially methylates hemi-methylated DNA and is responsible for maintenance of DNA methylation patterns during replication, while DNMT3A, DNMT3B, and DNMT3L act on unmethylated DNA and are responsible for *de novo* methylation [24,25]. DNA demethylation involves the ten-eleven translocation family of enzymes TET(1–3) that convert 5mC to 5-hydroxymethylcytosine (5hmC) [26]. Additional epigenetic DNA modifications are known, however, their identification is technically more challenging and their function is less well studied [27–29]. Cancer development in general is associated with global DNA demethylation (hypomethylation) affecting intergenic regions, DNA repetitive sequences, gene bodies, including regulatory sequences; and aberrant *de novo* methylation of CpG islands (hypermethylation) in promoter regions of tumor suppressor genes [reviewed in [30]]. CpG islands refer to regions with high density of CpGs within a sequence and are often located in the regulatory region of promoters and are unmethylated in non-cancerous tissue [31]. Epigenetic gene silencing following CpG island methylation is mediated through methyl-CpG-binding domain (MBD) proteins such as MECP2 that recruit histone-modifying and chromatin-remodeling complexes to the methylated sites. DNA methylation profiles of cancer are highly characteristic and retain some traits of cell of origin. They have been successfully employed for re-defining/refining classification of brain tumors [12,32,33] or to determine the origin of metastasis of unknown primary cancer [34]. Most of the aforementioned studies reviewed here have been performed on the

Illumina DNA methylation BeadChip platform that interrogates genome-wide DNA methylation and allows in addition gene copy number analysis. Hence, there are multiple efforts to develop molecular classifying algorithms based on data derived on the Illumina DNA methylation platform for WHO classification of brain tumors (e.g. The Heidelberg platform for next generation neuropathology can be used at: MolecularNeuropathology.org) [35]. Aberrant methylation of CpG islands in gene promoters leads to gene silencing affecting cancer relevant pathways associated with the hallmarks of cancer [36]. In glioblastomas activation of the WNT pathway is mediated by aberrant promoter methylation of multiple negative regulators, such as the gene encoding the WNT inhibitory factor 1 (WIF1) or the family of secreted frizzled-related proteins (sFRPs), dickkopf (DKK), and naked (NKDs) [37,38]. Similarly, negative regulators of the Ras pathway are silenced, such as the Ras association (RalGDS/AF-6) domain family member RASSF1A [39].

2.3. The glioma CpG Island methylator phenotype associated with IDH1 or IDH2 mutations

Gliomas with mutations in the metabolic genes *IDH1* or *IDH2* display a striking signature of DNA hypermethylation that is completely different from IDHwt gliomas, and has been termed Glioma CpG Island Methylator Phenotype (G-CIMP) [11]. This fairly recent discovery has indicated a novel driver mechanism in tumor development, consequently IDHmt gliomas are now considered a different disease as reflected in the WHO 2016 classification [17]. *IDH* mutations are early lesions in the development of gliomas and cluster in the substrate binding site of these enzymes, at codon 132 of *IDH1* or codon 172 of *IDH*2, respectively [40,41]. These mutations are always heterozygous and confer a gain of function that favors a neomorphic reaction catalyzing the conversion of α-ketoglutarate into D-2-hydroxyglutarate (2HG) [41]. 2HG acts as a so-called oncometabolite by accumulating to high concentrations that inhibit α-ketoglutarate-dependent enzymes. α-Ketoglutarate-dependent enzymes comprise epigenetic modifiers such as the enzyme TET2 involved in DNA demethylation or the lysine-specific histone demethylase KDM2A [28,29,42–45]. However, α-ketoglutarate-dependent enzymes are also involved in other cellular functions that are inhibited by 2HG, such as the DNA repair enzymes of the ALKBH family, thereby altering response to chemotherapy [46], or HIF1α regulating proteins, affecting hypoxia sensing/signalling [47]. Obviously, the cell metabolism is seriously disturbed. Respective vulnerabilities have been identified and proposed as treatment opportunities [45,48]. Similarly, acute myeloid leukemia (AML) display CIMP in presence of a mutation in *IDH1* or *IDH2,* with a preference for *IDH2,* or a mutation in *TET2*. These mutations are mutually exclusive, and

2

have been shown to preclude hematopoietic differentiation [44]. These insights have contributed to the elucidation of the underlying mechanisms of CIMP. IDH mutations are considered the drivers for the development of G-CIMP through the production of the oncometabolite 2HG that among other effects mediates DNA hypermethylation through inhibition of TET2 [44,49]. Moreover, IDHmt gliomas regardless of tumor grade display a distinct immune phenotype characterized by reduced expression of immune response signatures and by less infiltration of tumor-associated immune cells [50–52]. This may be mediated by various mechanisms, including G-CIMP associated hypermethylation of immune response related genes in the tumor, as shown recently for *CD274* (*PD-L1*) in IDHmt glioma [50], and by down-regulation of leukocyte chemotaxis [51,52]. Altogether the plethora of G-CIMP associated silenced genes, affecting multiple cancer relevant pathways, may hold opportunities for novel therapeutic approaches.

2.4. Clinically relevant epigenetic biomarkers

2.4.1. IDH status

Determination of the IDH mutation status is key for integrated glioma classification. An antibody specific for the most common mutant, IDH1R132H that accounts for > 90% of all IDH mutations in gliomas, facilitates diagnosis [40,53]. Alternatively, the associated G-CIMP status can be easily determined based on the characteristic DNA methylation profile [11,12]. The oncometabolite 2HG can be detected in patients by magnetic resonance spectroscopy and may be used for longitudinal follow-up of patients, although this has not reached the clinic yet [54,55]. The reliable measurement of 2HG in easily accessible body fluids is hampered by the blood brain barrier and has not yielded a useful clinical test [56]. In IDHwt glioma of brain midline structures of young adults, a histone H3K27M mutation needs to be considered, which can be detected by immunohistochemistry with a H3K27M-specific antibody [20].

2.4.2. MGMT promoter methylation status predictive biomarker in glioblastoma

The DNA repair gene O6-methylguanine-DNA methyltransferase (*MGMT*) is the most prominent epigenetically silenced gene in gliomas [57–59]. In glioblastomas promoter methylation of *MGMT* is predictive for benefit from the alkylating agent temozolomide, as shown in several phase III clinical trials, and the *MGMT* methylation status has become the first predictive biomarker in neuro-oncology [57,60–63]. MGMT repairs the most toxic lesion, O6-methylguanine, induced by alkylating agents, thereby blunting the treatment effects. This is reflected by the fact that patients with an unmethylated *MGMT* basically do not profit from the addition of temozolomide concomitant and adjuvant to radiotherapy [57]. Routine determination of the *MGMT* status allows for stratified treatment, and is used for selecting glioblastoma patients for clinical trials omitting temozolomide in the experimental arm [64–66]. The role of the *MGMT* methylation status on benefit from temozolomide in IDHmt lower grade gliomas is less clear [6], although most (> 80%) show methylation at the *MGMT* promoter, probably as part of G-CIMP [67]. However, unlike glioblastomas who usually lose one copy of chromosome 10 on which *MGMT* resides, IDHmt lower grade gliomas usually retain both copies and *MGMT* may not be completely silenced, resulting in residual repair capacity of MGMT contributing to resistance to temozolomide therapy [68]. The most commonly used tests to determine the *MGMT* methylation status employ methylation specific PCR [69], as reviewed elsewhere [61]. A *MGMT* status classifier (MGMT-STP27) is available for samples analyzed on the Illumina DNA methylation platform (HM27 K, HM450 K, EPIC) [68,70] and is widely used, including in clinical trials [6,13,71].

2.5. Histone code

The DNA molecule is packed in the nucleus of the cell by anchoring proteins called histones. The formed complex of DNA and 8 histone components of the nucleosome is referred to as chromatin. The chromatin is the essential environment through which transcription factors and signalling pathways alter gene activity. Histones serve not only for spatial organization of the DNA double helix, but also exhibit covalent marks that orchestrate chromatin accessibility. Each of the 8 core histones has a N-terminal tail hanging from the nucleosome that is subjected to multiple post-translational modifications at specific residues, comprising methylation, acetylation, sumoylation, ubiquitination, phosphorylation, and others. In fact, over 500 distinct histone modifications have been described, whereas the function of only a fraction of them has been studied (reviewed in [72]). The histone marks are recognized by a class of epigenetic proteins called readers, which in concert with recruited proteins remodel particular genomic regions to modulate target gene expression. The histone marks may be removed by erasers and added by writers, thereby dynamically regulating the chromatin code [73]. Active genes have been associated with tri-methylation of lysine 4 (H3K4me3) and acetylation of lysine 9 (H3K9ac), while inactive genes may be decorated with H3K9me3 and H3K27me3. However, many active and inactive genes have overlapping patterns of histone modifications. In fact bivalent histone marks are a hallmark of embryonic stem cells (H3K27me3/H3K4me3) that keep genes in a poised state for rapid changes and may predispose important regulatory genes to inactivation by aberrant DNA hypermethylation, resulting in malignant transformation and tumor progression [74].

A recent study using the TCGA GBM and LGG datasets exposed that at least one of a set of 36 genes involved in chromatin organization was targeted by genetic alterations in 54% of gliomas [16]. Interestingly, most gliomas with alterations in this set of genes belonged to the molecular subgroup of IDHmt non-codeleted gliomas (n = 230, 87%) [16]. Among the genes predicted to be potential glioma drivers, several have epigenetic functions, such as ATRX (n = 226 mutations, 25% of all cases), SETD2 (n = 24, 1%), ARID2 (n = 20, 1%), DNMT3A (n = 11, 1%), SMARCA4 (n = 29, 3%), and ARID1A (n = 15, 1%) [16].

In addition to histone modifications, genes coding for histones are mutated in high grade glioma of children and adolescents [23]. Nearly 30% of pediatric high grade gliomas (WHO grades III and IV) harbor point mutations at specific sites (K27M/I and G34R/V) of histone 3 (H3) gene variants (*H3F3A*, approximately 85%; *HIST1H3B/C* mutually exclusive, 14%; and other more rare variants [75]). Of note, there are thirty H3 variants in the human genome, and therefore the mutant allele is present only in a minor proportion (7.6-17.6%) of the total H3 proteins [76]. Lysines (K) are key residues in histone tails subjected to post-translational modifications by methylation or acetylation. Therefore, substitution of K27 with methionine or isoleucine in H3 has an impact on the epigenetic state of cells. Mechanistically it was shown that mutated histones H3K27M/I directly bind to histone-lysine N-methyltransferase (EZH2), thereby inhibiting the enzymatic activity of the Polycomb repressive complex 2. The transgene encoding H3K27M was demonstrated to efficiently reduce H3K27me3 levels *in vitro* and *in vivo* [76]. Whereas the global levels of H3K27me3 are diminished in H3K27M mutated gliomas, certain genes were shown to consistently preserve their H3K27me3 mark [77].

2.6. Chromatin organization

Gene expression is also regulated by the overall 3D chromatin organization, which is modulated by several factors, including DNA methylation and histone marks. The structure of the chromatin is composed of loops or topology associated domains (TADs), which are conserved evolutionarily, and are largely cell type invariant. The organization of TADs is responsible for placing the enhancer regions and promoter regions into spatial proximity in order to activate target gene expression. Originally TADs have been considered to be invariant building blocks of chromosomes [78]. However, recent findings by the

3
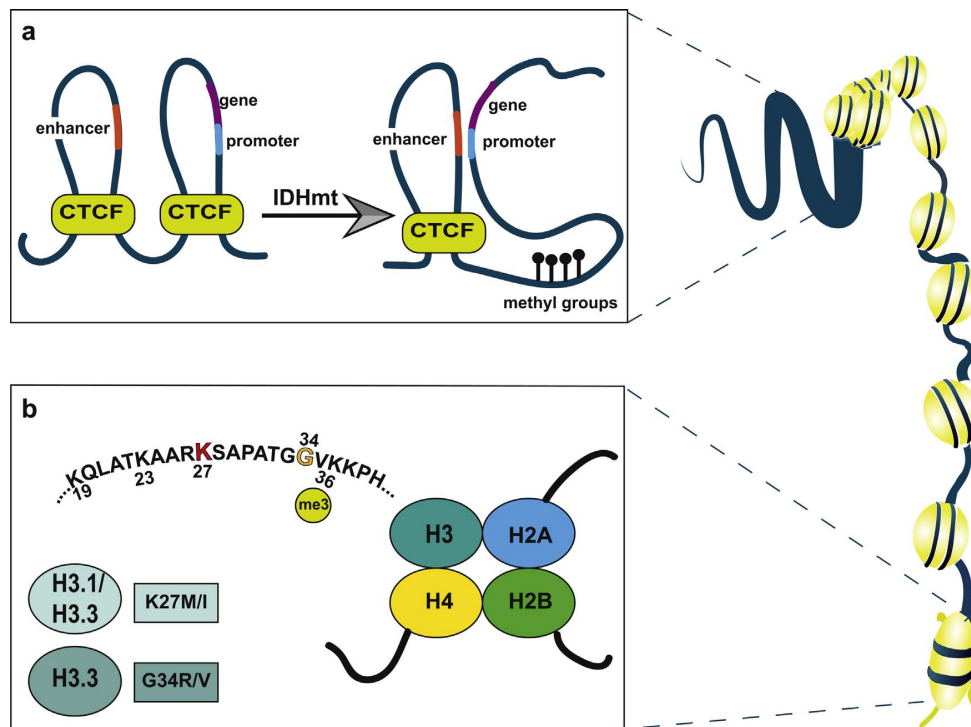
Fig. 2. Chromatin dysorganization and histone mutations in glioma. (a) Cell insulator protein CTCF separates topologically associated domains, depicted as loops. Flavahan and others showed that in IDH1mt glioma CTCF binding sites are often methylated reducing CTCF–DNA binding [78]. This allows aberrant associations between enhancers and the promoter regions of oncogenes. (b) Histone genes are mutated in about 50% of gliomas in children and young adults. Majority of mutations (85%) are found in histone variant H3.3, and 14% are found in variant H3.1. H3K27M and H3G34R/V mutations are associated with different patient age, different location of the tumor, and distinct methylation phenotype (reviewed in the text).

group of Bernstein suggested that the architecture of TADs is disturbed in IDHmt glioma, allowing aberrant interactions between strong enhancers and oncogenes (Fig. 2). As a result of the reorganization of TADs, the transcription of tumor promoting factors (e.g. oncogenes and anti-apoptotic factors) is enhanced and promotes neoplastic growth [79]. These observations were associated with the finding that IDH1mt gliomas exhibit hypermethylation at cohesin and CCCTC- binding factor (CTCF)-binding sites, which inhibits the binding of insulator protein that is crucial for proper organization of TADs.

Overall, the functional impact of G-CIMP goes well beyond promoter hypermethylation-related effects and may be responsible for disrupting chromosomal topology and allowing aberrant regulatory interactions that may induce oncogene expression [79].

3. Targeting the glioma epigenome

Several different approaches of targeting epigenetic alterations have been or are being tested in clinical trials: those targeting mutant IDH either by small molecule inhibitors, or as target for vaccination in the respective patient population; and those targeting epigenetic modifiers affecting large parts of the epigenome such as BETi, HDACi, DNMTi, and EZH2i (Fig. 3). Respective clinical trials, as available on clinical-trials.gov, are summarized in Table 1.

3.1. Inhibitors of mutant IDH (mtIDHi)

Inhibitors of mutant IDH are currently tested in several trials for patients with IDHmt gliomas with the aim to block the production of the oncometabolite 2HG to normalize the function of α-ketoglutarate dependent enzymes. Encouraging results from first preclinical studies

suggested differentiation promoting effects and attenuation of growth *in vitro* and *in vivo* (subcutaneous xenografts) of glioma cells with an endogenous heterozygous *IDH* mutation, while no appreciable changes of overall DNA methylation was observed [80]. However, later reports indicated that inhibition of IDHmt may not inhibit growth of IDHmt glioma cells or propagation of orthotopic tumor xenografts [48,81]. On the contrary, inhibition of IDHmt was suggested to promote the growth of most tested IDHmt glioma lines *in vitro* [48]. A recent report adds to this controversy, 10% (6/50) of a set of paired samples (first resection/ recurrence) was found to lose the IDHmt allele upon malignant progression. Overall G-CIMP was preserved, however, exhibiting some alterations in DNA methylation [82]. The latter may overlap with "G-CIMP-low" where progression related specific loss of methylation has been postulated to enhance expression of cell cycle related genes associated with worse prognosis [16]. The progression related loss of the IDHmt allele questions its importance for tumor maintenance and consequently the suitability as single drug target. This question is also of relevance for the vaccination trials targeting IDH1R132H, for which encouraging preclinical studies have been presented [83]. Interestingly, it has been suggested that reversing the inhibitory effect of 2HG on STAT1 mediated expression of IFN-γ–inducible chemokines may improve the vaccination approach [51]. The complexity of the different effects on tumor biology linked to targeting the IDHmt renders the outcome predictions difficult. Thus, the results of the clinical trials are eagerly awaited.

3.2. EZH2 inhibitors (EZH2i)

EZH2 is an interesting target within the polycomb repressor complex 2 (PRC2) in pediatric glioma, since the H3K27M mutation has been

4
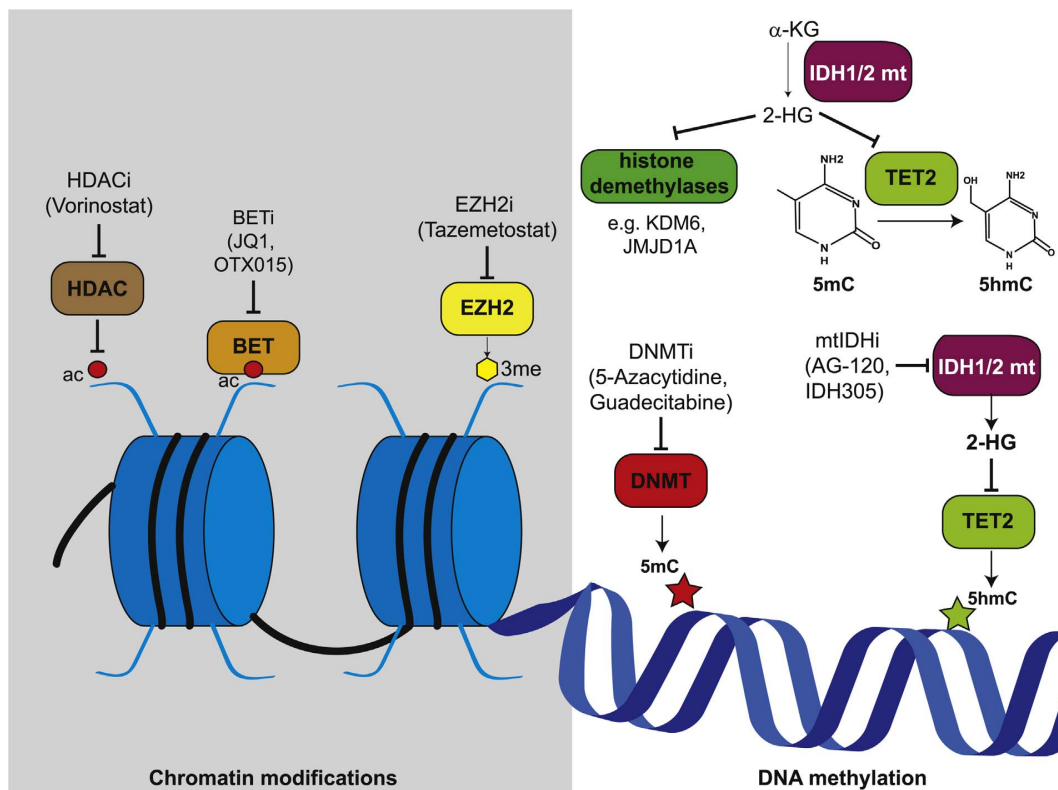
Fig. 3. Epigenetic inhibitors and drugs currently under investigation in preclinical glioma models and clinical trials. DNMT, DNA methylases; HDAC, histone deacetylase, BET, bromodomain and extra-terminal tail protein; EZH2, Enhancer of zeste homolog 2, histone-lysine N-methyltransferase; ac, acetylation; 3me, tri-methylation, 5mc, 5-methylcytosine; 5hmc, 5-hydroxymethylcytosine.

shown to inhibit PRC2 activity [76]. The EZH2i Tazemetostat is currently tested in pediatric glioma with a gain of function mutation in EZH2 or loss of function mutations in the chromatin remodeling complex subunits SMARCB1 or SMARCA4 (Table 1). However, these mutations are rare in pediatric gliomas [18,75,84].

Preclinical studies of the EZH2i Tazemetostat show a mixed picture. While the EZH2i Tazemetostat was suggested to lack activity in pediatric glioma cells *in vitro* independent of H3.3 mutations [85], a recent study provided evidence that Tazemetostat may affect growth of primary H3K27M-positive glioma cells in presence of functional p16INK4A [86].

Short-term EZH2 depletion in glioblastoma cells without H3 or IDH mutations, has been associated with reduced proliferation [87], while recent results suggest that prolonged EZH2 inhibition may cause a switch in cell fate, enhancing proliferation and DNA damage repair, resulting in tumor progression [88].

3.3. DNA methylation inhibitors (DNMTi)

Preclinical studies have suggested efficacy of DNA methylation inhibitors (DNMTi) in *in vitro* and *in vivo* models of IDHmt glioma [81,89]. However, this has not translated into successful treatments with DNMTi in glioma patients, possibly because 5-Azacytidine and Decitabine are S-phase-specific and have relatively short half lives [90]. The novel second-generation hypomethylating drug guadecitabine with better pharmacodynamic characteristics is currently tested in a phase III study in AML [91]. However, it remains controversial whether general demethylation is desired in glioma, as unwanted proto-oncogenes may be activated, and demethylation of the repair gene *MGMT*

may render glioblastomas resistant to alkylating agents that are part of the standard of care. Interestingly, low dose demethylating agents impact immune regulation and may induce innate immune response by re-activating retroviruses [92,93].

3.4. Histone deacetylase inhibitors (HDACi)

The underlying rationale of using HDACi as cancer therapeutics is to reverse dysregulated target gene expression by modulating histone acetylation marks [94]. Dynamic regulation of the chromatin state is mediated by mechanisms such as covalent modification of chromatin, which includes histone acetylation and methylation, and ATP-dependent chromatin remodeling. Histone 3 lysine acetylation is a mark of active enhancers that control the expression of associated distal genes. Generally, exposure to HDACi results in hyperacetylation of histones, which globally affects gene expression.

Vorinostat has been tested in phase II trials of recurrent glioblastomas, first as single agent that has shown good tolerability. Moreover, the study also indicated that the drug affected target pathways in glioblastomas [95]. Taken to the next step, vorinostat was tested in combination with the protease inhibitor bortezomib that however, in the dosing scheme used showed no efficacy [96]. In newly diagnosed glioblastoma the addition of vorinostat to the standard of care of radiochemotherapy did not meet the primary endpoint of efficacy in a phase I/II trial. However, indications from molecular subgroup analyses may provide criteria for future patient selection [97].

5

Table 1

Ongoing clinical trials testing epigenetic drugs in gliomas.
Source, https://clinicaltrials.gov.

Drug	Target	Age group (years)	Clinical trial identifier*	Trial phase	Malignancy
IDH inhibitors					
AG-881	mutant IDH1 and/or mutant IDH2	18 +	NCT02481154	I	Glioma with *IDH1* and/or *IDH2* mutation
AG-120 (Ivosidenib)	mutant IDH1	18 +	NCT02073994	II	Glioma with *IDH1* mutation
AG-221 (IDHIFA, Enasidenib)	mutant IDH2	18 +	NCT02273739	I/II	Glioma with *IDH2* mutation
BAY1436032	mutant IDH1	18 +	NCT02746081	I	Glioma with *IDH1* mutation
DS-1001b	mutant IDH1	20 +	NCT03030066	I	Glioma with *IDH1* mutation
IDH305	mutant IDH1	18 +	NCT02381886	I	Glioma with *IDH1* mutation
IDH305	mutant IDH1	18 +	NCT02977689	II	Glioma grade II or III with *IDH1* mutation
IDH1R132H peptide vaccine	IDH1R132H	18 +	NCT02454634	I	Glioma grade III-IV with *IDH1* mutation
IDH1R132H peptide vaccine	IDH1R132H	18 +	NCT02193347	I	Recurrent glioma grade II with*IDH1* mutation
IDH1R132H dendritic cell vaccine	IDH1R132H	18–70	NCT02771301	safety	Glioma with *IDH1* mutation
EZH2 inhibitors					
Tazemetostat	mt and wt EZH2	1–21	NCT03155620	II	Glioma with *EZH2*, *SMARCB1*, or *SMARCA4* mutation
HDAC inhibitors					
Valproic acid	HDAC, class I and II	3–17	NCT03243461	III	Pediatric glioma
Entinostat	HDAC, class I	1–21	NCT02780804	I	Recurrent childhood visual pathway glioma
Panobinostat (LBH589)	HDAC, class I, II, and IV	2–21	NCT02717455	I	Diffuse intrinsic pontine glioma
Vorinostat (SAHA)	HDAC, class I and II	3–21	NCT01189266	I/II	Diffuse intrinsic pontine glioma
Vorinostat (SAHA)	HDAC, class I and II	0.5– 21	NCT02420613	I	Diffuse intrinsic pontine glioma
Vorinostat (SAHA)	HDAC, class I and II	18 +	NCT00268385	I	Glioma
Vorinostat (SAHA)	HDAC, class I and II	3–21	NCT01236560	II/III	Pediatric high grade glioma
Vorinostat (SAHA)	HDAC, class I and II	18 +	NCT00555399	I/II	Glioblastoma
Belinostat	HDAC, class I and II	18 +	NCT02137759	II	Glioblastoma
Vorinostat (SAHA)	HDAC, class I and II	18 +	NCT00731731	I/II	Glioblastoma
DNMT inhibitors					
5-Azacytidine (Vidaza)	DNMT	1–21	NCT02940483	I	Recurrent posterior fossa ependymoma
5-Azacytidine (Vidaza)	DNMT	1–18	NCT03206021	I/Ib	Recurrent ependymoma
5-Azacytidine (Vidaza)	DNMT	18 +	NCT02223052	I	Glioblastoma

3.5. BET inhibitors (BETi)

Another way to target enhancer elements is to inhibit readers of the acetylated histone tails (Fig. 3). Bromodomain and extra-terminal tail (BET) proteins are chromatin readers, they recognize and bind to the H3K9 and H3K27 acetyl marks, recruit mediator complex and promote transcription of target genes. BET proteins were shown to be essential for high-level expression of oncogenes. Moreover, BETi were demonstrated to reduce the transcription of oncogenes by attenuating enhancer activity at so-called super-enhancers [98]. Super-enhancers are referred to as large clusters of transcriptional enhancers driving expression of genes that control cell identity and disease including cancer [99]. In an *in vivo* RNAi screen, testing chromatin regulators required for survival of glioblastoma cells in an intact environment, BRD4 was among the top hits [100]. Preclinical studies in orthotopic mouse glioblastoma xenografts have reported efficiency of several BETi, such as the tool drug JQ1, I-BET151, and OTX015 [101–103]. Moreover, IDHmt primary glioma cells were reported to be very sensitive to BETi JQ1 and GS-626510 with half-maximal inhibitory concentrations 1 000 times lower than the one of Temozolomide [104].

A phase IIa trial for dose optimization of OTX015 in recurrent glioblastoma patients was terminated in 2015 due to lack of efficacy in this patient population [105]. Other BETi with different pharmacokinetic properties are currently in preclinical evaluation.

3.6. Potential of epigenetic drugs in treatment resistance

The combinations of epigenetic drugs with conventional chemo/radiation therapy or with targeted compounds are still in the early stages of preclinical research in glioma. Recent reports suggested that both conventional chemotherapy [106] and tyrosine kinase inhibitors [107] may facilitate the growth of pre-existing resistant clones.

Importantly, these resistant clones were shown to be sensitive to epigenetic drugs. Dirks and co-workers have reported that Temozolomide-resistant clones displayed epigenetic changes that rendered them sensitive to the inhibitor of Menin-MLL (MI-2-2) [106]. Furthermore, the group of Bernstein demonstrated that Dasatinib-tolerant persisters were dependent on the H3K27me3 demethylases KDM6A/B and were therefore highly sensitive to the KDM6A/B small molecule inhibitor GSKJ4 [107]. Overall, the insights of these preclinical studies suggest that epigenetic drugs combined with conventional therapy, such as alkylating drugs or tyrosine kinase inhibitors may act synergistically to eliminate refractory tumor cells and potentially inhibit the expansion of resistant clones.

4. Conclusions

Discoveries of the last decade have completely changed our view on the genomic and epigenetic landscape of human gliomas. Driver mutations in epigenetic regulator genes have clarified their etiology and defined molecular subtypes with distinct biology. Consequently, epigenetic biomarkers play now a central role in tumor classification and decision making for stratified therapies. A whole arsenal of epigenetic drugs promises to target epigenetically deregulated pathways by interfering on several levels. However, the complex interplay between gene expression, DNA methylation, histone modifications, and chromatin organization presents challenges for rational trial designs. Moreover, the dynamic epigenetic changes in response to therapy (resistance) or the interaction with the tumor microenvironment yield challenges and opportunities. At present a number of trials have been initiated and await completion (Table 1). The insights from basic and preclinical research, and first clinical trials reviewed here, suggest that single epigenetic agents are likely not sufficient, and molecularly informed combinations with other epigenetic drugs, or other targeted/

6

ARTICLE IN PRESS

conventional therapies will be required. Furthermore, the glioma methylome, in particular in IDHmt/G-CIMP positive gliomas, still awaits exploration for potential vulnerabilities of cancer relevant pathways that may be amenable to specific treatments, beyond Temozolomide for glioblastomas with *MGMT* promoter methylation. Further insights on the effects of epigenetic drugs on the modulation of the tumor immune environment; and the exploration of 2HG- dependent metabolic vulnerabilities in IDHmt gliomas may provide additional opportunities. We are just at the beginning of an exciting new era.

Funding sources

Conflict of interest statement

References

[1] Q.T. Ostrom, H. Gittleman, J. Xu, C. Kromer, Y. Wolinsky, C. Kruchko, et al., CBTRUS Statistical report: primary brain and other central nervous system tumors diagnosed in the United States in 2009–2013, Neuro Oncol. 18 (Suppl. 5) (2016) v1–v75.

[2] R. Stupp, M.E. Hegi, W.P. Mason, M.J. van den Bent, M.J. Taphoorn, R.C. Janzer, et al., Effects of radiotherapy with concomitant and adjuvant temozolomide versus radiotherapy alone on survival in glioblastoma in a randomised phase III study: 5-year analysis of the EORTC-NCIC trial, Lancet Oncol. 10 (5) (2009) 459–466.

[3] R. Stupp, S. Taillibert, A.A. Kanner, S. Kesari, D.M. Steinberg, S.A. Toms, et al., Maintenance therapy with tumor-treating fields plus temozolomide vs temozolomide alone for glioblastoma: a randomized clinical trial, JAMA 314 (23) (2015) 2535–2543.

[4] M. Weller, M. van den Bent, J.C. Tonn, R. Stupp, M. Preusser, E. Cohen-Jonathan-Moyal, et al., European Association for Neuro-Oncology (EANO) guideline on the diagnosis and treatment of adult astrocytic and oligodendroglial gliomas, Lancet Oncol. 18 (6) (2017) e315–e329.

[5] H. Suzuki, K. Aoki, K. Chiba, Y. Sato, Y. Shiozawa, Y. Shiraishi, et al., Mutational landscape and clonal architecture in grade II and III gliomas, Nat. Genet. 47 (5) (2015) 458–468.

[6] B.G. Baumert, M.E. Hegi, M.J. van den Bent, A. von Deimling, T. Gorlia, K. Hoang-Xuan, et al., Temozolomide chemotherapy versus radiotherapy in high-risk low-grade glioma (EORTC 22033–26033): a randomised, open-label, phase 3 intergroup study, Lancet Oncol. 17 (11) (2016) 1521–1532.

[7] J.C. Buckner, E.G. Shaw, S.L. Pugh, A. Chakravarti, M.R. Gilbert, G.R. Barger, et al., Radiation plus procarbazine, CCNU, and vincristine in low-grade glioma, N. Engl. J. Med. 374 (14) (2016) 1344–1355.

[8] M.J. van den Bent, B. Baumert, S.C. Erridge, M.A. Vogelbaum, A.K. Nowak, M. Sanson, et al., Interim results from the CATNON trial (EORTC study 26053-22054) of treatment with concurrent and adjuvant temozolomide for 1p/19q non-co-deleted anaplastic glioma: a phase 3, randomised, open-label intergroup study, Lancet 8 (17) (2017) 31442–31443.

[9] R. Ruda, R. Soffietti, Controversies in management of low-grade gliomas in light of new data from clinical trials, Neuro Oncol. 19 (2) (2017) 143–144.

[10] H. Yan, D.W. Parsons, G. Jin, R. McLendon, B.A. Rasheed, W. Yuan, et al., IDH1 and IDH2 mutations in gliomas, N. Engl. J. Med. 360 (8) (2009) 765–773.

[11] H. Noushmehr, D.J. Weisenberger, K. Diefes, H.S. Phillips, K. Pujara, B.P. Berman, et al., Identification of a CpG island methylator phenotype that defines a distinct subgroup of glioma, Cancer Cell 17 (2010) 419–420.

[12] D. Sturm, H. Witt, V. Hovestadt, D.A. Khuong-Quang, D.T. Jones, C. Konermann, et al., Hotspot mutations in H3F3A and IDH1 define distinct epigenetic and biological subgroups of glioblastoma, Cancer Cell 22 (4) (2012) 425–437.

[13] C.W. Brennan, R.G. Verhaak, A. McKenna, B. Campos, H. Noushmehr, S.R. Salama, et al., The somatic genomic landscape of glioblastoma, Cell 155 (2) (2013) 462–477.

[14] T. Ozawa, M. Riester, Y.-K. Cheng, J.T. Huse, M. Squatrito, K. Helmy, et al., Most human-non-GCIMP glioblastoma subtypes evolve from a common proneural-like precursor glioma, Cancer Cell 26 (2) (2014) 288–300.

[15] D.J. Brat, R.G. Verhaak, K.D. Aldape, W.K. Yung, S.R. Salama, L.A. Cooper, et al., Comprehensive, integrative genomic analysis of diffuse lower-grade gliomas, N. Engl. J. Med. 372 (26) (2015) 2481–2498.

[16] M. Ceccarelli, F.P. Barthel, T.M. Malta, T.S. Sabedot, S.R. Salama, B.A. Murray, et al., Molecular profiling reveals biologically discrete subsets and pathways of progression in diffuse glioma, Cell 164 (3) (2016) 550–563.

[17] D.N. Louis, H. Ohgaki, O.D. Wiestler, W.K. Cavenee, WHO Classification of tumours of the central nervous system, in: F.T. Bosman, E.S. Jaffe, L.S.R.H. Ohgaki (Eds.), World Health Organization Classification of Tumours, IARC, Lyon, 2016.

[18] J. Schwartzentruber, A. Korshunov, X.Y. Liu, D.T. Jones, E. Pfaff, K. Jacob, et al., Driver mutations in histone H3.3 and chromatin remodelling genes in paediatric glioblastoma, Nature 482 (7384) (2012) 226–231.

[19] G. Wu, A. Broniscer, T.A. McEachron, C. Lu, B.S. Paugh, J. Becksfort, et al., Somatic histone H3 alterations in pediatric diffuse intrinsic pontine gliomas and non-brainstem glioblastomas, Nat. Genet. 44 (3) (2012) 251–253.

[20] G. Reifenberger, H.G. Wirsching, C.B. Knobbe-Thomsen, M. Weller, Advances in the molecular genetics of gliomas ? implications for classification and therapy, Nat. Rev. Clin. Oncol. 29 (10) (2016) 204.

[21] D.E. Reuss, A. Kratz, F. Sahm, D. Capper, D. Schrimpf, C. Koelsche, et al., Adult IDH wild type astrocytomas biologically and clinically resolve into other tumor entities, Acta Neuropathol. 129 (2015) 407–417.

[22] H. Ohgaki, P. Kleihues, The definition of primary and secondary glioblastoma, Clin. Cancer Res. 19 (4) (2013) 764–772.

[23] D. Sturm, S.M. Pfister, D.T.W. Jones, Pediatric gliomas: current concepts on diagnosis, biology, and clinical management, J. Clin. Oncol. 35 (21) (2017) 2370–2377.

[24] A. Hermann, H. Gowher, A. Jeltsch, Biochemistry and biology of mammalian DNA methyltransferases, Cell. Mol. Life Sci. 61 (19–20) (2004) 2571–2587.

[25] A.S. Quina, M. Buschbeck, L. Di Croce, Chromatin structure and epigenetics, Biochem. Pharmacol. 72 (11) (2006) 1563–1569.

[26] Y. Huang, A. Rao, Connections between TET proteins and aberrant DNA modification in cancer, Trends Genet. 30 (10) (2014) 464–474.

[27] G. Ficz, J.G. Gribben, Loss of 5-hydroxymethylcytosine in cancer: cause or consequence? Genomics 104 (5) (2014) 352–357.

[28] Y.W. Zhang, Z. Wang, W. Xie, Y. Cai, L. Xia, H. Easwaran, et al., Acetylation enhances TET2 function in protecting against abnormal DNA methylation during oxidative stress, Mol. Cell 65 (2) (2017) 323–335.

[29] L. Scourzic, E. Mouly, O.A. Bernard, TET proteins and the control of cytosine demethylation in cancer, Genome Med. 7 (1) (2015) 9.

[30] A. Portela, M. Esteller, Epigenetic modifications and human disease, Nat. Biotech. 28 (10) (2010) 1057–1068.

[31] A.M. Deaton, A. Bird, CpG islands and the regulation of transcription, Genes Dev. 25 (10) (2011) 1010–1022.

[32] D. Sturm, B.A. Orr, U.H. Toprak, V. Hovestadt, D.T. Jones, D. Capper, et al., New brain tumor entities emerge from molecular classification of CNS-PNETs, Cell 164 (5) (2016) 1060–1072.

[33] S. Fukushima, S. Yamashita, H. Kobayashi, H. Takami, K. Fukuoka, T. Nakamura, et al., Genome-wide methylation profiles in primary intracranial germ cell tumors indicate a primordial germ cell origin for germinomas, Acta Neuropathol. 11 (10) (2017) 017–1673.

[34] S. Moran, A. Martinez-Cardus, S. Sayols, E. Musulen, C. Balana, A. Estival-Gonzalez, et al., Epigenetic profiling to classify cancer of unknown primary: a multicentre, retrospective analysis, Lancet Oncol. 17 (10) (2016) 1386–1395.

[35] J. Eckel-Passow, P. Decker, E. Hughes, T. Kollmeyer, M. Kosel, D. Burgenske, et al., PATH-47. Clinical sensitivity and specificity of illumina methylation array for classifying adult gliomas into WHO groups, Neuro-oncol 19 (Suppl. 6) (2017) vi181.

[36] N. Azad, C.A. Zahnow, C.M. Rudin, S.B. Baylin, The future of epigenetic therapy in solid tumours-lessons from the past, Nat. Rev. Clin. Oncol. 10 (5) (2013) 256–266.

[37] W.L. Lambiv, I. Vassallo, M. Delorenzi, T. Shay, A.C. Diserens, A. Misra, et al., The Wnt inhibitory factor 1 (WIF1) is targeted in glioblastoma and has a tumor suppressing function potentially by induction of senescence, Neuro Oncol. 13 (7) (2011) 736–747.

[38] S. Gotze, M. Wolter, G. Reifenberger, O. Muller, S. Sievers, Frequent promoter hypermethylation of Wnt pathway inhibitor genes in malignant astrocytic gliomas, Int. J. Cancer 126 (11) (2010) 2584–2593.

[39] K. Horiguchi, Y. Tomizawa, M. Tosaka, S. Ishiuchi, M. Kurihara, M. Mori, et al., Epigenetic inactivation of RASSF1A candidate tumor suppressor gene at 3p21. 3 in brain tumors, Oncogene 22 (49) (2003) 7862–7865.

[40] C. Hartmann, J. Meyer, J. Balss, D. Capper, W. Mueller, A. Christians, et al., Type and frequency of IDH1 and IDH2 mutations are related to astrocytic and oligodendroglial differentiation and age: a study of 1,010 diffuse gliomas, Acta Neuropathol. 118 (4) (2009) 469–474.

[41] B. Pietrak, H. Zhao, H. Qi, C. Quinn, E. Gao, J.G. Boyer, et al., A tale of two subunits: how the neomorphic R132H IDH1 mutation enhances production of αHG, Biochemistry 50 (21) (2011) 4804–4812.

[42] L. Dang, D.W. White, S. Gross, B.D. Bennett, M.A. Bittinger, E.M. Driggers, et al., Cancer-associated IDH1 mutations produce 2-hydroxyglutarate, Nature 462 (7274) (2009) 739–744.

[43] W. Xu, H. Yang, Y. Liu, Y. Yang, P. Wang, S.-H. Kim, et al., Oncometabolite 2-hydroxyglutarate is a competitive inhibitor of [alpha]-ketoglutarate-dependent dioxygenases, Cancer Cell 19 (1) (2011) 17–30.

[44] M.E. Figueroa, O. Abdel-Wahab, C. Lu, P.S. Ward, J. Patel, A. Shih, et al., Leukemic IDH1 and IDH2 mutations result in a hypermethylation phenotype, disrupt TET2 function, and impair hematopoietic differentiation, Cancer Cell 18 (6) (2010) 553–567.

[45] J.R. Prensner, A.M. Chinnaiyan, Metabolism unhinged: IDH mutations in cancer, Nat. Med. 17 (3) (2011) 291–293.

[46] P. Wang, J. Wu, S. Ma, L. Zhang, J. Yao, K.A. Hoadley, et al., Oncometabolite D-2-Hydroxyglutarate inhibits ALKBH DNA repair enzymes and sensitizes IDH mutant cells to alkylating agents, Cell Rep. 13 (11) (2015) 2353–2361.

[47] P. Koivunen, S. Lee, C.G. Duncan, G. Lopez, G. Lu, S. Ramkissoon, et al.,

7

Transformation by the (R)-enantiomer of 2-hydroxyglutarate linked to EGLN activation, Nature 483 (7390) (2012) 484–488.

[48] K. Tateishi, H. Wakimoto, A.J. Iafrate, S. Tanaka, F. Loebel, N. Lelic, et al., Extreme vulnerability of IDH1 mutant cancers to nad+ depletion, Cancer Cell 28 (6) (2015) 773–784.

[49] S. Turcan, D. Rohle, A. Goenka, L.A. Walsh, F. Fang, E. Yilmaz, et al., IDH1 mutation is sufficient to establish the glioma hypermethylator phenotype, Nature 483 (7390) (2012) 479–483.

[50] A.S. Berghoff, B. Kiesel, G. Widhalm, D. Wilhelm, O. Rajky, S. Kurscheid, et al., Correlation of immune phenotype with IDH mutation in diffuse glioma, Neuro Oncol. 19 (11) (2017) 1460–1468.

[51] G. Kohanbash, D.A. Carrera, S. Shrivastav, B.J. Ahn, N. Jahan, T. Mazor, et al., Isocitrate dehydrogenase mutations suppress STAT1 and CD8+ T cell accumulation in gliomas, J. Clin. Invest. 127 (4) (2017) 1425–1437.

[52] N.M. Amankulor, Y. Kim, S. Arora, J. Kargl, F. Szulzewsky, M. Hanke, et al., Mutant IDH1 regulates the tumor-associated immune system in gliomas, Genes Dev. 31 (8) (2017) 774–786.

[53] D. Capper, S. Weissert, J. Balss, A. Habel, J. Meyer, D. Jager, et al., Characterization of R132H mutation-specific IDH1 antibody binding in brain tumors, Brain Pathol. 20 (2009) 245–254.

[54] C. Choi, S.K. Ganji, R.J. DeBerardinis, K.J. Hatanpaa, D. Rakheja, Z. Kovacs, et al., 2-hydroxyglutarate detection by magnetic resonance spectroscopy in IDH-mutated patients with gliomas, Nat. Med. 18 (4) (2012) 624–629.

[55] C. Choi, J.M. Raisanen, S.K. Ganji, S. Zhang, S.S. McNeil, Z. An, et al., Prospective longitudinal analysis of 2-hydroxyglutarate magnetic resonance spectroscopy identifies broad clinical utility for the management of patients with IDH-mutant glioma, J. Clin. Oncol. 34 (33) (2016) 4030–4039.

[56] D. Capper, M. Simon, C.D. Langhans, J.G. Okun, J.C. Tonn, M. Weller, et al., 2-hydroxyglutarate concentration in serum from patients with gliomas does not correlate with IDH1/2 mutation status or tumor size, Int. J. Cancer 131 (3) (2011) 766–768.

[57] M.E. Hegi, A.C. Diserens, T. Gorlia, M.F. Hamou, N. de Tribolet, M. Weller, et al., MGMT gene silencing and benefit from temozolomide in glioblastoma, N. Engl. J. Med. 352 (10) (2005) 997–1003.

[58] M. Esteller, J.G. Herman, Generating mutations but providing chemosensitivity: the role of O6-methylguanine DNA methyltransferase in human cancer, Oncogene 23 (1) (2004) 1–8.

[59] G. Ciriello, M.L. Miller, B.A. Aksoy, Y. Senbabaoglu, N. Schultz, C. Sander, Emerging landscape of oncogenic signatures across human cancers, Nat. Genet. 45 (10) (2013) 1127–1133.

[60] A. Malmstrom, B.H. Gronberg, C. Marosi, R. Stupp, D. Frappaz, H. Schultz, et al., Temozolomide versus standard 6-week radiotherapy versus hypofractionated radiotherapy in patients older than 60 years with glioblastoma: the Nordic randomised, phase 3 trial, Lancet Oncol. 13 (9) (2012) 916–926.

[61] W. Wick, M. Weller, M. van den Bent, M. Sanson, M. Weiler, A. von Deimling, et al., MGMT testing-the challenges for biomarker-based glioma treatment, Nat. Rev. Neurol. 10 (7) (2014) 372–385.

[62] M.R. Gilbert, M. Wang, K.D. Aldape, R. Stupp, M.E. Hegi, K.A. Jaeckle, et al., Dose-dense temozolomide for newly diagnosed glioblastoma: a randomized phase III clinical trial, J. Clin. Oncol. 31 (32) (2013) 4085–4091.

[63] J.R. Perry, N. Laperriere, C.J. O'Callaghan, A.A. Brandes, J. Menten, C. Phillips, et al., Short-course radiation plus temozolomide in elderly patients with glioblastoma, N. Engl. J. Med. 376 (11) (2017) 1027–1037.

[64] M.E. Hegi, R. Stupp, Withholding temozolomide in glioblastoma patients with unmethylated MGMT promoter-still a dilemma? Neuro Oncol. 17 (11) (2015) 1425–1427.

[65] W. Wick, T. Gorlia, P. Bady, M. Platten, M.J. van den Bent, M.J. Taphoorn, et al., Phase II study of radiotherapy and temsirolimus versus radiochemotherapy with temozolomide in patients with newly diagnosed glioblastoma without MGMTpromoter hypermethylation (EORTC 26082), Clin. Cancer Res. 22 (19) (2016) 4797–4806.

[66] U. Herrlinger, N. Schafer, J.P. Steinbach, A. Weyerbrock, P. Hau, R. Goldbrunner, et al., Bevacizumab plus irinotecan versus temozolomide in newly diagnosed O6-methylguanine-DNA methyltransferase nonmethylated glioblastoma: the randomized GLARIUS trial, J. Clin. Oncol. 34 (14) (2016) 1611–1619.

[67] P. Bady, D. Sciuscio, A.C. Diserens, J. Bloch, M.J. van den Bent, C. Marosi, et al., MGMT methylation analysis of glioblastoma on the Infinium methylation BeadChip identifies two distinct CpG regions associated with gene silencing and outcome, yielding a prediction model for comparisons across datasets, tumor grades, and CIMP-status, Acta Neuropathol. 124 (4) (2012) 547–560.

[68] P. Bady, M. Delorenzi, M.E. Hegi, Sensitivity analysis of the MGMT-STP27 model and impact of genetic and epigenetic context to predict the MGMT methylation status in gliomas and other tumors, J. Mol. Diagn. 18 (3) (2016) 350–361.

[69] I. Vlassenbroeck, S. Califice, A.C. Diserens, E. Migliavacca, J. Straub, I. Di Stefano, et al., Validation of real-time methylation-specific PCR to determine O6-methylguanine-DNA methyltransferase gene promoter methylation in glioma, J. Mol. Diagn. 10 (4) (2008) 332–337.

[70] P. Bady, A.C. Diserens, V. Castella, S. Kalt, K. Heinimann, M.F. Hamou, et al., DNA fingerprinting of glioma cell lines and considerations on similarity measurements, Neuro Oncol. 14 (6) (2012) 701–711.

[71] M.J. van den Bent, L. Erdem Eraslan, A. Idbaih, J.J. de Rooi, P.H. Eilers, W. Spliet, et al., MGMT-STP27 methylation status as predictive marker for response to PCV in anaplastic oligodendrogliomas and oligoastrocytomas. A report from EORTC study 26951, Clin. Cancer Res. 19 (19) (2013) 5513–5522.

[72] T. Kouzarides, Chromatin modifications and their function, Cell 128 (4) (2007) 693–705.

[73] C.D. Allis, T. Jenuwein, The molecular hallmarks of epigenetic control, Nat. Rev. Genet. 17 (8) (2016) 487–500.

[74] J.E. Ohm, K.M. McGarvey, X. Yu, L. Cheng, K.E. Schuebel, L. Cope, et al., A stem cell-like chromatin pattern may predispose tumor suppressor genes to DNA hypermethylation and heritable silencing, Nat. Genet. 39 (2) (2007) 237–242.

[75] A. Mackay, A. Burford, D. Carvalho, E. Izquierdo, J. Fazal-Salom, K.R. Taylor, et al., Integrated molecular meta-Analysis of 1,000 pediatric high-Grade and diffuse intrinsic pontine glioma, Cancer Cell 32 (4) (2017) 520–537 (e5).

[76] P.W. Lewis, M.M. Muller, M.S. Koletsky, F. Cordero, S. Lin, L.A. Banaszynski, et al., Inhibition of PRC2 activity by a gain-of-function H3 mutation found in pediatric glioblastoma, Science 340 (6134) (2013) 857–861.

[77] S. Bender, Y. Tang, A.M. Lindroth, V. Hovestadt, D.T. Jones, M. Kool, et al., Reduced H3K27me3 and DNA hypomethylation are major drivers of gene expression in K27 M mutant pediatric high-grade gliomas, Cancer Cell 24 (5) (2013) 660–672.

[78] J.H. Gibcus, J. Dekker, The hierarchy of the 3D genome, Mol. Cell 49 (5) (2013) 773–782.

[79] W.A. Flavahan, Y. Drier, B.B. Liau, S.M. Gillespie, A.S. Venteicher, A.O. Stemmer-Rachamimov, et al., Insulator dysfunction and oncogene activation in IDH mutant gliomas, Nature 529 (7584) (2016) 110–114.

[80] D. Rohle, J. Popovici-Muller, N. Palaskas, S. Turcan, C. Grommes, C. Campos, et al., An inhibitor of mutant IDH1 delays growth and promotes differentiation of glioma cells, Science 340 (6132) (2013) 626–630.

[81] S. Turcan, A.W. Fabius, A. Borodovsky, A. Pedraza, C. Brennan, J. Huse, et al., Efficient induction of differentiation and growth inhibition in IDH1 mutant glioma cells by the DNMT Inhibitor Decitabine, Oncotarget 4 (10) (2013) 1729–1736.

[82] T. Mazor, C. Chesnelong, A. Pankov, L.E. Jalbert, C. Hong, J. Hayes, et al., Clonal expansion and epigenetic reprogramming following deletion or amplification of mutant IDH1, Proc. Natl. Acad. Sci. U. S. A. 15 (201708914) (2017) 1708914114.

[83] T. Schumacher, L. Bunse, S. Pusch, F. Sahm, B. Wiestler, J. Quandt, et al., A vaccine targeting mutant IDH1 induces antitumour immunity, Nature 512 (7514) (2014) 324–327.

[84] G. Wu, A.K. Diaz, B.S. Paugh, S.L. Rankin, B. Ju, Y. Li, et al., The genomic landscape of diffuse intrinsic pontine glioma and pediatric non-brainstem high-grade glioma, Nat. Genet. 46 (5) (2014) 444–450.

[85] M. Wiese, F. Schill, D. Sturm, S. Pfister, E. Hulleman, S.A. Johnsen, et al., No significant cytotoxic effect of the EZH2 inhibitor tazemetostat (EPZ-6438) on pediatric glioma cells with wildtype histone 3 or mutated histone 3. 3, Klin. Padiatr. 228 (3) (2016) 113–117.

[86] F. Mohammad, S. Weissmann, B. Leblanc, D.P. Pandey, J.W. Hojfeldt, I. Comet, et al., EZH2 is a potential therapeutic target for H3K27M-mutant pediatric gliomas, Nat. Med. 23 (4) (2017) 483–492.

[87] F. Orzan, S. Pellegatta, P.L. Poliani, F. Pisati, V. Caldera, F. Menghi, et al., Enhancer of Zeste 2 (EZH2) is up-regulated in malignant gliomas and in glioma stem-like cells, Neuropathol. Appl. Neurobiol. 37 (4) (2011) 381–394.

[88] N.A. de Vries, J. Hulsman, W. Akhtar, J. de Jong, D.C. Miles, M. Blom, et al., Prolonged Ezh2 depletion in glioblastoma causes a robust switch in cell fate resulting in tumor progression, Cell Rep. 14 (14) (2015) 1057–1062.

[89] A. Borodovsky, V. Salmasi, S. Turcan, A.W. Fabius, G.S. Baia, C.G. Eberhart, et al., 5-azacytidine reduces methylation, promotes differentiation and induces tumor regression in a patient-derived IDH1 mutant glioma xenograft, Oncotarget 4 (10) (2013) 1737–1747.

[90] D.J. Stewart, J.P. Issa, R. Kurzrock, M.I. Nunez, J. Jelinek, D. Hong, et al., Decitabine effect on tumor global DNA methylation and other parameters in a phase I trial in refractory solid tumors and lymphomas, Clin. Cancer Res. 15 (11) (2009) 3881–3888.

[91] H.M. Kantarjian, G.J. Roboz, P.L. Kropf, K.W.L. Yee, C.L. O'Connell, R. Tibes, et al., Guadecitabine (SGI-110) in treatment-naive patients with acute myeloid leukaemia: phase 2 results from a multicentre, randomised, phase 1/2 trial, Lancet Oncol. 18 (10) (2017) 1317–1326.

[92] H. Li, K.B. Chiappinelli, A.A. Guzzetta, H. Easwaran, R.W. Yen, R. Vatapalli, et al., Immune regulation by low doses of the DNA methyltransferase inhibitor 5-azacitidine in common human epithelial cancers, Oncotarget 5 (3) (2014) 587–598.

[93] K.B. Chiappinelli, P.L. Strissel, A. Desrichard, H. Li, C. Henke, B. Akman, et al., Inhibiting DNA methylation causes an interferon response in cancer via dsRNA including endogenous retroviruses, Cell 162 (5) (2015) 974–986.

[94] S. Ropero, M. Esteller, The role of histone deacetylases (HDACs) in human cancer, Mol. Oncol. 1 (1) (2007) 19–25.

[95] E. Galanis, K.A. Jaeckle, M.J. Maurer, J.M. Reid, M.M. Ames, J.S. Hardwick, et al., Phase II trial of vorinostat in recurrent glioblastoma multiforme: a north central cancer treatment group study, J. Clin. Oncol. 27 (12) (2009) 2052–2058.

[96] B.B. Friday, S.K. Anderson, J. Buckner, C. Yu, C. Giannini, F. Geoffroy, et al., Phase II trial of vorinostat in combination with bortezomib in recurrent glioblastoma: a north central cancer treatment group study, Neuro Oncol. 14 (2) (2012) 215–221.

[97] E. Galanis, S.K. Anderson, C.R. Miller, J.N. Sarkaria, K. Jaeckle, J.C. Buckner, et al., Phase I/II trial of vorinostat combined with temozolomide and radiation therapy for newly diagnosed glioblastoma: final results of Alliance N0874/ABTC 02, Neuro Oncol. 22 (10) (2017).

[98] J. Loven, H.A. Hoke, C.Y. Lin, A. Lau, D.A. Orlando, C.R. Vakoc, et al., Selective inhibition of tumor oncogenes by disruption of super-enhancers, Cell 153 (2) (2013) 320–334.

[99] D. Hnisz, B.J. Abraham, T.I. Lee, A. Lau, V. Saint-Andre, A.A. Sigova, et al., Super-enhancers in the control of cell identity and disease, Cell 155 (4) (2013) 934–947.

[100] T.E. Miller, B.B. Liau, L.C. Wallace, A.R. Morton, Q. Xie, D. Dixit, et al., Transcription elongation factors represent in vivo cancer dependencies in glioblastoma, Nature 547 (7663) (2017) 355–359.

8

ARTICLE IN PRESS

O. Gusyatiner, M.E. Hegi

[101] Z. Cheng, Y. Gong, Y. Ma, K. Lu, X. Lu, L.A. Pierce, et al., Inhibition of BET bro-modomain targets genetically diverse glioblastoma, Clin. Cancer Res. 19 (7) (2013) 1748–1759.

[102] C. Pastori, M. Daniel, C. Penas, C.H. Volmar, A.L. Johnstone, S.P. Brothers, et al., BET bromodomain proteins are required for glioblastoma cell proliferation, Epigenetics 9 (4) (2014).

[103] C. Berenguer-Daize, L. Astorgues-Xerri, E. Odore, M. Cayol, E. Cvitkovic, K. Noel, et al., OTX015 (MK-8628), a novel BET inhibitor, displays in vitro and in vivo antitumor effects alone and in combination with conventional therapies in glio-blastoma models, Int. J. Cancer 139 (9) (2016) 2047–2055.

[104] H. Bai, A.S. Harmanci, E.Z. Erson-Omay, J. Li, S. Coskun, M. Simon, et al., Integrated genomic characterization of IDH1-mutant glioma malignant progression, Nat. Genet. 48 (1) (2016) 59–66.

[105] A.F. Hottinger, M. Sanson, E. Moyal, J.-P. Delord, R.D. Micheli, K. Rezai, et al., Dose optimization of MK-8628 (OTX015), a small molecule inhibitor of bromo-domain and extra-terminal (BET) proteins, in patients (pts) with recurrent glio-blastoma (GB), J. Clin. Oncol. 34 (Suppl. 15) (2016) e14123.

[106] X. Lan, D.J. Jörg, F.M.G. Cavalli, L.M. Richards, L.V. Nguyen, R.J. Vanner, et al., Fate mapping of human glioblastoma reveals an invariant stem cell hierarchy, Nature 549 (7671) (2017) 227–232.

[107] B.B. Liau, C. Sievers, L.K. Donohue, S.M. Gillespie, W.A. Flavahan, T.E. Miller, et al., Adaptive chromatin remodeling drives glioblastoma stem cell plasticity and drug tolerance, Cell Stem Cell 20 (2) (2017) 233–246 (e7).

9

1.5 BET inhibitors (BETi) in cancer

1.5.1 BET proteins

Bromodomain and extra-terminal tail (BET) proteins belong to a class of epigenetic proteins called "readers", since their function is to recognize (or read) the acetylated Lysines on histone tails and promote the signal downstream. BET proteins are a family of 4 proteins BRD2, BRD3, BRD4, and BRDT, which is only expressed in the testis.

BET proteins are localized on the promoters and active enhancer elements, they recruit mediator complexes to promote target gene transcription. It was recently shown that enhancer elements are not functioning equally, on the contrary, out of a few thousands of enhancers in a human cell, a few hundred are nick-named super-enhancers that are characterized by high binding of mediator complex and master transcription factors (Fig.1:4) (Hnisz et al., 2013; Loven et al., 2013; Whyte et al., 2013). Super-enhancers are highly cell-type specific and were shown to drive cell identity (Whyte et al., 2013). In cancer super-enhancers were suggested to be responsible for high expression levels of oncogenes and anti-apoptotic factors (Loven et al., 2013).
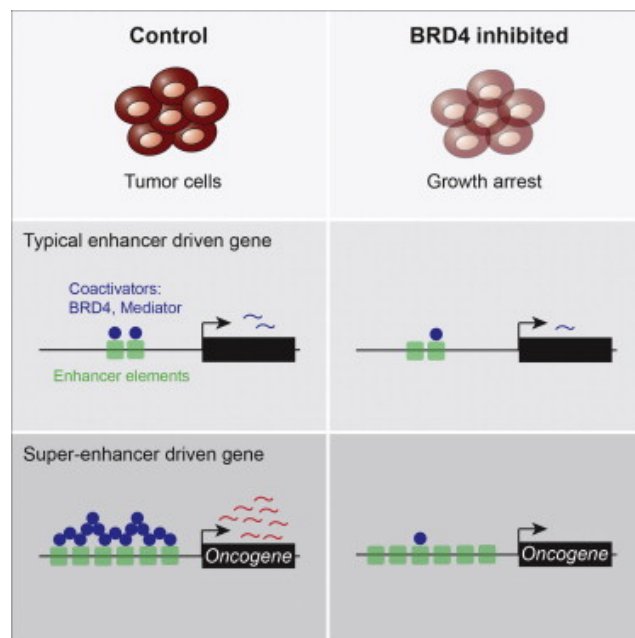
Figure 1:4. BRD4 inhibition represses transcription of super-enhancer driven oncogenes. In cancer cells super-enhancers are occupied by BRD4, mediator complex and master transcription factor regulators. Loven and others showed that super-enhancers may drive transcription of oncogenes, which can inhibited by BETi. Adapted from graphical abstract (Loven et al., 2013).

1.5.2 The rationale behind using BET inhibitors in cancer

BET inhibitors are certainly of interest for the disease called NUT midline carcinoma. There, the BRD4 locus (19p13.1) is fused to the locus of nuclear protein in

testis (NUT) (15q14), which forms a new in-frame transcript that is believed to be a driver event for this malignancy (Fig.1:5). When NUT midline carcinoma cells were treated with BETi JQ1, the cells were terminally differentiating and G1 arrested (Filippakopoulos et al., 2010); whereas in clinic partial remission was reported from phase I trials in NUT midline carcinoma patients (Massard et al., 2016; O'Dwyer et al., 2016; Stathis et al., 2016).
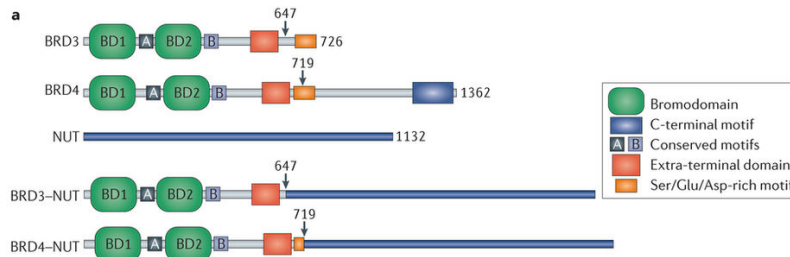
Figure 1:5. Fusions of *BRD3* or *BRD4* with *NUT* in NUT midline carcinoma.
The arrows point at the breakpoints where the fusions occur. Adapted from (Filippakopoulos et al., 2010).

In several cancers genetic screens pointed out at BET proteins to be essential for tumour cell survival (Baratta et al., 2015; Marcotte et al., 2016; Zuber et al., 2011). Some cancers were reported to exhibit high expression level BRD2 and BRD4 (Delmore et al., 2011; Marcotte et al., 2016).

1.5.3 Response to BET inhibitors in the clinic

There is a strong evidence of response to BETi in hematological malignancies. In preclinical studies leukemia and B-cell lymphoma cell lines displayed cell-cycle arrest and apoptosis when exposed to low concentrations of BETi (Berthon et al., 2016; Boi et al., 2015). Some leukemia patients responded well to BETi treatment (2/41 complete remission, and 3/41 partial remission), whereas no biomarkers of response were identified in responders versus non-responders (Berthon et al., 2016). Lymphoma patients showed responses similar to that of leukemia with 2/33 complete remissions, and 1/33 partial remission. Whereas multiple myeloma patients included in the same trial did not show evidence of response (Amorim et al., 2016). One more trial testing a different BETi in Non-Hodgkin lymphoma patients reported 2/44 complete remissions and 1/44 partial remission (Abramson et al., 2015). The mentioned clinical trials were phase I and therefore tested the compounds in a dose escalation setting with 3/10 (Massard et al., 2016) partial responses. So, the response was limited to 20-30% of patients. Moreover, all the patients relapsed during

the treatment (O'Dwyer et al., 2016). A bigger study in a defined cohort of patients with confirmed NUT-BRD4 fusions should be done in order to address the efficacy of BETi in NUT midline carcinoma.

In other solid cancers, reported results from clinical trials for BETi are more pessimistic with 1/36 prostate cancer with a partial response (Massard et al., 2016), and no evidence of response reported in lung cancer (Massard et al., 2016) and in GBM (Hottinger et al., 2016), the latter was in part performed in CHUV (OTX015 drug).

1.5.4 Reported clinical toxicities of BETi

The toxicities with BETi are somewhat expected, since BET proteins are essential for transcription; and both *BRD2* and *BRD4* knockout mice are embryonically lethal (Gyuris et al., 2009; Houzelstein et al., 2002; Shang et al., 2009). Moreover, mice treated with BETi were reported to lose their long-term memory (Korb et al., 2015) and to develop autism-like syndrome (Sullivan et al., 2015). Lastly, male mice treated with BETi are infertile, since one of the BETi targets, BRDT, is essential for spermatogenesis (Matzuk et al., 2012).

In the clinic, cancer patients treated with various BETi commonly exhibited thrombocytopenia, an abnormally low levels of platelets in the blood. The other reported toxicities included anemia, headaches, fatigue, gastrointestinal tract toxicities, diarrhea and an increase of bilirubin (reviewed in (Stathis and Bertoni, 2017)).

1.6   Aims of the project

Glioblastoma remains to be largely incurable with limited treatment options available. It has become clear that single agent drugs fail in clinical trials, and new strategies for combination therapies are urgently needed. In this project we aim at targeting enhancer elements, which are crucial for epigenetic regulation of gene expression, in GBM models in order to identify novel drug combination strategies. The project entailed:

1. Characterization of cellular response to pharmacological BET inhibition *in vitro*
2. Identification of gene expression signatures induced by JQ1 in an *in vitro* glioblastoma sphere model
3. Validation of obtained signatures
4. Prediction of compounds that can used in combination with BETi
5. Testing the predicted drug combinations *in vitro* and *in vivo*

1.7   Advantage of Glioma sphere cell lines (GS-lines)

Most of the experiments in this project were performed with a 3D model of glioblastoma GS-lines that were patient derived and established in our laboratory. GS-lines grow in neurobasal medium without FBS and form cell clusters or gliomaspheres. GS-lines represent a better model of GBM compared to regular adherent cell lines for multiple reasons. First, GS-lines grow very invasively when injected orthotopically in immunocompromised mice. Moreover, GS-lines conserve certain tumour stem-cell properties, and *EGFR* amplification that is normally present in 50% of GBMs, but for unknown reasons is lost among adherent GBM models (Balvers et al., 2013). Moreover, GS-lines represent the molecular subtypes of GBM. The experiments were performed with 6 GS-lines, and every experiment was performed in LN-2683-GS. Importantly, LN-2683-GS was derived from a recurrent GBM, the patient was treated with TMZ/RT-TMZ in first line, hence representing a "naturally resistant" model (Table 6:1).

Chapter 2   Materials and Methods

2.1   Cell culture

Glioblastoma derived sphere lines (GS) LN-2207-GS, LN-2683-GS, LN-2540-GS, LN-2669-GS were established in our laboratory, molecularly characterized (Bady et al., 2012; Kurscheid et al., 2015; Sciuscio et al., 2011), and authenticated (Bady et al., 2012). The corresponding GEO accession numbers are GSE60274, GSE108098, and GSE104291 for DNA methylation, aCGH, and gene expression data, respectively. LN-3704-GS, LN-3708-GS, and LN3397 were recently derived in our laboratory (authentication pending). LN-18, LN-428 were established in our laboratory (Bady et al., 2012; Ishii et al., 1999). U87MG, PEO1, and OVCAR3 originate from ATCC. BS-153 originates from the laboratory of Adrian Merlo. U87MG, LN-18, LN-428, and BS-153 were grown in DMEM Glutamax (Gibco) with 5% FBS (Hyclone or PAA). Ovarian cancer cell lines OVCAR3 and PEO1 were grown in RPMI (Gibco) supplemented with 10% FBS (PAA).

GS-lines were cultured under stem-cell conditions in Dulbecco's modified Eagle medium/F12 containing B27 supplement and 20ng/ml of epidermal growth factor (EGF, Peprotech) and 20ng/ml of fibroblast growth factor (FGF, Peprotech). For setting up experiments, the spheres were separated into a single cell suspension by treatment with Accutase (Gibco), followed by separation with fire treated Pasteur pipettes with cotton plugs for a maximum of 10 minutes. The cell counter (EVE) was used to count live cells using tryptan blue exclusion assay. The cell density used was 1 M of live cells per 9 ml of B27 media unless stated otherwise.

For Interferon priming of GS-lines, the interferon-alpha (Peprotech or PBL assay Science) was added to the final concentration of 1000 units/ml, and interferon-gamma (GenWay Biotech) to the final concentration of 20 ng/ml. B27 medium was added to respective control dishes.

Mycoalert kit (Lonza) was used for routine mycoplasma contamination testing.

2.2   JQ1 and TSA treatment

(+)-JQ1 and its inactive enantiomer (-)-JQ1 (ApexBio Technology LLC) were dissolved to 10mM in DMSO, stored at -20 C aliquoted. Trichostatin A (Sigma) was a ready-made solution supplied as 5mM in DMSO and stored aliquoted at -20C. The drugs were added to the GS-lines cells 3 days after seeding to allow the sphere formation. For long (10 days) exposures, the media and drugs were refreshed on day 6.

2.3   Senescence-associated β-Gal assay

120,000 of U87MG cells for JQ1, and 80,000 cells for DMSO per well were seeded in 12-well plates. The next day 1μM (+)-JQ1, (-)-JQ1 or DMSO was added for 72 hours. Plates were stained for the activity of β-Gal using the β-Galactosidase staining Kit (Biovision) according to manufacturer's instructions, and incubated overnight at 37°C. Imaging of 5 random fields per condition was performed by stereomicroscope (Leica M205FA). The quantification of proportion of β-Gal positive cells was done manually with ImageJ by two researchers independently.

2.4   Immunofluorescence of GS-lines

Single cells of LN-2683-GS were seeded at density 500,000 cells per 3ml, and one day later, 1μM JQ1 or DMSO was added. The spheres were fixed and permeabilized 10 day after drug addition for 3 hours at 4°C in a fixing/permeabilizing buffer (4% Formaldehyde, 1% Triton X-100). The spheres were then washed in 1X PBS/0.1% Tween and blocked in blocking buffer (PBS/5% donkey serum/0.1%Tween) for 60 minutes at room temperature. Incubation with primary antibodies was done overnight at 4°C in blocking buffer with the anti-TUJ1 antibody (Cell Signalling, 1:400). The spheres were then washed once in PBST and incubated with fluorochrome-conjugated anti-rabbit Alexa 647 (Abcam, 1:500). Then the spheres were washed with PBS and resuspended in 15 μl of mounting medium Vectashield containing DAPI (Vector), and mounted on glass slides. Image acquisition was performed with 64x objective of Leica SP5 tandem confocal microscope. For the figure brightness and contrast of images were adjusted equally in JQ1 and DMSO in Photoshop CC (2015) to increase visibility for the reader.

2.5   Cell viability assay

2.5.1   Cell viability assay of adherent GBM cell lines

4000 cells/well of LN-18, LN-428, and U-87MG; or 4500 cells/well of BS-153 were seeded in 100 µl of complete medium. Next day (+)-JQ1, (-)-JQ1 was added to the plate as a 10-point serial dilution 1:3 starting form 30 µM. For 0% viability control cytotoxic concentration of of Actinomycin D (1 µg/ml) was added, and for 100% viability just DMSO. 72 hours later medium was aspirated and 10% Cell Titer Blue in complete medium was added. Plates were incubated for 1 hour at 37C. And cell viability was measured with Tecan plate reader. The data was analyzed with Graphpad Prism 6 using drug-response curve fitting algorithm with variable Hill slope.

2.5.2   Cell viability assay of GS-lines

3750 cells of LN-2207-GS, LN-2540-GS, and LN-2683-GS per well of 96-well plate were plated in 75 µl in B27 media. 3 days after seeding JQ1, (-)-JQ1 was added to the plate in 75 µl. 10-point serial 1:2 dilution starting with 30 µM was used. After 72 hours 20 µl of Cell Titer Blue was added and incubated for 4 hours at 37C. Fluorescence was measured by Tecan plate reader and data was analyzed in GraphPad Prism 7. The wells without drugs were set to 100% viability and wells treated with lethal concentration of Actinomycin D (1µg/ml) were set to have 0% of the viability. A curve-fitting algorithm with variable Hill slope was applied to the intensity values to derive IC50 values. The experiment was repeated at least 3 times for each GS-line.

2.6   Drug combination assay

3750 cells of LN-2683-GS and LN-3708-GS per well of 96-well plate were plated in 75 µl in B27 media. 3 days after seeding the drugs were added to the plate in 75 µl four each drug. 7-point serial 1:2 dilution starting with 20 µM was used. The drugs were added as in a chessboard pattern (8 by 8), so that every concentration of JQ1 is tested with every concentration of TSA. DMSO was used as a control.

After 5 days 22.5 µl of Cell Titer Blue was added and incubated for 4 hours at 37 C. For 10 days the cells were set as above, but JQ1 and TSA were added at a serial dilution starting from 2µM. After 5 days the plate was centrifuged for 5 min at 300g and 150 µl of the supernatant was removed from each well. JQ1 and TSA were

added in 75 µl of B27 each in the corresponding concentration. Fluorescence was measured with Tecan plate reader and data was analyzed in R. The package synergyfinder was used to access the combination score (combination of Lowe and Bliss combination indexes) (He et al., 2016). The experiment was repeated at least three times for each GS-line and both time points.

2.7   Neurosphere Formation Assay

The protocol was adapted from (Cheng et al., 2013). Briefly, single cells were seeded into a 48-well plate with 100 cells per well in 100µl F12/B27 medium containing EGF and FGF (LN-2207-GS, LN-2540-GS, LN-2683-GS) and with 1000 cells per well for LN-2669-GS. Then, JQ1 diluted in 100µL F12/B27 to a final concentration of 0, 0.25, 0.5, 1, 2 or 4 µM was added, with 4 replicates per condition. EGF and FGF to a final concentration of 20ng/ml in 2µl F12/B27 were added to each well on day 8 and 15. The spheres with a diameter exceeding 50µm were counted after 14 and 21 days. The experiment was repeated 3 times.

2.8   RNA Extraction, qRT-PCR

Total RNA was isolated from the cell lines with the ReliaPrep^{TM} RNA cell miniprep kit (Promega, WI, USA). mRNA from xenografts was isolated with RNeasy Mini Kit (Qiagen). The quantity and quality of the extracted RNA was assessed by Nanodrop (Thermo Fisher Scientific, Waltham, MA, USA) and by Fragment Analyzer for xenografts samples. DNAse treatment was performed with RapidOut DNA Removal Kit (Thermo Fisher Scientific).

cDNA was synthesized with PrimeScript RT reagent kit (Takara, Kyoto, JPN). Real-time qPCR was done using the Kapa Sybr® Fast Universal qPCR kit (Kapa Biosystems, MA, USA), on a Rotor Gene 6000 real-time PCR system (Qiagen, Venlo, NLD). The qPCR conditions were the following: 95°C (100s) followed by 40 cycles at 95°C (3s) to 60°C (20s). The quality of the products was controlled with the melting curve. The expression levels were normalized to *GAPDH*, and to geometrical mean of *hGAPDH* and *C1orf43* for cDNA derived from mouse xenografts. The primers were designed with Universal Probe Library System Assay Design (Roche). Gene-specific primers used in this study are in Table 6:2.

2.9   Protein Extraction

Cells were collected by centrifugation for GS-lines or by scraping for adherent cells, washed with PBS, snap-frozen. The pellets were lysed in RIPA buffer (50mM Tris-HCL, 150mM NaCl, 2mM EDTA, 1mM EGTA, 1% Triton, 0.5mM Phenylmethyl-sulfonyl fluoride), supplemented with protease inhibitor cocktail (Roche) and PhoS-TOP (Phosphatase Inhibitor Cocktail, Roche). The pellets were lysed by passing them 5 times through a 25-gauge needle. The proteins were then separated from the cell debris by centrifugation at 15,000g for 15 minutes at 4°C. For Nuclear and Cyto-plasmic fractions extraction NE-PER kit (Thermo Scientific) was used with the follow-ing modifications. Nuclei were lysed in 30µl NER buffer supplemented with protease inhibitor cocktail (Roche) and PhoSTOP (Phosphatase Inhibitor Cocktail, Roche) and sonicated on ice at 30% amplitude for 5 sec or until homogenized with Bandelin Sonoplus Sonifier with 2.5mm needle. Protein quantification was done using the Bradford assay (Bio-Rad, Hercules, USA) with BSA as a standard in a 96-well plate.

2.10   Western Blot

Western Blot was performed as described previously (Lenain et al., 2015). Briefly, 20-40 µg of protein extracts were separated on SDS polyacrylamide gradient (4-20%, Biorad) or homemade gels of desired concentration. The proteins were then transferred to nitrocellulose 0.45µm blotting membrane (GE, Healthcare Life Scienc-es or Biorad). Equal loading was verified with Ponceau S (Sigma) and membranes were blocked for 1 hour in 5%BSA (ApexBio) or 5% non-fat skimmed milk (Migros) at room temperature. The membranes were probed in 5% milk or 5% BSA overnight at 4°C with the following antibodies: anti-BRD4 (Bethyl Laboratories, A301, 1:7,000), anti-PARP (Cell Signalling, #9542, 1:5000), anti-α-tubulin (Sigma, T5168, 1:10,000), anti-C-MYC (Abcam, #32072, 1:10,000), anti-TUJ1 (Cell Signalling, #5568, 1:10,000), anti-GAPDH (Sigma, #G9545, 1:10,000), anti-Histone H3 (Abcam, ab1791, 1:1,000), anti-PD-L1 (Cell Signalling, #13684, 1:2,000), anti-STAT1 (Cell Signalling, #9172, 1:1,000), anti-pSTAT1 (Cell Signalling, 7649, 1:1,000), anti-Vinculin (Sigma, V91131, 1:4,000).

2.11 Cell cycle analysis

Spheres were dissociated, and single cells were seeded into a 6-well plate with 0.3M cells per well (LN-2207-GS) and 0.45M cells per well (LN-2683-GS), in 3ml F12/B27 supplemented with 20 ng/ml of EGF and FGF. (+)-JQ1, (-)-JQ1 or DMSO diluted in 1ml F12/B27 was added to the wells on day 4 for a final concentration of 1µM. Cells were incubated with BrdU for 1 hour at 37C on day 5 and 10 after drug addition. For the condition "5 days on drug / 5 days off drug", the medium of the cells was changed on day 6 to a normal F12/B27 medium. The cells were stained with anti-BrdU antibody conjugated with FITC and 7-AAD using BD Pharmingen™ BrdU Flow Kits (BD Biosciences). Acquisition was done with FACS (Calibur) on up to 1M cells. Cell cycle distribution was analyzed with FlowJo software (FlowJO LLC, version 7).

2.12 RNA sequencing and differential expression analysis

LN-2683-GS cells were seeded at a density of 0.35 M per 6-cm petri dishes in 3 ml of B27. 2 days after (+)-JQ1 or DMSO were added to a final concentration of 1µM. The cells were lysed in RLT buffer and snap-frozen at 4, 12, 24, and 48 hours. Untreated cells in quadruplicate at baseline (0 hours) were harvested directly without treatment.

For RNA sequencing Qiagen RNeasy Mini Kit was used according to the manufacturer's instructions. Quality of RNA was assessed by Fragment Analyzer. The library preparation was performed with TruSeq Stranded Total RNA Library Prep Kit (Illumina). Samples were multiplexed as 7 samples per lane and ran in single read mode on Illumina HiSeq 2500. The preprocessing of RNAseq data was performed following the standard pipeline and recommendations from bcbio-nextgen (version 0.8, http://bcbio-nextgen.readthedocs.org/en/latest/). After trimming of adapter and polyA; and standard quality control checking, the alignment to human reference genome (assembly GRCh37) was performed by STAR aligner (version 2.4.0). Differential Expression was performed with edgeR package (version * 3.12.0) using model with full interaction between treatment and time. Genes with Bonferroni adjusted P-values<0.001 were considered differentially expressed. Gene set enrichment analysis was performed with PGSEA package (version* 1.44.0) and GAGE package (version * 2.20.1) using and The Molecular Signatures Database (MSigDB

version 5, Broad Institute). Hallmark gene set H collection was used for primary assessment and the results from running enrichment on all 8 collections are reported here. The gene sets with FDR adjusted P-value <0.05 were considered significant.

2.13 Analysis of reproducibility of cluster G12 in TCGA dataset

To estimate the similarity among the distance matrices of NCHaffy (Murat et al., 2008), TCGAaffy, and TCGArnaseq (Brennan et al., 2013) expression data frames, we used the RV-coefficient (Escoufier, 1973). Pairwise RV coefficient permutation tests were performed on the distance matrices with R package ade4 (Chessel et al., 2004).

2.14 Analysis of *CD274* expression in glioma cell lines

To assess the expression of *CD274* in glioma cell lines we used affymetrix expression data from The Cancer Cell Line Encyclopedia (CCLE) (Barretina et al., 2012). Expression values were RMA normalized and the background was corrected with R package affy. Results are shown for the most variable probe 227458_at.

2.15 Chromatin Immunoprecipitation (ChIP)

LN-2683-GS cells were plated at 2.2M per 9 ml of B27 in 10 cm petri dishes. Three days after plating 1µM JQ1, or 0.1% DMSO as control was added to the plate together with 1000 Units/ml of Interferon-alpha (Peprotech). The cells were harvested 2 hours after and washed with PBS. ChIP was performed using iDeal ChIP-seq kit for Histones x24 from Diagenode. Briefly, cells were cross-linked by adding methanol free formaldehyde (Thermo Fisher Scientific) to a final concentration of 1% in PBS for 8 minutes, then 125 mM Glycine was added for 5 minutes to quench the formaldehyde. After the cells were kept on ice and washed twice with 1ml cold PBS. The pellets were snap frozen and kept in -80C until further use. Then, the cell membranes were lysed and nuclei extracted. The shearing was performed in 200µl iS1 shearing buffer supplemented with protease inhibitors (Diagenode or Roche) and 20mM Sodium Butyrate (Sigma). The chromatin was sheared on ice with 50% amplitude at 10x 30 second cycles of 1 sec on /1 sec off, with 2 minute incubation on ice in between by Bandelin Sonoplus Sonifier with 2.5mm needle. The chromatin was cleared by 10 minutes centrifugation at 16,000g at 4C. 50µl of the supernatant were

kept for sheared chromatin analysis and the rest (150µl) was snap-frozen for further immunoprecipitation.

For sheared chromatin analysis, RNA was eliminated by adding 1µl of RNAse (10 mg/ml, Sigma) and 3.125 µl of 5M NaCl and incubating for 1 hour at 37 C. Then the sample was reverse cross-linked by overnight incubation at 65 C. DNA was extracted with phenol/chloroform/isoamyl alcohol and precipitated in ethanol at -80C. The ethanol was removed and the dried pellets were dissolved in 15µl TE buffer. 10 µl were used for 1.5% agarose gel analysis and 5 µl for Fragment analyzer. The samples with the fragment length100-600 bps were used for subsequent immuno-precipitation.

2.16   Stereotactic Orthotopic Xenograft Injections into the Mouse Brain

6-8 weeks NOD scid gamma knockout (NSG (Jax name: NOD.Cg-Prkdcscid Il2rgtm1Wjl/SzJ)) males born in-house were used. The injection was performed as described in (Vassallo et al., 2016), which was sterotactically in the striatum (coordinates: bregma 0.5mm anterior, 2mm lateral and 3mm ventral). 100,000 U87MG cells in 5µl of HBSS with phenol red, no calcium, no magnesium (Thermo Fisher Scientific) were injected with a micro pump in 1 minute. The syringe was slowly (1min) lifted 5 minutes after the injection to avoid cell reflux. The end-point criteria were either 15% weight loss, or the presence of neurological symptoms (paresis, ataxia, rotation).

(+)-JQ1 was dissolved in DMSO at 100 mg/ml and then diluted 1:10 in 10% (2-Hydroxypropyl)-b-cyclodextrin (Sigma). The control was DMSO dissolved 1:10 in 10% (2-Hydroxypropyl)-b-cyclodextrin (Sigma). The mixture was sonicated at 37C for 5 minutes to dissolve and injected i.p. at 1% of the body weight (final concentration 100 mg/kg). 4 hours later mice were sacrificed by CO_2 inhalation.

2.17   Tissue Processing and immunohistochemistry

The fresh mouse brain was cut using a brain mold. The central part of the brain (5mm) was frozen in O.C.T. compound (Tissue-Tek) in isopentane on liquid nitrogen. Hematoxylin and Eosin (H&E) staining of frozen block was done to determine the location of the tumour in the mouse brain and used as a reference to

macrodissect the tumour from mouse brain with Cryostat. 15 mg of frozen tissue were used for subsequent mRNA isolation.

The remaining tissue was fixed in 4% formalin for 4 hours, rinsed with water and transferred to 70% ethanol. The tissue was dehydrated through the series of ethanol baths in a tissue processor and embedded in paraffin. The sections were cut and human PD-L1 staining PD-L1 was performed with anti-PD-L1 antibody (clone SP263, Roche Ventana, #790-4905) was used for. H&E staining of adjacent sections was performed to verify the tumour location.

2.18   Statistical analysis of experiments

Statistical analysis of the experiments was performed using GraphPad Prism 7 Software and with R-3.2.2 (R Core Team, 2015). Bioconductor (Gentleman et al., 2004) packages for specific tasks are listed in the relevant sections. The Student t-test was used to compare the variables between two groups, and 2-way ANOVA to compare the variables for more complex experimental design. P-values lower than 0.05 were considered statistically significant. Significance is indicated with asterisks: 1 asterisk (*) meaning that $P < 0.05$, 2 (**) when $P < 0.01$, 3 (***) when $P < 0.001$, and 4 (****) when $P < 0.0001$. Data are presented as mean values, error bars represent standard deviation unless indicated otherwise.

Chapter 3   Results

3.1   Effects of BETi JQ1 on cell viability of GBM cell lines

First, we assessed cell viability of a panel of adherent GBM cell lines in response to a small-molecule inhibitor of BET proteins ((+)-JQ-1, hereafter JQ1) (Fig. 3:1 A, B). As a result, cell viability of 4 tested GBM cell lines was reduced upon 72-hour exposure to JQ1, and remained constant when treated with inactive enantiomer (-)-JQ1. U87MG showed slightly higher sensitivity to JQ1 than LN-18, LN-428 and BS-153. Even when GBM cells were treated with the highest concentration 30 μM JQ1, a proportion of cells visually appeared as viable. With this observation and the reports published in other cancer cell lines (Delmore et al., 2011; Tolani et al., 2014), we tested whether U87MG cells exhibited β-Galactosidase activity, a marker of cellular senescence (Kuilman et al., 2010) (Fig. 3:1 C, D). Indeed, we detected an increase of the fraction of β-Gal positive cells exposed to (+)-JQ1 compared to inactive enantiomer (-)-JQ1 or DMSO.
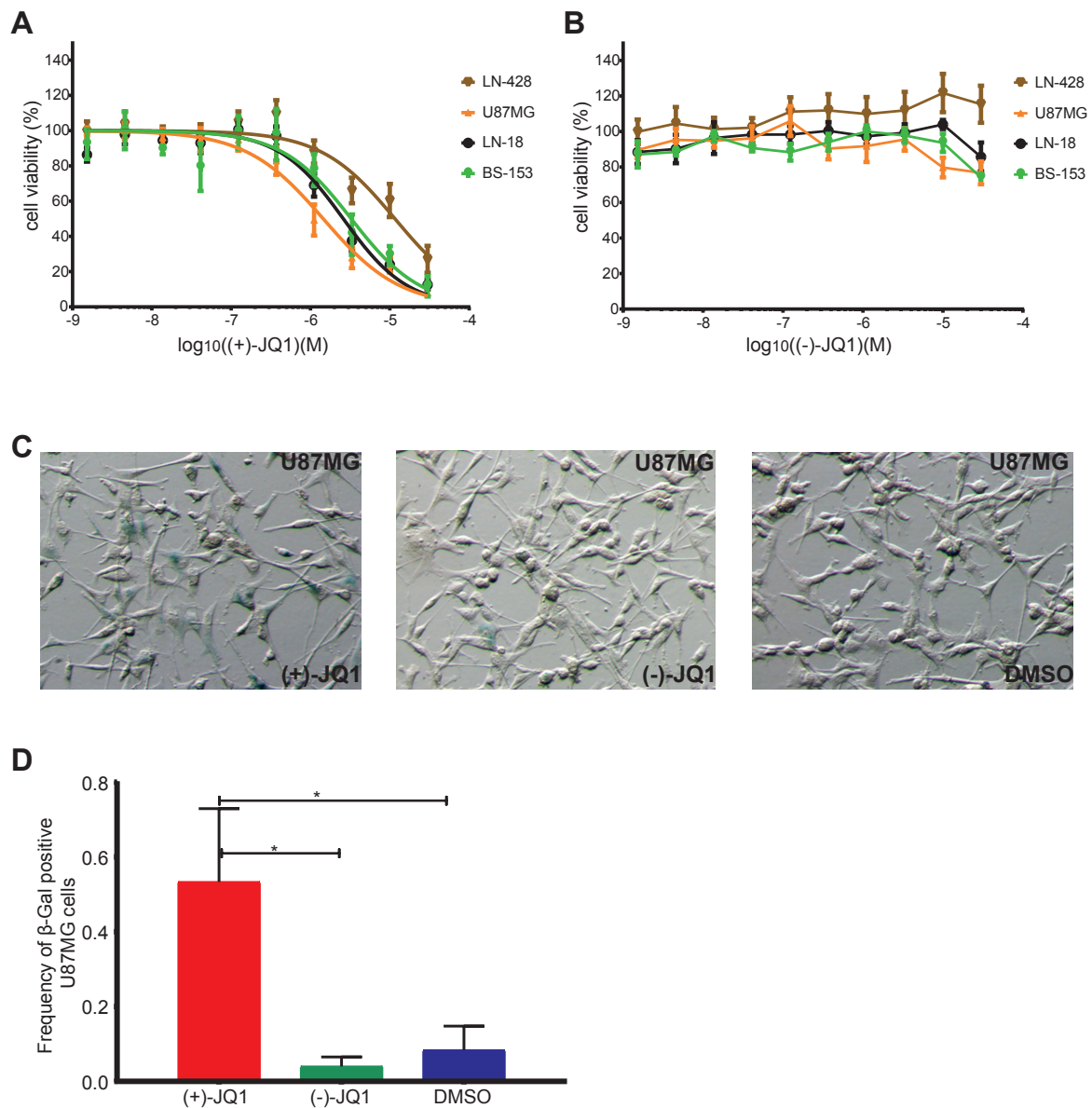
Figure 3:1. JQ1 decreases cell viability of adherent GBM cell lines, and induces β-Galactosidase in U87MG.

(A) Cell viability of LN-18, LN-428, BS-153, and U87MG was determined after 72-hour incubation with 3-fold serial dilutions of (+)-JQ1 and normalized to DMSO treated control. Data represent a mean of 3 independent experiments; error bars are SEM.

(B) The same as (A) for (-)-JQ1.

(C) Representative microphotographs of Senescence-Associated β-Gal assay. U87MG cells were treated with 1μM (+)-JQ1, (-)-JQ1 or DMSO for 72 hours.

(D) Quantification of Senescence associated β-Gal assay for U87MG cells. The results represent a summary of 3 independent experiments. Error bars are SD, significance determined with unpaired one-sided t-test.

3.2   Effects of JQ1 treatment on glioma sphere lines

Next, we focused of glioma sphere lines (GS-lines) that, in our opinion, represent a better model of GBM (see chapter 1.7). Of note, LN-2540-GS and LN-2669-GS were contaminated with mycoplasma, whereas all the other cell lines were negative for mycoplasma. Cell viability of three tested GS-lines was reduced after 72-hour exposure to (+)-JQ1 and remained unchanged when treated with its inactive enantiomer (-)-JQ1 (Fig.3:2 A). There was no difference in response between the tested GS-lines; half maximal inhibitory concentrations (IC_{50}) were about 15 µM for all three tested GS-lines. When compared to published data of cancer cell lines (IC_{50} from 3nM to 6 µM) treatment (Todaro et al., 2014) or to previously obtained data with adherent GBM cell lines, GS-lines seemed to be more resistant to JQ1 (Table 3:1, Fig. 3:2 A). The observed reduced sensitivity could have been due to the fact that GS-lines are slow-growing with population doubling times between 4-15 days (Table 6:1), which is longer than most of the commonly used cancer cell lines.

Cell line	(+)-JQ1 IC_{50}
U87MG	1.4 µM
LN-18	2.6 µM
BS-153	3.3 µM
LN-428	11.6 µM
LN-2683-GS	18.6 µM
LN-2540-GS	8.9 µM
LN-2207-GS	5.8 µM

Table 3:1. IC_{50} values (concentrations of JQ1 that give half-maximal inhibition) of a panel of glioblastoma cell lines including sphere lines.

Next, we focused on more long-term effects and performed neurosphere formation assay in the presence of JQ1 (serial dilution in DMSO starting from 4 µM) (Fig.3:2 B, D). Here we set the cells as single cell suspension and added the drugs on the same day before neurospheres were formed. Twenty-one days after seeding, we counted the number of spheres and observed that JQ1 impaired the capacity of gliomasphere formation of all four tested GS-lines, but to different extend. As little as 0.25µM JQ1 was sufficient to reduce 4 times the number of spheres of LN-2207-GS, while for LN-2669-GS a concentration of 1µM was required. Importantly, 2µM of JQ1 was sufficient to completely block sphere formation in 3 of 4 tested GS-lines.

Then we assessed whether decreased cell viability and sphere formation were due to cell cycle arrest or programmed cell death. The proportion of cells in S-phase, as determined by the BrdU incorporation assay (Fig.3:2 E) was lower in LN-2207-GS cells treated with 1µM JQ1 for 5 days, whereas we did not observe difference in cell cycle distribution for LN-2683-GS. The effect on the reduced number of cells in S-phase was fully reversible upon drug withdrawal after 5-days of treatment in LN-2207-GS, indicating the absence of cell cycle G1 arrest that was previously associated with BETi treatments in cancer models (Boi et al., 2015; Delmore et al., 2011). Finally, we observed that 5-day treatment with 1µM JQ1 was sufficient to induce apoptosis in LN-2207-GS and LN-2683-GS evaluated by the presence of band of cleaved poly (ADP-ribose) polymerase (c-PARP).

3.3 MYC is down regulated upon pharmacological BET inhibition

Since MYC downregulation had been previously associated with pharmacological BET inhibition (Delmore et al., 2011), we examined the expression of MYC on mRNA and protein levels after 48-hour treatment of GS-lines with 1µM JQ1. As a result, *C-MYC* and *N-MYC* levels were reduced in all glioma models tested (Fig.3:2 F-H). Moreover, the protein levels of C-MYC were significantly reduced upon treatment with JQ1 in 3 tested GS-lines and not affected by (-)-JQ1. While MYC overexpression or hyper activation is believed to be one of the most common drivers of cancer, GBM is certainly not a MYC-driven malignancy. Indeed, *MYC* is not commonly amplified in GBM. And only 16 cases out of 129 IDH wild type GBMs appeared to have copy number alterations or mRNA up regulation according to TCGA (http://www.cbioportal.org/, (Gao et al., 2013)).
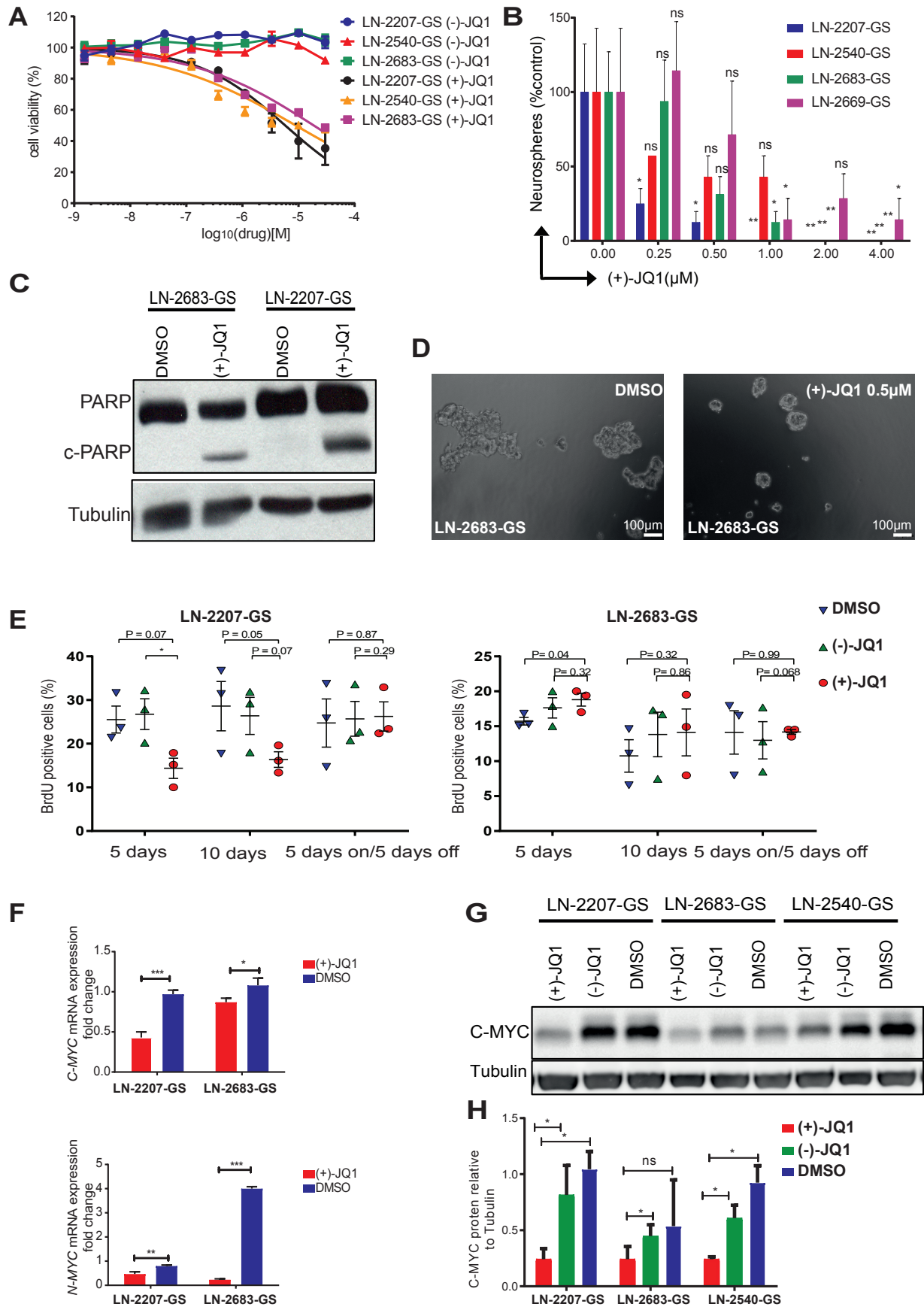
Figure 3:2. Effects of JQ1 on glioma sphere lines.

(A) Cell viability of LN-2207-GS, LN-2540-GS, and LN-2683-GS was determined after 72 hour incubation with 3-fold serial dilutions of (+)-JQ1 and (-)-JQ1 and was normalized to DMSO treated control. Data represent a mean of 3 independent experiments; error bars are SEM.

(B) Quantification of neurosphere formation assay of LN-2207-GS, LN-2540-GS, LN-2683-GS, and LN-2669-GS. The spheres with a diameter larger than 50 µm were counted 21 days after addition of indicated concentration of (+)-JQ1. Data represent the mean of 4 wells; error bars are SD. Representative of at least 3 independent experiments. Reported P-values are determined by 2-way ANOVA and adjusted to account for multiple testing using statistical hypothesis Dunnett test.

(C) Western blot for total PARP, cleaved PARP (c-PARP) and Tubulin (loading control) of lysates of LN-2683-GS and LN-2207-GS 10 days after treatment with 1µM (+)-JQ1 or DMSO control.

(D) Representable image of neurosphere formation assay taken after a 21-day incubation of LN-2683-GS with 0.5µM (+)-JQ1 and DMSO control.

(E) BrdU incorporation assay of LN-2207-GS and LN-2683-GS treated with 1µM (+)-JQ1, (-)-JQ1, and DMSO. For 5 days on/5 days off condition the medium was changed to DMSO containing normal medium after 5 days of treatment. Data represent summary of 3 independent experiments. *, P-value<0.05 by paired t-test.

(F) qRT-PCR analysis of *C-MYC* and *N-MYC* gene expression after 48 hours treatment with 1µM (+)-JQ1. The data represent one of at least 3 independent experiments; P-values were determined by paired t-test.

(G) Western blot analysis of C-MYC and Tubulin loading control of GS-lines treated with 1µM (+)-JQ1, 1µM (-)-JQ1 or DMSO for 48 hours.

(H) Densitometry of Western blots (G). Data represent mean of 3 independent experiments, error bars are SD. *, P-value<0.05, by paired t-test.

3.4   BET inhibition induces differentiation-like phenotype in LN-2683-GS

Interestingly, we observed that after as short as 24-hour incubation with 1μM JQ1, LN-2683-GS tends to become adherent and the cells form protrusions (Fig.3:3 A). This observation raised the question whether LN-2683-GS undergoes differentiation upon pharmacological BET inhibition. First, we assessed markers of neuronal (TUJ1, neuronal specific class III beta-tubulin) and astrocytic (GFAP, glial fibrillary acidic protein) differentiation by qRT-PCR after 24-hour treatment with 1μM JQ1. And we observed that *TUBB3* (gene coding for TUJ1) was almost 4 times up regulated after 24-hour treatment with 1μM JQ1 compared to DMSO control (Fig.3:3 B). On the protein level elevation of TUJ1 was detected 5 and 10 days after JQ1 addition on Western Blot (Fig.3:3 C) and confirmed by Immunofluorescence 10 days after JQ1 addition (Fig.3:3 D). Induction of the neuronal specific beta-tubulin III indicates that JQ1 may stimulate a program of differentiation into neuron-like cells that was not reversible upon drug withdrawal after 5 days (data not shown).
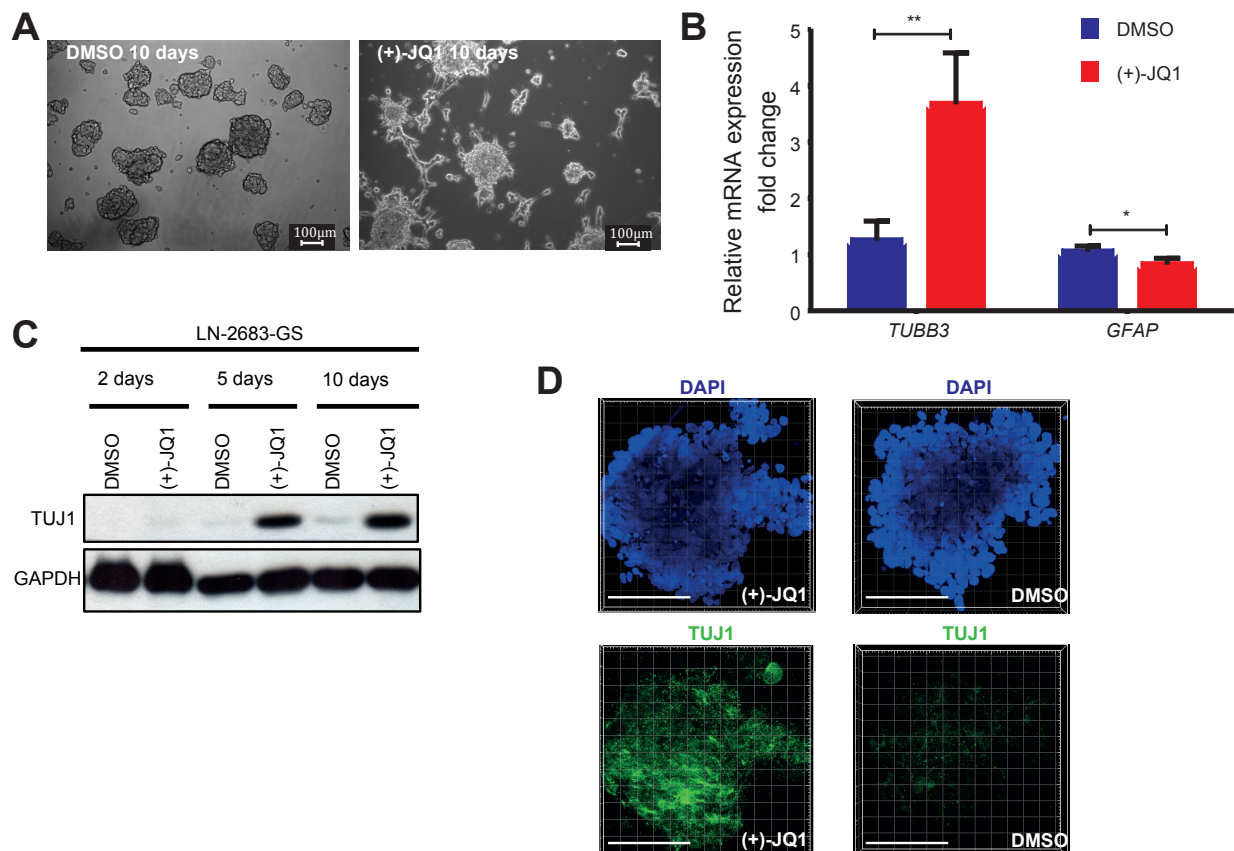
Figure 3:3. JQ1 induces differentiation-like phenotype in LN-2683-GS.

(A) Representative microphotographs of LN-2683-GS treated with JQ1 or DMSO control for 10 days.

(B) qRT-PCR analysis of *TUBB3* (TUJ1) and *GFAP* after 48 hour treatment with 1µM (+)-JQ1 or DMSO control. Data represent mean of 4 independent experiments, error bars are SD, and P-values were determined by paired t-test.

(C) Western blot analysis of TUJ1 and loading control GAPDH of lysates of LN-2683-GS treated with 1µM (+)-JQ1 for 2, 5, and 10 days.

(D) Representative immunofluorescence images of LN-2683-GS spheres after 10-day treatment with JQ1, or with DMSO stained with anti-TUJ1 antibody (green) and DAPI (blue). Scale bar is 100 µm.

3.5 BET protein inhibition causes extensive changes of transcriptome

In order to identify the pathways that are affected by pharmacological BET inhibition we performed differential gene expression profiling by RNA-sequencing (Fig.3:4 A). First, we performed principal coordinate analysis on distance matrix of raw read counts. The factorization of distance matrix aids at visualizing the differences between the expression profiles of different samples in two dimensions (Fig.3:4 B). Different replicates clustered together, while samples from different time points formed distinct clusters. Importantly, we obtained perfect separation between JQ1 treated and control on the first principal coordinate (x-axis). While the second principal coordinate (y-axis) was explanatory for the different time lapses that LN-2683-GS cells were treated with JQ1.

After that, we performed differential gene expression analysis with R package edgeR. We detected that over a thousand genes were significantly differently expressed between JQ1 treated and control conditions. As many as 598 genes were identified to be up regulated and 1278 genes were down regulated after filtering for genes whose expression changed 2 folds compared to the baseline (0 hours) in at least one time point and that pass 0.001 threshold for Bonferonni corrected P-value. The top 100 genes are visualized in an expression heatmap (Fig.3:4 C). It is worth mentioning that among the top up regulated genes there was *HEXIM1*, which is a negative regulator of the positive transcription elongation factor b (P-TEFb), the master modulator of RNA polymerase II during transcriptional elongation (Chen et al., 2014) (Michels et al., 2004). Remarkably, *HEXIM1* was reported to be increased after treatment with JQ1 in T cells (Banerjee et al., 2012) in lymphoma (Chapuy et al.,

2013), and in neuroblastoma (Puissant et al., 2013), and in adherent GBM models (Berenguer-Daize et al., 2016).

In order to identify gene sets that are affected by pharmacological BET inhibition we performed gene set enrichment analysis (GSEA) and reported here the top 15 down regulated and the 15 up regulated gene sets (Fig.3:4 D,E). GSEA of JQ1-treated and control GS cells revealed that signatures of Interferon-α response genes were significantly decreased in JQ1-treated cells. Moreover, in both up regulated and down regulated signatures, HDAC targets or gene sets of cells treated with HDACi Trichostatin A were detected (marked in bold in Fig.3:4 D,E). Interferon-α response and HDAC targets are the signatures that we decided to focus on in the current study.
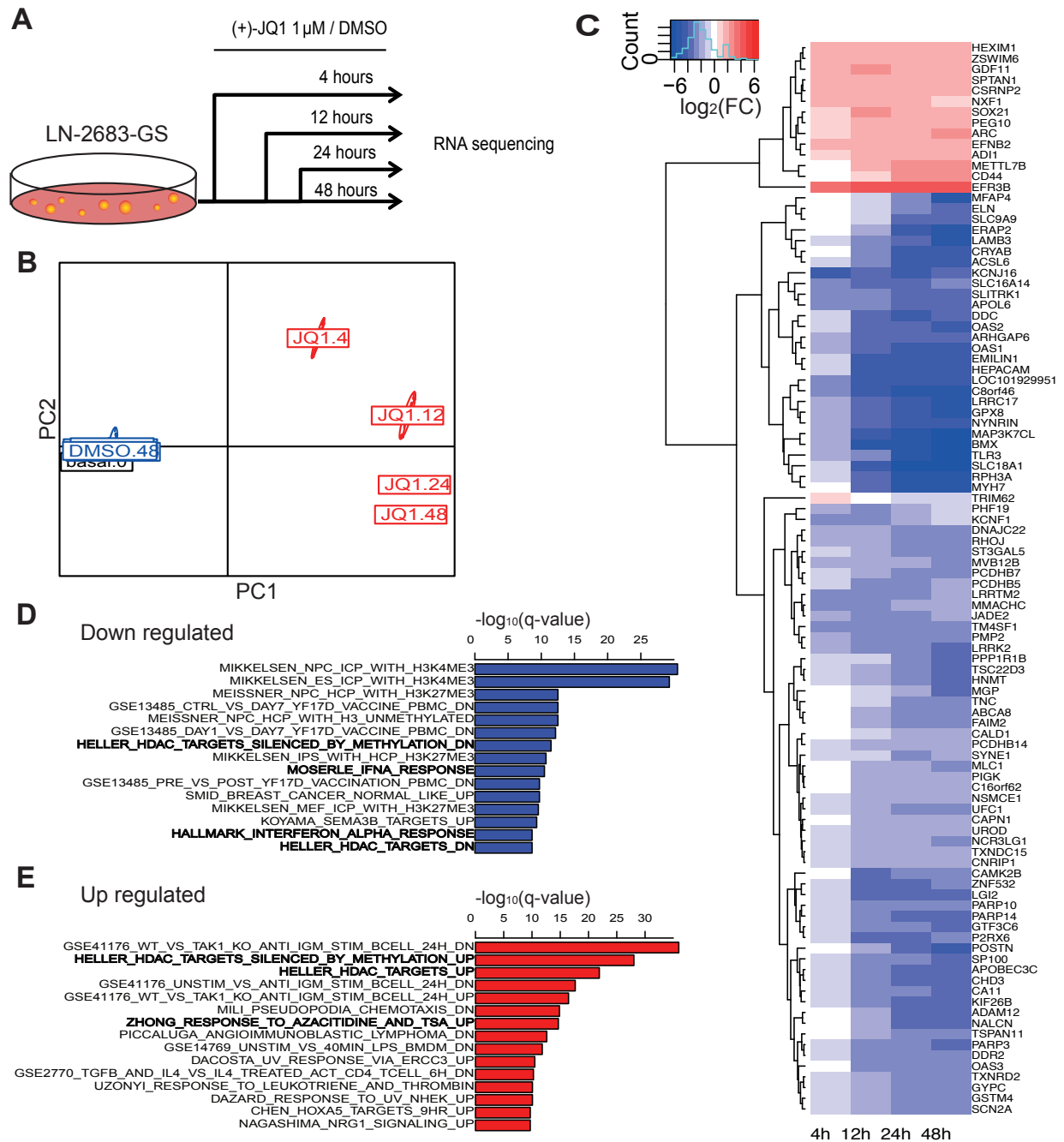
Figure 3:4. Transcriptome-wide analysis of the effects of JQ1.

(A) Experimental set-up of differential gene expression analysis by RNA-seq. LN-2683-GS cells were treated with 1μM (+)-JQ1 or DMSO control for 4, 12, 24, and 48 hours, experiment was repeated 3 times, and mRNA was subjected to sequencing.

(B) Principal coordinate analysis of the raw read counts of RNA-seq data. PC1, PC2; principal coordinates 1 and 2. FC; fold change.

(C) Heatmap of log$_2$FC of top 100 differentially expressed genes (log$_2$FC>1) based on Bonferroni adjusted P-value.

(D-E) Top 15 down regulated (D) and up regulated (E) gene sets based on gene set enrichment analysis with MSigDB database. q-value is Bonferroni corrected for multiple testing. Gene sets in bold were selected for subsequent analysis and validation.

3.6   Expression of interferon stimulated genes is reduced upon JQ1 treatment.

Interferon signature in GBM was previously reported by our laboratory when gene expression profiles of 80 GBMs were interrogated in order to identify expression signatures (Murat et al., 2008). One of the identified expression signatures was cluster called G12 that consisted of ISGs. Probes were re-annotated to GRCh37 genome assembly and GBMs were assigned to four molecular subtypes (Verhaak et al., 2010) (Fig.3:5 A). Interestingly, the probes in G12 cluster that had not been annotated in 2008 currently belonged to ISGs. We did not observe enrichment of mesenchymal GBMs in ISG positive (right) part of the heatmap, and non-tumoural brain was found to have no expression of ISGs, as one would have expected. Furthermore, we validated the consistency of the cluster structure in TCGA GBM expression data (Fig.3:5 B).

From HALLMARK_INTERFERON_ALPHA_RESPONSE gene set we chose two genes *OAS1* and *MX1* for validation experiments, since they are among the most down regulated. (Fig. 3:6 A), they belong to G12 cluster (Fig.3:5 A), and they appeared to be classical ISGs that had ISRE element in the promoter. In order to increase the translation value of the work we also included *CD274* (PD-L1), which is a member of G12 cluster (Fig.3:5 A) in the validation experiments.

In order to validate the reduction of ISGs upon JQ1 treatment, we boosted the signalling by priming GS-lines with IFN-α for 4 hours and then added JQ1 for subsequent 4 hours. We detected a strong reduction of ISGs *OAS1*, *MX1* and *CD274* mRNA in JQ1 treated GS-lines compared to DMSO control (Fig.3:6 B, D). Since *CD274* is an IFN-γ response gene (Garcia-Diaz et al., 2017) we repeated the experiment with IFN-γ and confirmed repression of induced *CD274* gene upon JQ1 treatment in the GS-lines. We validated the repression of IFN-induced PD-L1 upon JQ1 treatment also on the protein level (Fig. 3:6 F,G). Importantly, BET inhibition by JQ1 greatly diminished both IFN-α and IFN-γ-induced PD-L1 on the protein level in GS-lines.

Both IFN-α and IFN-γ signal through the Janus Activated Kinase (JAK)-Signal Transducer and Activator of Transcription (STAT) pathway. To activate the transcription of target genes (ISGs), pSTAT1 needs to translocate to the nucleus as homodimer or heterodimer with pSTAT2. In order to exclude possible effects of JQ1 on JAK/STAT signalling *per se* we examined pSTAT1 levels in the nucleus of GS-lines after priming with IFN-α or IFN-γ. While total STAT1 and pSTAT1 were increased in the nucleus after IFN priming, we did not observe any change in JQ1 treated GS-lines compared to DMSO control (Fig.3:7 and Fig. 6:1).
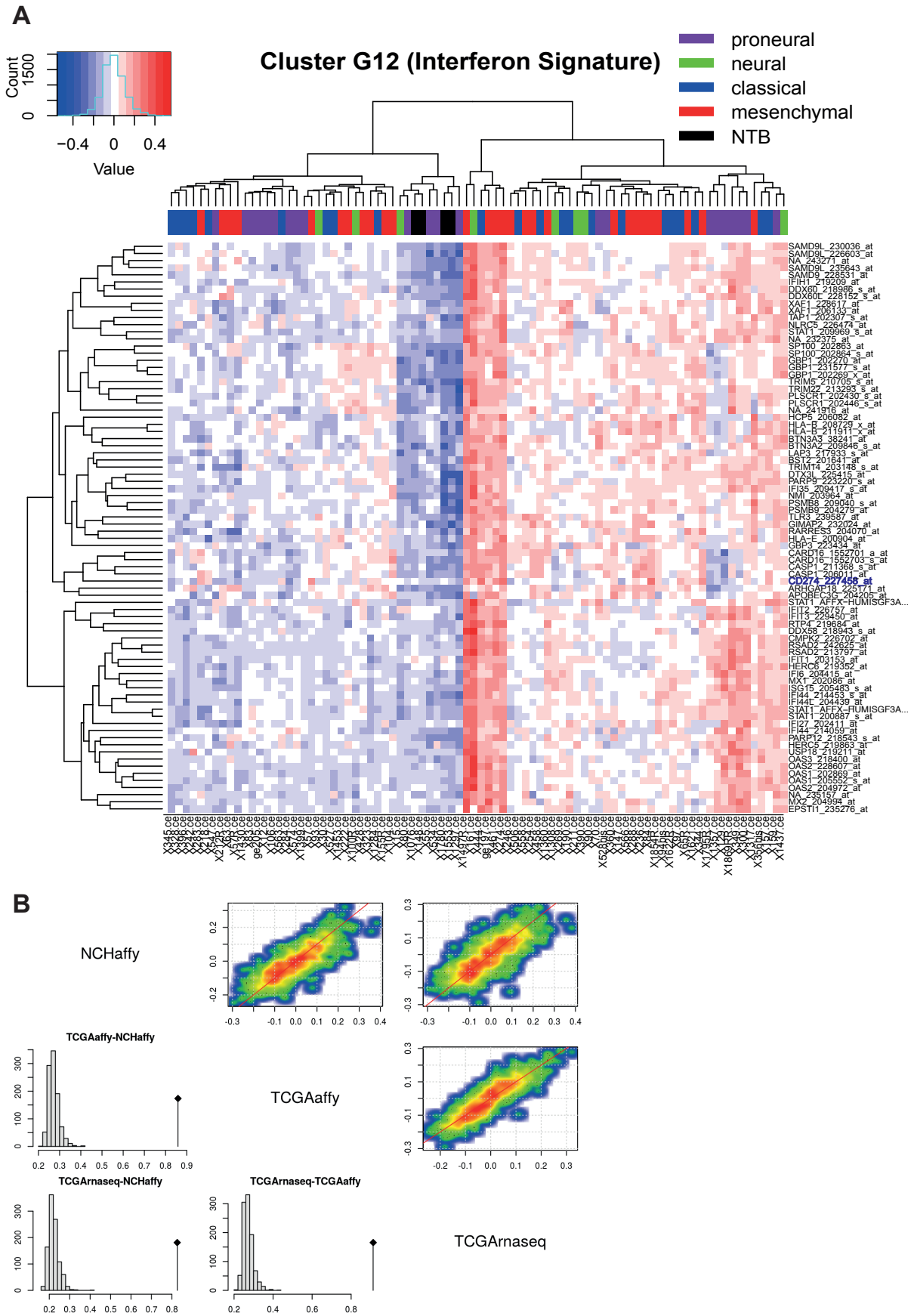
Figure 3:5. Interferon response gene signature in GBM.

(A) Heatmap of the interferon gene cluster (G12) identified in the GBM transcriptome (Murat et al., 2009). The expression values (Affymetrix gene probes) are log transformed, centered and normalized. The GBM samples are annotated with a colour code according to the expression subtypes (Verhaak et al., 2010). NTB, non-tumoural brain. CD274, a member of the G12 cluster, is marked in violet.

(B) Plots of pair-wise RV coefficient tests between NCHaffy (Murat et al., 2009), TCGAaffy and TCGArnaseq datasets (Brennan et al., 2013). Histograms of simulated values and observed value (straight line); and bivariate scatterplots between semi-matrices of distances.
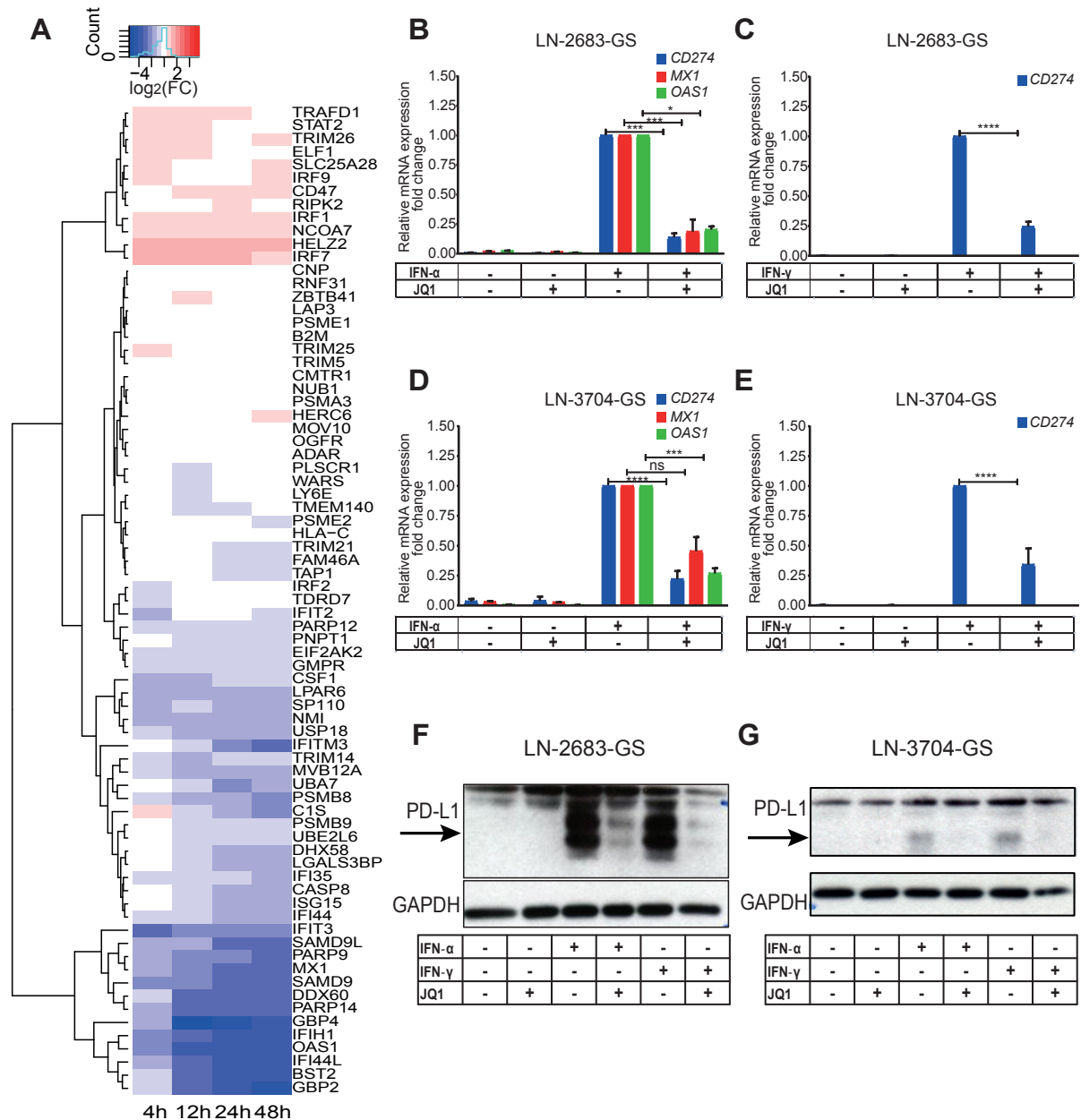
Figure 3:6. Expression of interferon-stimulated genes is reduced upon JQ1 treatment.

(A) Heatmap of log$_2$FC of expression of Interferon response gene set from MSigDB database (HALLMARK_INTERFERON_ALPHA_RESPONSE) in LN-2683-GS treated with 1µM JQ1 for 4, 12, 24 and 48 hours.

(B, D) qRT-PCR analysis of *CD274*, *MX1*, and *OAS1* in (B) LN-2683-GS and (D) LN3704-GS primed with Interferon-α (1000 U/ml) for 4 hours, then with JQ1 (1µM) for 4 hours. Data represent mean of 3 independent experiments. Error bars are SD. Reported P-values were defined by 2-way ANOVA and adjusted to account for multiple testing using statistical hypotheses Sidak test.

(C, E) qRT-PCR analysis of *CD274* in (C) LN-2683-GS, and (E) LN-3704-GS primed with Interferon-γ (20 ng/ml) for 4 hours, then with JQ1 (1µM) for 4 hours. Data repre-

sent mean of 3 independent experiments. Error bars are SD. Reported P-values are defined by 2-way ANOVA and adjusted to account for multiple testing using statistical hypothesis Sidak test.

(F-G) Western blot for PD-L1 and GAPDH (loading control) in (F) LN-2683-GS and (G) LN-3704-GS primed with Interferon-α (1000 U/ml) or Interferon-γ (20 ng/ml) for 4 hours, and then treated with JQ1 (1μM) for 4 hours. Data is representative of 3 independent experiments. Arrows point at specific band for PD-L1.

A

B

C
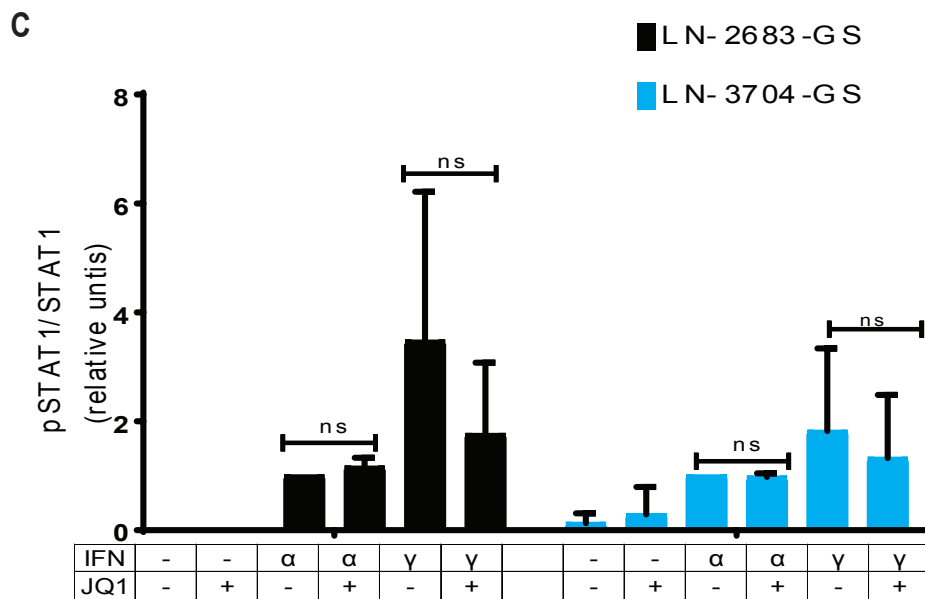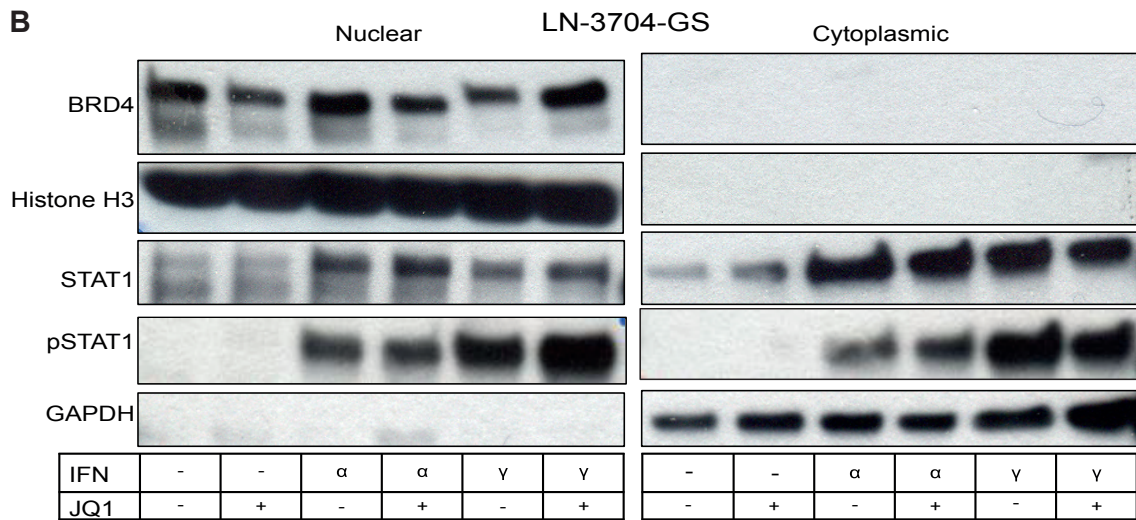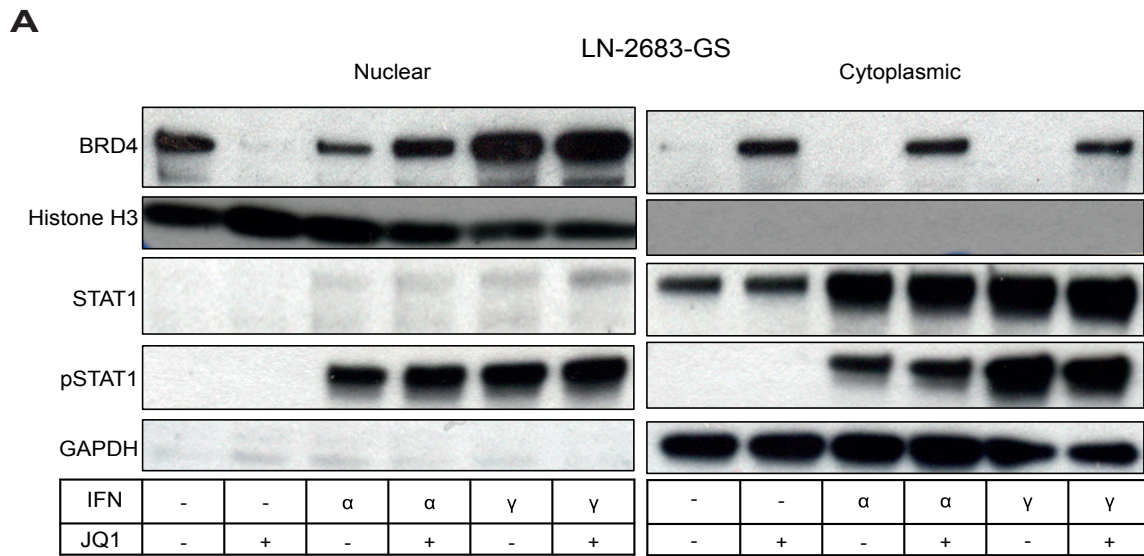
Figure 3:7. pSTAT1 levels in the nucleus are not affected by JQ1.

(A) Western blot analysis of nuclear and cytosolic fractions of LN-2683-GS (A) that were primed with IFN-α (1000 U/ml) or IFN-γ (20ng/ml) for 4 hours, then JQ1 (1µM) was added for 4 hours. Histone H3 and GAPDH were used to verify separation of fractions.

(B) The same as (A) for LN-3704-GS.

(C) Densitometry of pSTAT1 versus STAT1 bands of (A-B). The data represent a summary of 3 independent experiments, error bars are SD. ns, P-value>0.05, by paired t-test. Uncropped blots can be found in Supplementary Fig. 6:1.

3.7 GBM cell lines may endogenously express ISGs including *CD274* (PD-L1), and their expression is reduced upon JQ1 treatment.

Bradner and others demonstrated that some ovarian cancer cell lines may endogenously express PD-L1 and its expression was regulated by BRD4, hence BETi suppressed PD-L1 expression (Zhu et al., 2016). Like in ovarian cancer cell lines (Zhu et al.) CD274 is expressed endogenously in some commonly used GBM cell lines like U87MG and LN-18 (Fig. 3:8 F). We confirmed PD-L1 expression on protein level in U87MG *in vitro* (Fig. 3:8 A) and observed membranous staining on the immunohistochemistry of U87MG orthotopic mouse xenografts (Fig. 3:8 E). To determine whether JQ1 reduced expression of endogenous *MX1*, *OAS1*, and *CD274* we treated U87MG and LN-18 cells with 1µM JQ1 for 48 hours. As a result, mRNA of tested ISGs was largely reduced, and PD-L1 was diminished on protein level as well (Fig. 3:8 B-D).
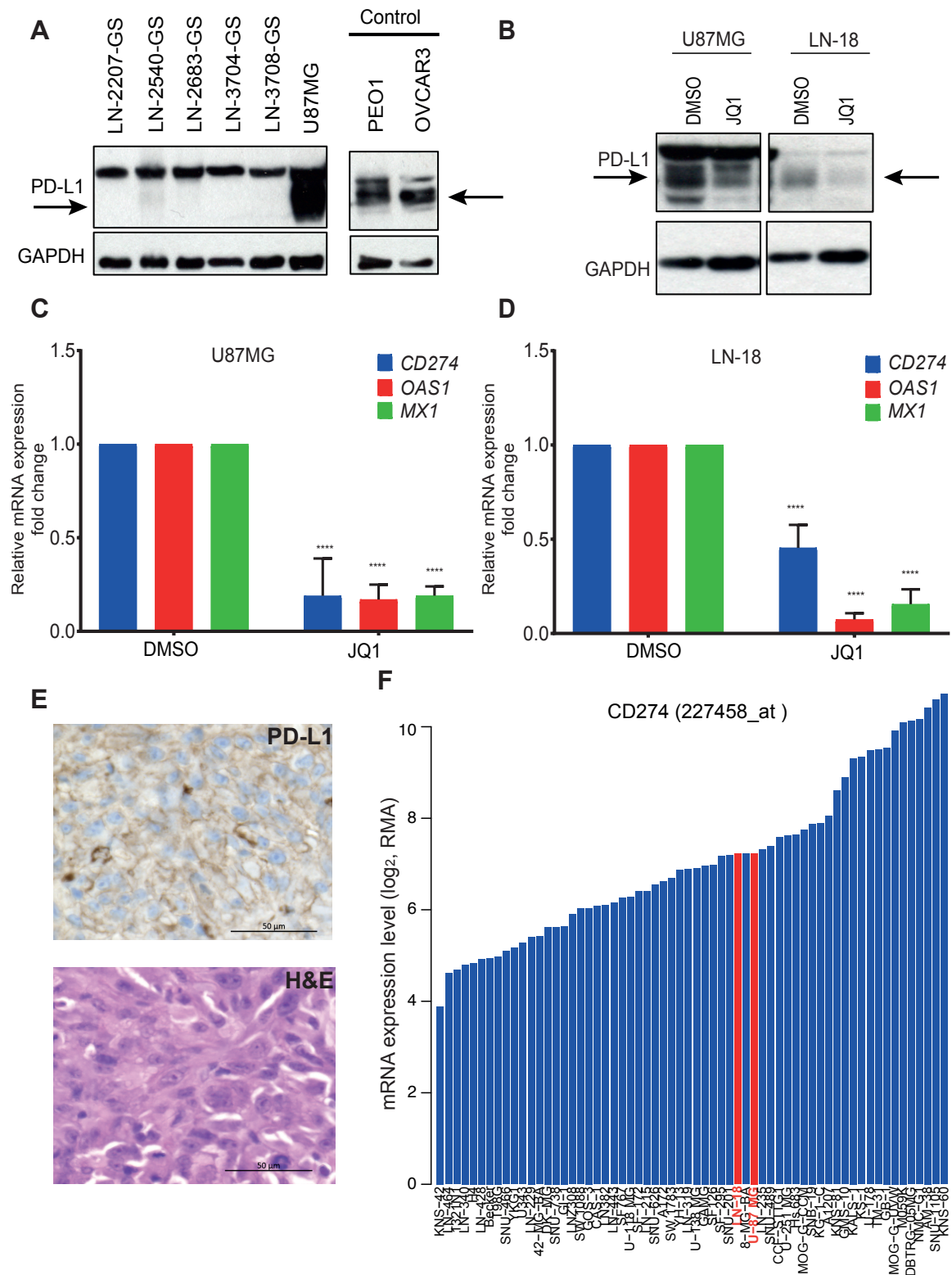
Figure 3:8. GBM cell lines may endogenously express ISGs including *CD274* (PD-L1), and their expression is reduced upon JQ1 treatment.

(A) Western blot analysis of endogenous PD-L1 levels in a panel of GS-lines, U87MG and ovarian cancer cell line PEO1 and OVCAR3 previously reported to have endogenous PD-L1 expression (Zhu et al., 2016) that were used as a positive control for the antibody. The arrow points the specific band for PD-L1 protein.

(B) Western blot analysis of PD-L1 in U87MG and LN-18 cell lines that were treated with 1µM JQ1 for 48 hours. GAPDH served as a loading control.

(C-D) qRT-PCR analysis of *CD274*, *MX1*, *OAS1* in (C) U87MG and (D) LN-18 cell lines treated with 1µM JQ1 for 48 hours. Reported P-values are determined by 2-way ANOVA and adjusted to account for multiple testing using statistical hypothesis Sidak test.

(E) Representative images of immunohistochemistry of PD-L1 and H&E of adjacent sections of U87MG xenograft in NSG mice. Scale bar is 50µm.

(F) Relative expression of *CD274* (227458_at probe) in glioma cell lines from CCLE (Barretina et al., 2012). Bar plots for LN-18 and U87MG are marked in blue. RMA, Robust Multi-Array Average.

3.8   *CD274* (PD-L1) is endogenously expressed in U87MG orthotopic xenografts and its expression is reduced upon a single injection of JQ1.

In order to determine the effects of JQ1 on ISGs expression *in vivo* we utilized orthotopic mouse xenografts of U87MG cells (Fig. 3:9 A). This model forms a fast-growing aggressive tumour, often hypoxic (Berenguer-Daize et al., 2016). Of note, excellent brain permeability by JQ1 was previously reported in healthy mice (Matzuk et al., 2012). Survival benefit of mice bearing orthotopic U87MG xenografts treated with BETi OTX015 compared to vehicle control was already shown (Berenguer-Daize et al., 2016). We thus decided to focus on short-term treatment effects on the gene transcription level. For *in vivo* experiments the injected mice were allowed to develop brain tumours for 15-22 days. First, we confirmed that PD-L1 expression was preserved in U87MG xenografts (Fig. 3:8 E). When mice exhibited weight loss and/or neurological symptoms they were treated with 100 mg/kg JQ1 or vehicle DMSO control (i.p.). After 4 hours the brains were harvested and *CD274*, *OAS1*, *MX1* and *C-MYC* expression was determined in marcodissected brain tumours. Indeed, a significant decrease in *CD274* and *OAS1* expression was detected, whereas *MX1* and *C-MYC* mRNAs were not affected by 4-hour JQ1 treatment (Fig. 3:9 B).
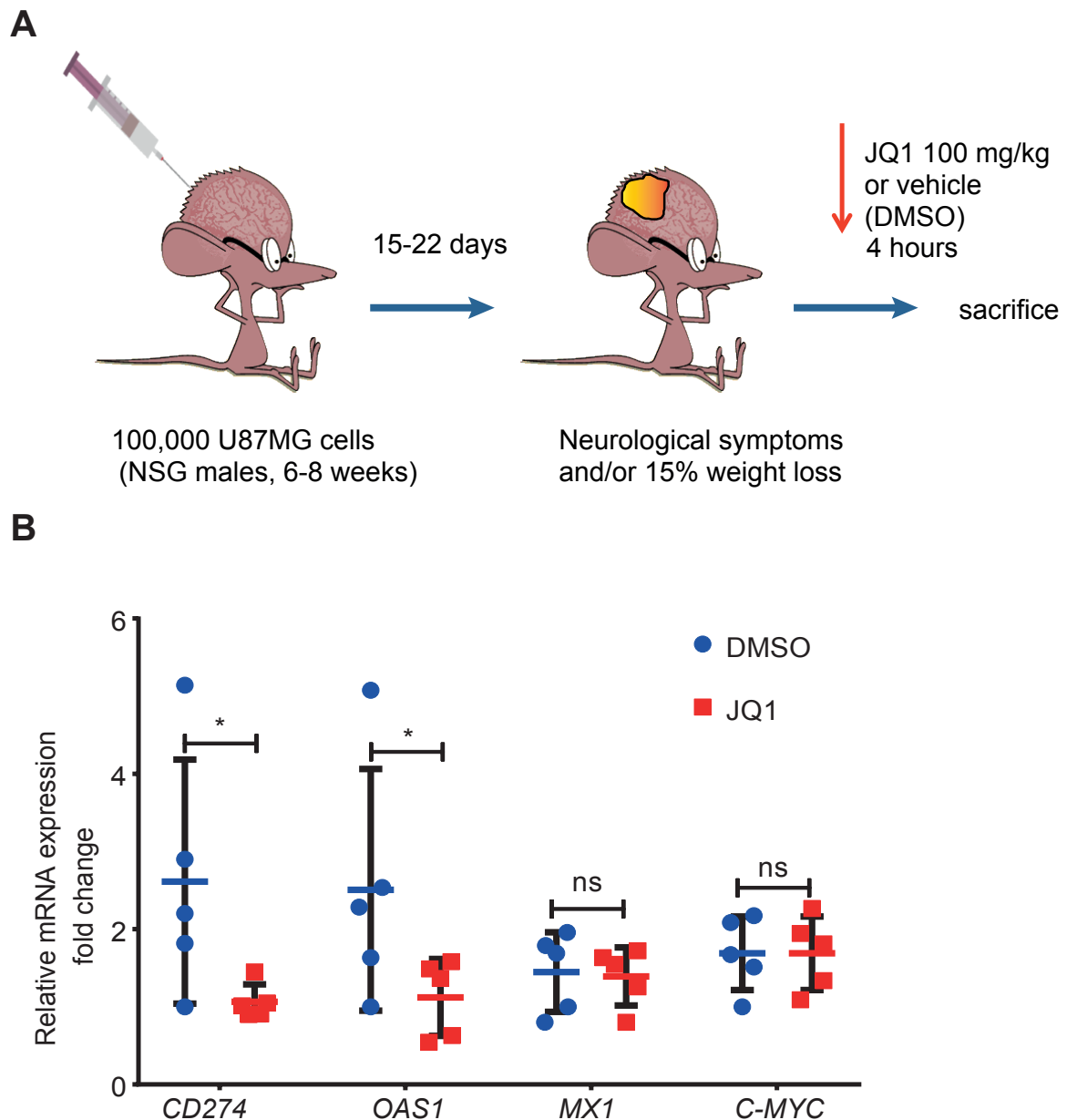
Figure 3:9. *CD274* **(PD-L1) is endogenously expressed in U87MG orthotopic xenografts and its expression is reduced upon a single injection of JQ1.**

(A) Schematic representation of the *in vivo* experiment. Nod-skid gamma knockout male mice were stereotaxically injected with 100,000 U87MG cells. After 15-22 days mice exhibited symptoms and were injected with 100 mg/kg JQ1 or DMSO vehicle control i.p. for 4 hours, and then sacrificed.

(B) qRT-PCR analysis of *CD274*, *MX1*, *OAS1*, and *C-MYC* in U87MG xenografts. n=5 mice per group pulled from 3 independent experiments. Reported P-values were determined by 2-way ANOVA adjusted to account for multiple testing using FDR approach by two-stage linear step-up procedure of Benjamini, Krieger and Yekutieli.

3.9   JQ1 and TSA act synergistically to reduce cell viability of GS-lines

GSEA of JQ1 treated LN-2683-GS also revealed enrichment of several gene sets related to HDACi (marked in bold in Fig. 3:5 D,E). Interestingly, all the identified gene sets were discovered in cells treated with Trichostatin A (TSA), a small molecule inhibitor of HDACi. In the literature, similarity between the effects of HDACi and BETi on the transcriptome level has been described from normal cells and cancer models (Bernasconi et al., 2016; Bhadury et al., 2014; Vazquez et al., 2017). Given the resemblance, we decided to test whether the combination of JQ1 with the HDACi TSA would be synergistic in GS-lines. For this we treated LN-2683-GS and LN-3708-GS with 64 possible combinations of JQ1 and TSA from 0µM to 10µM for a 3-day assay and from 0µM to 2µM for a 10-day assay (Fig. 3:10 A-D). We performed analysis of dose-response matrix (Fig. 3:10 B) and determined the range of concentrations where synergistic drug interactions occur (red part of JQ1-TSA interaction landscape (Fig. 3:10 C)). Importantly, the shape of drug interaction landscapes remained the same for 3 biological experiments (data not shown) that confirmed the validity of chosen synergy analysis methodology. Based on the performed analysis, 5% of LN-2683-GS cells after 3 days and 9% after 10 days die due to the synergistic drug interactions (for LN-3708-GS 15% after 3 days, and 4% after 10 days). Next step would be to test this drug combination in mouse xenografts.

3.10   JQ1 and TSA produce synergistic effects to repress transcription of IFN-induced, but not endogenously expressed, ISGs

In order to test whether TSA produces effects on transcription level of ISGs similar to the ones observed with JQ1, GS-lines primed with IFN-α were treated with 1µM JQ1, 1µM TSA or the combination of 0.5µM JQ1 and 0.5µM TSA (Fig. 3:10 F). Indeed, TSA reduced the expression of *MX1*, *OAS1*, and *CD274* to the same extend as JQ1, apart from *CD274* in LN-3704-GS, which was significantly higher in TSA treated cells. Moreover, the combination of TSA and JQ1 reduced the expression of ISGs more than JQ1 alone in both GS-lines, indicating synergistic effects of the therapy on gene transcription level as well as on cell viability.

Given the effects of the combination of TSA and JQ1 on IFN-induced ISGs, we tested whether TSA is potent to reduce the expression of innate ISGs in adherent GBM cell lines as well. Surprisingly, we marked a completely different effect (Fig.

3:10 G, H). In fact, TSA was not reducing the expression of innate ISGs, even slightly induced expression of *CD274* in LN-18. In addition, TSA did not affect endogenous PD-L1 expression on the protein level either (Fig. 3:10 I,K). Hence, there are fundamental differences in modulation ISGs expression by JQ1 in GS-lines and GBM cell lines will be discussed in the next chapter.

A — Inhibition (%) vs TSA (µM)

B

TSA(µM)	0	0.03	0.06	0.12	0.25	0.5	1	2
2	98.62	98.89	98.56	98.7	98.59	98.62	98.39	98.99
1	97.51	97.72	97.86	98.2	98.32	98.32	98.19	97.98
0.5	59.86	66.49	70.03	83.7	93.89	97.77	98.11	98.08
0.25	46.25	42.84	39.81	52.59	67.71	80.94	86.6	90.42
0.12	23	23.94	33.21	47.2	53.17	67.44	76.7	81.93
0.06	20.53	13.65	4.07	28.86	36.25	61.44	66.54	74.59
0.03	0.4	-2.43	6.97	-12.25	29.41	42.74	56.45	70.99
0	-9.59	-15.98	-20.73	-3.11	14.87	29.18	47.31	52.85

JQ1 (µM)

C — 3D surface plot of Inhibition (%) vs JQ1 (µM) and TSA (µM)

D — Inhibition (%) vs JQ1 (µM)

E IFN-α primed LN-2683-GS — Relative mRNA expression fold change (CD274, MX1, OAS1)

F IFN-α primed LN-3704-GS — Relative mRNA expression fold change (CD274, MX1, OAS1)

G U87MG — Relative mRNA expression fold change (CD274, MX1, OAS1)

H LN-18 — Relative mRNA expression fold change (CD274, MX1, OAS1)

I — Western blot: U87MG and LN-18; PD-L1, Vinculin; JQ1 / TSA

K — PD-L1 protein relative to Vinculin (U87MG, LN-18); JQ1 / TSA

Figure 3:10. Combination of JQ1 with TSA shows synergy in reduction of cell viability and repression of Interferon stimulated genes in GS-lines.

(A-D) Combination assay in LN-2683-GS treated with serial 2-fold dilutions of JQ1 and TSA starting with 2µM for 10 days. Representative of 3 independent experiments.

(A, D) Single drug cell viability curves for LN-2683-GS treated with (A) TSA and (D) JQ1. Data represent mean of 3 plates (technical replicates).

(B) Combination matrix of cell inhibition. 100% is inhibition of LN-2683-GS cells treated with lethal 1µg/ml Actinomycin D, 0% is inhibition of LN-2683-GS exposed to DMSO control. Data represent mean of 3 wells (technical replicates).

(C) Combination landscape showing the synergistic range of concentrations of TSA and JQ1 in red, and additive in green.

(E-F) qRT-PCR analysis of *CD274*, *MX1*, and *OAS1* in (E) LN-2683-GS and (F) LN-3704-GS primed with Interferon-α (1000 U/ml) for 4 hours and then treated with 1µM JQ1, 1µM TSA or the combination of 0.5µM JQ1 and 0.5µM TSA for 4 hours. Data represent mean of 3 independent experiments, error bars are SD. Reported P-values were determined by 2-way ANOVA and are adjusted to account for multiple testing using statistical hypothesis Sidak test.

(G-H) qRT-PCR analysis of *CD274*, *MX1*, and *OAS1* in (G) U87MG and (H) LN-18 treated with 1µM JQ1, 1µM TSA or the combination of 0.5µM JQ1 and 0.5µM TSA for 48 hours. Reported P-values were determined by 2-way ANOVA and adjusted to account for multiple testing using statistical hypothesis Sidak test.

(I) Western blot analysis of PD-L1 and Vinculin loading control of U87MG and LN-18 treated with 1µM JQ1, 1µM TSA or the combination of 0.5µM JQ1 and 0.5µM TSA for 48 hours.

(J) Densitometry of (I). Data represent mean of 3 independent experiments. Error bars are SD. Reported P-values were determined by 2-way ANOVA and adjusted to account for multiple testing using statistical hypothesis Sidak test.

Chapter 4 Discussion

4.1 JQ1 treatment seems to induce senescence-like phenotype in adherent GBM cell lines

BET inhibitors such as JQ1 have demonstrated efficacy in various cancer models, and clinical analogues of JQ1 have been tested in several malignancies according to the rapidly expanding literature (reviewed in (Stathis and Bertoni, 2017)). In this study, we evaluated the potential efficacy of JQ1 in glioblastoma (GBM) models. At first, we observed a reduction of cell viability of regular GBM cell lines (Fig.3:1 A). Moreover, GBM cell lines exhibited markers of senescence, reduction of cells in S-phase (data not shown) and presence of SA-β-Gal activity (Fig.3:1 C, D). In fact, the induction of SA-β-Gal with incomplete growth arrest in response to BETi was already reported in cancer models *in vitro* (Boi et al., 2015; Delmore et al., 2011).

4.2 Long exposure to JQ1 blocks the ability of GS-lines to form secondary gliomaspheres

Next, we focused on glioma sphere lines (GS-lines), and observed that cell viability of GS-lines was reduced upon JQ1 exposure. However, compared to published reports and the results obtained with adherent cell lines previously, the tested GS-lines would fall into the resistant category, since even the highest concentration tested (30μM) was not lethal (Fig.3:2 A) (Todaro et al., 2014). This resistance might have been linked to the slow-cycling nature of GS-lines (population doubling times from 4 to 15 days, Table 6:1) and a neurobasal growth medium without serum that we use specifically to culture GS-lines.

Then, we confirmed the results of Cheng and colleagues (Cheng et al., 2013) that JQ1 compromised the ability of glioma spheres to form secondary gliomaspheres. This observation is important, since it is commonly believed that retraction of GBM to cancer therapies is due to a small population of cells with stem cell

like features (Bao et al., 2006). Notably, 2µM JQ1 was sufficient to completely block the sphere formation capacity of GS-lines, and this concentration of BETi OTX015 was therapeutically achievable in patients' plasma. However, OTX015 did not show to be efficient in recurrent GBM patients (Hottinger et al., 2016).

4.3 JQ1 seems to drive GS-lines to apoptosis

Moreover, JQ1 did not increase the population of cells arrested in G1 of GS-lines, as it was demonstrated in other cancer models (Boi et al., 2015; Delmore et al., 2011; Pastori et al., 2014). In fact, we only observed a decrease of cells in S-phase in LN-2207-GS, which was reversible upon drug withdrawal. However, GS-lines seemed to die apoptotically after prolonged exposure of 5 or 10 days to JQ1 (presence of Annexin V, not shown; and cleaved PARP (Fig 3:2 C).

4.4 MYC is down regulated upon JQ1 exposure in GS-lines

Importantly, MYC was reported to play a central role in the rational of using BET inhibitors in cancer in virtually all cancer related studies published (Boi et al., 2015; Delmore et al., 2011; Mertz et al., 2011; Ott et al., 2012). BET inhibition was postulated to be a therapeutic strategy to target MYC, which in its turn mediated transcriptional changes and repressed cell cycle progression (Delmore et al., 2011). In GBM models contradictory results were published concerning MYC. Pastori and colleagues reported that I-BET (a clinical analogue of JQ1) did not alter MYC expression in U87MG *in vitro* (Pastori et al., 2014). Whereas, Cheng and colleagues showed down regulation of MYC on both mRNA and protein levels after treatment of GS-lines and in their adherent pairs with JQ1 *in vitro* (Cheng et al., 2013). According to our results, MYC is down regulated after JQ1 treatment in all tested GBM models *in vitro*. Of note, our GS-line with the lowest intrinsic level of C-MYC protein LN-2683-GS did not appear to be more sensitive to JQ1.

4.5 LN-2683-GS seems to exhibit neuronal differentiation-like phenotype

Furthermore, we discovered a differentiation-like phenotype of LN-2683-GS after exposure to JQ1, with an increased expression of neuronal differentiation marker neuronal specific class III beta-tubulin (TUJ1). To our knowledge, the observation that GS-lines may differentiate after treatment with JQ1 was not reported be-

fore in GBM models. Nevertheless, there are studies that showed differentiation phenotype in response to JQ1 of embryonic stem cells (Gonzales-Cope et al., 2016), neuroblastoma cell lines (Lee et al., 2015), and paediatric glioma cells (Piunti et al., 2017). JQ1 was also shown to inhibit differentiation of bone cells in the context of bone tumour osteosarcoma (Lamoureux et al., 2014), and T helper 17 cells (Cheung et al., 2017). In our results, a differentiation-like phenotype was only present in LN-2683-GS, and not in six other tested GS-lines. Hence, the differentiation phenotype in response to JQ1 was not prevalent in GS-lines.

4.6 Transcriptome-wide differential gene expression analysis revealed gene signatures affected by BET inhibition

In our study, over a thousand of genes were differentially expressed in JQ1 treated LN-2683-GS compared to DMSO control. This result was initially puzzling, since it had been shown that BETi affected a few hundreds of genes, most of which being associated with super-enhancers (Dawson et al., 2012; Loven et al., 2013). For instance, 88 genes were significantly down and 25 up regulated in multiple myeloma cell lines after JQ1 treatment (Delmore et al., 2011). Generally, drugs targeting chromatin regulators (such as HDAC, HAT or BET inhibitors) are thought to be unspecific due to the lack of specificity of the regulators themselves. So, it could be possible that BET proteins are not enriched at super-enhancers in GS-lines to the extent reported in other malignancies, where 33% of BRD4 is bound to 1.6% of genes in lymphoma (Chapuy et al., 2013).

Despite the observed major changes of the transcriptome, GSEA with MSigDB database helped us to make sense of the achieved RNA-seq data and resulted in two major discoveries: JQ1 represses the IFN response genes; and JQ1 produces similar effects as an HDACi in published data sets (Fig. 3:4). Whereas, the resemblance with HDACi could have been predicted by the mode of action and published reports (Bhadury et al., 2014; Mazur et al., 2015), the relevance of ISGs repression to GBM was difficult to decipher.

4.7 Epigenetic modulation of interferon response genes in cancer

First, it is unclear why we were able to detect ISGs in cell culture, where there should not be any IFN present. Major producers of IFN-α are believed to be macro-

phages, and IFN-γ is produced by T-cells in cancer microenvironment. In fact, cancer cells were shown to be able to produce type I IFNs themselves along with infiltrating immune cells in the tumour microenvironment (reviewed in (Parker et al., 2016)). Whereas, the expression of IFN-γ is only attributed to T cells and NK cells (Schroder et al., 2004). Moreover, if the ISGs expression was due to the presence of immune cells in the GBM microenvironment, the GBMs that express ISGs would have been of mesenchymal subtype, which is not the case based on the results from G12 cluster (Fig. 3:5). So, there might be a genetic or epigenetic innate mechanism of ISGs transcription by GBM cells.

Indeed, our experiments demonstrated that the expression of IFN-induced or endogenously expressed ISGs was repressed upon pharmacological BET inhibition; hence the transcription of ISGs was epigenetically regulated in *in vitro* GBM models. We discovered that expression of both endogenous or IFN-induced *CD274* (PD-L1) is reduced upon BETi treatment in line with the results recently reported in ovarian cancer human cell lines (Zhu et al., 2016), and in a large panel of breast, lymphoma, colon adenoma murine and human cancer cell lines (Hogg et al., 2017). Both studies demonstrated that BRD4 is a critical mediator of *CD274* expression, and regardless of the transcription factors present in *CD274* locus, BETi were shown to block transcription elongation of *CD274* gene. Importantly, this effect was MYC independent, which is somehow in controversy to earlier published report (Casey et al., 2016).

PD-1 inhibiting antibodies are currently being tested in the clinic for the treatment of glioblastoma (for example clinical trials NCT03430791, NCT02617589). Our results raise the possibility of targeting PD-L1 using small molecule BET inhibitors. It could be an interesting strategy for brain tumours since small molecules should better penetrate BBB than antibodies. However, our results alone cannot tell whether BETi facilitate a positive immune response to kill the tumor. In order to answer this question one must study effects of BETi on immune cells in glioma microenvironment (more details in perspectives section). Moreover, major limitation of BETi approach to PD-L1 blockade would be all other genes that are affected by BETi (Figure 4:1).

There is some reported evidence of epigenetic regulation of ISGs in cancer. For instance, *CD274* promoter is commonly silenced by methylation in IDHmt glioma, but not in IDHwt glioblastoma (Berghoff et al., 2015; Berghoff et al., 2017). Works pioneered by Stephen Baylin demonstrated that reversing aberrant methylation to normal pattern helps the tumour to reactivate its immune attraction systems (Chiappinelli et al., 2015). Mechanistically, they demonstrated that after exposure to DNMTi (5-Aza), cancer cell started to express RNA from endogenous retroviruses, which lead to an increased IFN signaling and viral defense gene expression, like the cancer cell had been exposed to a virus. In a follow-up work they showed that addition of HDACi to 5-Aza further augmented the induction of ISGs in NSCLC models (Topper et al., 2017). These finding are supported by the data from the clinic where NSCLC patients who were treated with 5-Aza (Vidaza) and HDACi Entinostat responded to immunotherapy better, that those who were treated with immunotherapy alone (Wrangle et al., 2013).

4.8   Synergy between BETi and HDACi

In our experiments combination of JQ1 and TSA showed synergism in reducing cell viability of GS-lines. Moreover, combination of TSA and JQ1 was also reducing the expression of ISGs, including PD-L1 in GS-lines. In fact, synergy between HDACi and BETi was previously reported in several cancers (Bhadury et al., 2014; Boi et al., 2015; Fiskus et al., 2014; Mazur et al., 2015; Shahbazi et al., 2016). The results obtained *in vitro* have to be validated in mouse xenografts of GS-lines, which will be discussed in perspectives.

4.9   The observed difference between GS-lines and adherent GBM cell lines

Intriguingly, the obtained results with GS-lines and adherent GBM cell lines concerning modulation of ISGs were profoundly different. We demonstrated that expression of endogenous ISGs in U87MG and LN-18 was not repressed by HDACi (even slightly, but significantly induced in LN-18). In fact, HDACi was shown to induce *CD274* expression in melanoma cell lines *in vitro* (Woods et al., 2015). Moreover, the combination of 5-Aza and HDACi was reported to increase ISGs expression in NSCLC and ovarian cancer models (Stone et al., 2017; Topper et al., 2017). Hence, adherent GBM cell lines gave results similar to the ones reported with 2D models of

other cancers in respect to response to HDACi treatment. Mario Suva mapped H3K27ac (mark of active genes and enhancers) in 3 GS-lines and their adherent pairs. Even though most of H3K27ac peaks were shared between a given GS-line and its adherent pair, a big part of H3K27ac peaks were specific only to a GS-line or only to its adherent pair. In fact, unsupervised clustering showed higher similarity between different GS-lines, rather than between the GS-line and its adherent pair (Suva et al., 2014). This suggests that the chromatin landscape, in regards to at least the H3K27ac mark, correlates better with the phenotypic state and probably culture conditions, rather than with tumour-specific characteristics. Hence, when one modulates the H3K27ac mark, with for example HDACi, the effects might be profoundly different, which is what we have observed in our experiments. In any case, mechanistic details of the effect have yet to be investigated, but our data demonstrated that the modulation of ISGs by HDACi is not a universal effect and is likely to be cell context-dependent.

4.10   Experiments with orthotopic mouse xenografts

First of all, excellent blood brain barrier permeability of JQ1 had already been reported in healthy mice (Matzuk et al., 2012). We first confirmed PD-L1 expression in U87MG xenografts by immunohistochemistry. Despite the presence of a staining background in mouse brain, which was probably due to the use of an anti-mouse and anti-rabbit cocktail of secondary antibodies (Ventana kit, Roche), U87MG xenografts exhibited a cytoplasmic staining of PD-L1.

In order to investigate modulation ISGs in response to JQ1, we chose to treat the mice bearing orthotopic xenografts with JQ1 for 4 hours, since this time was more than enough to induce massive changes on the transcriptome of GS-lines (RNA-seq data) and to reduce expression of ISGs in culture. Our results demonstrated that *OAS1* and *CD274* were down regulated, whereas *MX1* remained unchanged. It could have been due to the time point, since the drug needs to reach the brain first, and the genes modulation of which we detected were probably direct and early response genes. Expression of *C-MYC* was not affected either, but it was expected since even in culture it takes 48 hours to have significant changes in U87MG cells (data not shown).

4.11 Limitation of the current study

A big part of the current study was based on data we have achieved from RNA-seq that we performed in one GS-line. However, all the subsequent experiments were performed in at least 2 GS-lines, which is important to validate the results. Moreover, *in vivo* experiments were performed only in one model of GBM U87MG xenografts. This model does not recapitulate the important characteristics of glioblastoma, such as invasiveness. Furthermore, the origin of U87MG line is debated, however it was confirmed to be glioblastoma-derived (Allen et al., 2016). LN-2669-GS and LN-2540-GS were contaminated with mycoplasma. Mycoplasma was shown to affect the biology of cell lines, for example causing significant changes in gene expression (Olarerin-George and Hogenesch, 2015), metabolism and many other aspects of cell biology (Shannon et al., 2016; Young et al., 2010). GS-line LN-2207-GS is not tumourigenic in mice and therefore is a not a good model of the glioblastoma (Table 6:1). Furthermore, mice were immunocompromised, which does not allow recapitulating glioblastoma microenvironment. The reason we do not use mouse immunocompetent models of glioblastoma is that the murine tumour does not recapitulate the one of human origin; mutation burden of mouse glioma is low (Pyonteck et al., 2013; Uhrbom et al., 2002). Lastly, a major limitation of the current study is that all the experiments were conducted with a tool drug that has a short half-life and needs to be diluted in DMSO to be administered in the animals, and impossible to use for humans. Hence, there are a dozen of various BETi that are currently being tested in preclinical and clinical studies, most of which have limited blood brain barrier penetration in mice (example for I-BET (Pastori et al., 2014)).

4.12 Perspectives

4.12.1 Confirmation of the key results with clinically relevant BETi

We are currently testing a clinically relevant BETi ODM-207 in our GBM models in collaboration with a pharmaceutical company Orion Pharma (Bjorkman et al., 2016a; Bjorkman et al., 2016b). ODM-207 is now being tested in solid cancers (clinical trial identifier: NCT03035591). The results could not be included in this thesis due to the non-disclosure agreement.

4.12.2 Investigation of the mechanism of ISGs repression upon pharmacological BET inhibition
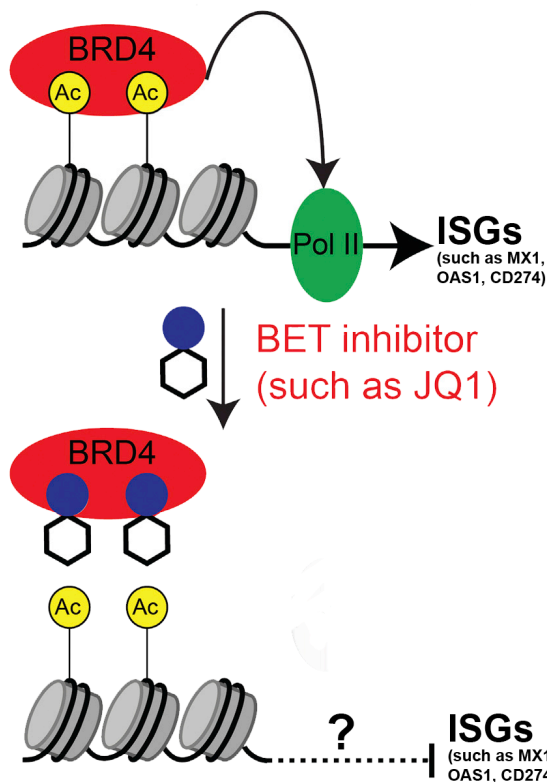
Figure 4:2. BETi suppress the expression of Interferon Stimulated genes.
Adapted from (Zhu et al., 2016). Ac, acetyl group; ISGs, interferon-stimulated genes; Pol II, polymerase 2.

Our results consistently demonstrate that JQ1 represses the expression of both endogenously expressed and IFN-induced ISGs in GBM models. Since, we observed a strong reduction in expression after as short as 4 hours, we think ISGs are direct response genes of BETi. It is supported by the literature at least concerning *CD274* gene, since BRD4 was shown to be required for tethering acetylated chromatin to RNA Pol2 and therefore directly promoting transcriptional elongation of *CD274* (Hogg et al., 2017). We hypothesize that the reported mechanism concerning transcriptional repression of *CD274* by BETi may possibly be extrapolated to the signature of ISGs (Fig. 4:1).

In order to test this hypothesis we are planning to perform ChIP in JQ1 and control conditions of IFN-primed GS-lines to assess Pol2 presence in TSSs of *CD274*, *MX1*, and *OAS1*. First, the read-out will be performed by qPCR, and if Pol2 is detected to be absent from TSS of tested ISGs, the chipped gDNA will be sequenced. It might be important to include the H3K27ac mark to define active enhancers/super-enhancers, as well as BRD4 in order to have a better mechanistic insight on the transcription of ISGs. Our preliminary experiments showed that Pol2 was present on TSS of *CD274* 2 hours after the induction (preliminary results, data

not shown). We encountered multiple technical difficulties when trying to perform ChIP of GS-lines, due to the absence of the standard procedure for GS-lines and limitation in cell number.

4.12.3 Validation of BETi and HDACi combination

Currently, we are working on characterizing LN-3708-GS xenografts *in vivo* in order to use this model for a preclinical trial of BETi. If BETi shows survival benefit of mice bearing orthotopic xenografts, we will proceed to test the combination of BETi and HDACi. In a second step, we are planning to validate the results obtained *in vitro*, but this time we will use clinically relevant analogues (such as ODM-207 and HDACi Vorinostat). The efficiency of the combination should be compared to stand-ard of care, so one arm of tested animals should be treated with Temozolomide.

4.12.4 Effects of BETi on the GBM microenvironment

It would have been interesting to investigate whether BETi provokes changes in the immune compartment of the glioblastoma microenvironment. In fact, in the above-mentioned studies by S. Baylin, ISGs re-expression by 5-Aza treatment tar-geted massive changes in immune compartment of tumour microenvironment (more CD45+ overall, more active CD8+Tcells, and NK cells) (Stone et al., 2017). In order to investigate the effects of BETi on glioblastoma microenvironment together with the effects on the cancer cells themselves, one must work with immunocompetent ani-mals, or co-culture GBM cells with immune cells such as macrophages that were shown to be abundant in the GBM microenvironment (Bowman et al., 2016). Howev-er, it might be not technically challenging, since immune cells might be dying in FBS free medium. To our knowledge, little is published on how BETi influences tumour microenvironment, except for one study that showed that BETi enhanced T cell per-sistence (Kagoya et al., 2016).

4.12.5 Future of epigenetic drugs as cancer therapies

It is clear that the epigenome of cancer cell is altered. Even cancers with low mutational burden, such as paediatric cancers or IDHmt gliomas exhibit drastic changes of the epigenome (Biegel et al., 2014; Flavahan et al., 2016; Mack et al., 2014). And several epigenetic drugs such as Decitabine, Azacitidine, Vorinostat showed a survival benefit and low toxicities in the clinics, and are currently FDA ap-

proved (reviewed in(Jones et al., 2016)). Despite significant successes, a lot of challenges remain, such as absence of response biomarkers, and unclear mechanisms of response. Epigenetic drugs of the class "broad reprogrammers" (BETi, HDACi, HATi, DNMTi) are not specific to cancer cells; in fact normal cells cannot exist without the functioning epigenome. So, clinical activity of drugs targeting "broad reprogrammers" might always be limited by their toxicities.

There is another type of more specific epigenetic drugs, such as inhibitors of mutant EZH2 or mutant IDH inhibitors. These drugs are designed to specifically target cancer cells with particular mutations; hence their toxicities should be limited.

Finally, it was shown multiple times that the flexibility of the epigenome is used by cancer cells to rapidly acquire resistance to anti-cancer agents (for example (Brown et al., 2014; Liau et al., 2017)). Therefore, epigenetic therapies would be more effective when used in combination with kinase inhibitors, conventional chemotherapy, or immunotherapy.

Chapter 5   References

Abramson, J.S., Blum, K.A., Flinn, I.W., Gutierrez, M., Goy, A., Maris, M., Cooper, M., O'Meara, M., Borger, D., Mertz, J.*, et al.* (2015). BET Inhibitor CPI-0610 Is Well Tolerated and Induces Responses in Diffuse Large B-Cell Lymphoma and Follicular Lymphoma: Preliminary Analysis of an Ongoing Phase 1 Study. Blood *126*.

Allen, M., Bjerke, M., Edlund, H., Nelander, S., and Westermark, B. (2016). Origin of the U87MG glioma cell line: Good news and bad news. Science Translational Medicine *8*, 354re353-354re353.

Amorim, S., Stathis, A., Gleeson, M., Iyengar, S., Magarotto, V., Leleu, X., Morschhauser, F., Karlin, L., Broussais, F., Rezai, K.*, et al.* (2016). Bromodomain inhibitor OTX015 in patients with lymphoma or multiple myeloma: a dose-escalation, open-label, pharmacokinetic, phase 1 study. Lancet Haematol *3*, e196-204.

Bady, P., Diserens, A.C., Castella, V., Kalt, S., Heinimann, K., Hamou, M.F., Delorenzi, M., and Hegi, M.E. (2012). DNA fingerprinting of glioma cell lines and considerations on similarity measurements. Neuro Oncol *14*, 701-711.

Balvers, R.K., Kleijn, A., Kloezeman, J.J., French, P.J., Kremer, A., van den Bent, M.J., Dirven, C.M., Leenstra, S., and Lamfers, M.L. (2013). Serum-free culture success of glial tumors is related to specific molecular profiles and expression of extracellular matrix-associated gene modules. Neuro Oncol *15*, 1684-1695.

Banerjee, C., Archin, N., Michaels, D., Belkina, A.C., Denis, G.V., Bradner, J., Sebastiani, P., Margolis, D.M., and Montano, M. (2012). BET bromodomain inhibition as a novel strategy for reactivation of HIV-1. Journal of leukocyte biology *92*, 1147-1154.

Bao, S., Wu, Q., McLendon, R.E., Hao, Y., Shi, Q., Hjelmeland, A.B., Dewhirst, M.W., Bigner, D.D., and Rich, J.N. (2006). Glioma stem cells promote radioresistance by preferential activation of the DNA damage response. Nature *444*, 756-760.

Baratta, M.G., Schinzel, A.C., Zwang, Y., Bandopadhayay, P., Bowman-Colin, C., Kutt, J., Curtis, J., Piao, H., Wong, L.C., Kung, A.L.*, et al.* (2015). An in-tumor genetic screen reveals that the BET bromodomain protein, BRD4, is a potential therapeutic target in ovarian carcinoma. Proc Natl Acad Sci U S A *112*, 232-237.

Barretina, J., Caponigro, G., Stransky, N., Venkatesan, K., Margolin, A.A., Kim, S., Wilson, C.J., Lehar, J., Kryukov, G.V., Sonkin, D.*, et al.* (2012). The Cancer Cell Line

Encyclopedia enables predictive modelling of anticancer drug sensitivity. Nature *483*, 603-607.

Berenguer-Daize, C., Astorgues-Xerri, L., Odore, E., Cayol, M., Cvitkovic, E., Noel, K., Bekradda, M., MacKenzie, S., Rezai, K., Lokiec, F.*, et al.* (2016). OTX015 (MK-8628), a novel BET inhibitor, displays in vitro and in vivo antitumor effects alone and in combination with conventional therapies in glioblastoma models. Int J Cancer *139*, 2047-2055.

Berghoff, A.S., Kiesel, B., Widhalm, G., Rajky, O., Ricken, G., Wohrer, A., Dieckmann, K., Filipits, M., Brandstetter, A., Weller, M.*, et al.* (2015). Programmed death ligand 1 expression and tumor-infiltrating lymphocytes in glioblastoma. Neuro Oncol *17*, 1064-1075.

Berghoff, A.S., Kiesel, B., Widhalm, G., Wilhelm, D., Rajky, O., Kurscheid, S., Kresl, P., Wohrer, A., Marosi, C., Hegi, M.E.*, et al.* (2017). Correlation of immune phenotype with IDH mutation in diffuse glioma. Neuro Oncol *19*, 1460-1468.

Bernasconi, E., Gaudio, E., Kwee, I., and Bertoni, F. (2016). Assessment of the Antiproliferative Activity of a BET Bromodomain Inhibitor as Single Agent and in Combination in Non-Hodgkin Lymphoma Cell Lines. Methods Mol Biol *1436*, 305-312.

Berthon, C., Raffoux, E., Thomas, X., Vey, N., Gomez-Roca, C., Yee, K., Taussig, D.C., Rezai, K., Roumier, C., Herait, P.*, et al.* (2016). Bromodomain inhibitor OTX015 in patients with acute leukaemia: a dose-escalation, phase 1 study. Lancet Haematol *3*, e186-195.

Bhadury, J., Nilsson, L.M., Muralidharan, S.V., Green, L.C., Li, Z., Gesner, E.M., Hansen, H.C., Keller, U.B., McLure, K.G., and Nilsson, J.A. (2014). BET and HDAC inhibitors induce similar genes and biological effects and synergize to kill in Myc-induced murine lymphoma. Proc Natl Acad Sci U S A *111*, E2721-2730.

Biegel, J.A., Busse, T.M., and Weissman, B.E. (2014). SWI/SNF chromatin remodeling complexes and cancer. Am J Med Genet C Semin Med Genet *166C*, 350-366.

Bjorkman, M., Mattila, E., Riikonen, R., Sekhar, C., Jaleel, M., Marappan, S., Ikonen, T., Nicorici, D., Samajdar, S., Ramachandra, M.*, et al.* (2016a). ODM-207, a novel BET-bromodomain inhibitor as a therapeutic approach for the treatment of patients with castration resistant prostate cancer. European Journal of Cancer *69*, S89-S90.

Bjorkman, M., Mattila, E., Riikonen, R., Sekhar, C., Jaleel, M., Marappan, S., Ikonen, T., Nicorici, D.N., Rantala, J., Samajdar, S.*, et al.* (2016b). ODM-207, a novel BET-bromodomain inhibitor as a therapeutic approach for the treatment of prostate and breast cancer. Cancer Research *76*.

Boi, M., Gaudio, E., Bonetti, P., Kwee, I., Bernasconi, E., Tarantelli, C., Rinaldi, A., Testoni, M., Cascione, L., Ponzoni, M.*, et al.* (2015). The BET Bromodomain

Inhibitor OTX015 Affects Pathogenetic Pathways in Preclinical B-cell Tumor Models and Synergizes with Targeted Drugs. Clin Cancer Res *21*, 1628-1638.

Bowman, R.L., Klemm, F., Akkari, L., Pyonteck, S.M., Sevenich, L., Quail, D.F., Dhara, S., Simpson, K., Gardner, E.E., Iacobuzio-Donahue, C.A.*, et al.* (2016). Macrophage Ontogeny Underlies Differences in Tumor-Specific Education in Brain Malignancies. Cell Rep *17*, 2445-2459.

Brennan, C.W., Verhaak, R.G., McKenna, A., Campos, B., Noushmehr, H., Salama, S.R., Zheng, S., Chakravarty, D., Sanborn, J.Z., Berman, S.H.*, et al.* (2013). The somatic genomic landscape of glioblastoma. Cell *155*, 462-477.

Brown, R., Curry, E., Magnani, L., Wilhelm-Benartzi, C.S., and Borley, J. (2014). Poised epigenetic states and acquired drug resistance in cancer. Nat Rev Cancer *14*, 747-753.

Casey, S.C., Tong, L., Li, Y., Do, R., Walz, S., Fitzgerald, K.N., Gouw, A.M., Baylot, V., Gutgemann, I., Eilers, M.*, et al.* (2016). MYC regulates the antitumor immune response through CD47 and PD-L1. Science *352*, 227-231.

Chapuy, B., McKeown, M.R., Lin, C.Y., Monti, S., Roemer, M.G., Qi, J., Rahl, P.B., Sun, H.H., Yeda, K.T., Doench, J.G.*, et al.* (2013). Discovery and characterization of super-enhancer-associated dependencies in diffuse large B cell lymphoma. Cancer Cell *24*, 777-790.

Chen, R., Yik, J.H., Lew, Q.J., and Chao, S.H. (2014). Brd4 and HEXIM1: multiple roles in P-TEFb regulation and cancer. BioMed research international *2014*, 232870.

Cheng, Z., Gong, Y., Ma, Y., Lu, K., Lu, X., Pierce, L.A., Thompson, R.C., Muller, S., Knapp, S., and Wang, J. (2013). Inhibition of BET bromodomain targets genetically diverse glioblastoma. Clin Cancer Res *19*, 1748-1759.

Chessel, D., Dufour, A.-B., and Thioulouse, J. (2004). The ade4 package - I : One-table methods, Vol 4.

Cheung, K., Lu, G., Sharma, R., Vincek, A., Zhang, R., Plotnikov, A.N., Zhang, F., Zhang, Q., Ju, Y., Hu, Y.*, et al.* (2017). BET N-terminal bromodomain inhibition selectively blocks Th17 cell differentiation and ameliorates colitis in mice. Proc Natl Acad Sci U S A *114*, 2952-2957.

Chiappinelli, K.B., Strissel, P.L., Desrichard, A., Li, H., Henke, C., Akman, B., Hein, A., Rote, N.S., Cope, L.M., Snyder, A.*, et al.* (2015). Inhibiting DNA methylation causes an interferon response in cancer via dsRNA including endogenous retroviruses. Cell *162*, 974-986.

Cimino, P.J., Zager, M., McFerrin, L., Wirsching, H.G., Bolouri, H., Hentschel, B., von Deimling, A., Jones, D., Reifenberger, G., Weller, M.*, et al.* (2017). Multidimensional scaling of diffuse gliomas: application to the 2016 World Health Organization classification system with prognostically relevant molecular subtype discovery. Acta Neuropathol Commun *5*, 39.

Dawson, M.A., Kouzarides, T., and Huntly, B.J. (2012). Targeting epigenetic readers in cancer. N Engl J Med *367*, 647-657.

Delmore, J.E., Issa, G.C., Lemieux, M.E., Rahl, P.B., Shi, J., Jacobs, H.M., Kastritis, E., Gilpatrick, T., Paranal, R.M., Qi, J.*, et al.* (2011). BET bromodomain inhibition as a therapeutic strategy to target c-Myc. Cell *146*, 904-917.

Escoufier, Y. (1973). Le traitement des variables vectorielles. Biometrics *29*, 750-760.

Filippakopoulos, P., Qi, J., Picaud, S., Shen, Y., Smith, W.B., Fedorov, O., Morse, E.M., Keates, T., Hickman, T.T., Felletar, I.*, et al.* (2010). Selective inhibition of BET bromodomains. Nature *468*, 1067-1073.

Fiskus, W., Sharma, S., Qi, J., Valenta, J.A., Schaub, L.J., Shah, B., Peth, K., Portier, B.P., Rodriguez, M., Devaraj, S.G.*, et al.* (2014). Highly active combination of BRD4 antagonist and histone deacetylase inhibitor against human acute myelogenous leukemia cells. Mol Cancer Ther *13*, 1142-1154.

Flavahan, W.A., Drier, Y., Liau, B.B., Gillespie, S.M., Venteicher, A.S., Stemmer-Rachamimov, A.O., Suva, M.L., and Bernstein, B.E. (2016). Insulator dysfunction and oncogene activation in IDH mutant gliomas. Nature *529*, 110-114.

Gao, J., Aksoy, B.A., Dogrusoz, U., Dresdner, G., Gross, B., Sumer, S.O., Sun, Y., Jacobsen, A., Sinha, R., Larsson, E.*, et al.* (2013). Integrative analysis of complex cancer genomics and clinical profiles using the cBioPortal. Sci Signal *6*, pl1.

Garcia-Diaz, A., Shin, D.S., Moreno, B.H., Saco, J., Escuin-Ordinas, H., Rodriguez, G.A., Zaretsky, J.M., Sun, L., Hugo, W., Wang, X.*, et al.* (2017). Interferon Receptor Signaling Pathways Regulating PD-L1 and PD-L2 Expression. Cell Rep *19*, 1189-1201.

Gentleman, R.C., Carey, V.J., Bates, D.M., Bolstad, B., Dettling, M., Dudoit, S., Ellis, B., Gautier, L., Ge, Y., Gentry, J.*, et al.* (2004). Bioconductor: open software development for computational biology and bioinformatics. Genome Biol *5*, R80.

Gonzales-Cope, M., Sidoli, S., Bhanu, N.V., Won, K.J., and Garcia, B.A. (2016). Histone H4 acetylation and the epigenetic reader Brd4 are critical regulators of pluripotency in embryonic stem cells. BMC Genomics *17*, 95.

Gyuris, A., Donovan, D.J., Seymour, K.A., Lovasco, L.A., Smilowitz, N.R., Halperin, A.L., Klysik, J.E., and Freiman, R.N. (2009). The chromatin-targeting protein Brd2 is required for neural tube closure and embryogenesis. Biochim Biophys Acta *1789*, 413-421.

He, L., Kulesskiy, E., Saarela, J., Turunen, L., Wennerberg, K., Aittokallio, T., and Tang, J. (2016). Methods for High-Throughput Drug Combination Screening and Synergy Scoring. Springer Protocol.

Hegi, M.E., Diserens, A.C., Gorlia, T., Hamou, M.F., de Tribolet, N., Weller, M., Kros, J.M., Hainfellner, J.A., Mason, W., Mariani, L.*, et al.* (2005). MGMT gene silencing and benefit from temozolomide in glioblastoma. N Engl J Med *352*, 997-1003.

Hegi, M.E., and Stupp, R. (2015). Withholding temozolomide in glioblastoma patients with unmethylated MGMT promoter-still a dilemma? Neuro Oncol *17*, 1425-1427.

Hnisz, D., Abraham, B.J., Lee, T.I., Lau, A., Saint-Andre, V., Sigova, A.A., Hoke, H.A., and Young, R.A. (2013). Super-enhancers in the control of cell identity and disease. Cell *155*, 934-947.

Hogg, S.J., Vervoort, S.J., Deswal, S., Ott, C.J., Li, J., Cluse, L.A., Beavis, P.A., Darcy, P.K., Martin, B.P., Spencer, A.*, et al.* (2017). BET-Bromodomain Inhibitors Engage the Host Immune System and Regulate Expression of the Immune Checkpoint Ligand PD-L1. Cell Rep *18*, 2162-2174.

Hottinger, A.F., Sanson, M., Moyal, E., Delord, J.-P., Micheli, R.D., Rezai, K., Leung, A.C.F., Perez, S., Bekradda, M., Lachaux, N.*, et al.* (2016). Dose optimization of MK-8628 (OTX015), a small molecule inhibitor of bromodomain and extra-terminal (BET) proteins, in patients (pts) with recurrent glioblastoma (GB). Journal of Clinical Oncology *34*, e14123-e14123.

Hottinger, A.F., Stupp, R., and Homicsko, K. (2014). Standards of care and novel approaches in the management of glioblastoma multiforme. Chinese journal of cancer *33*, 32-39.

Houzelstein, D., Bullock, S.L., Lynch, D.E., Grigorieva, E.F., Wilson, V.A., and Beddington, R.S. (2002). Growth and early postimplantation defects in mice deficient for the bromodomain-containing protein Brd4. Mol Cell Biol *22*, 3794-3802.

Ishii, N., Maier, D., Merlo, A., Tada, M., Sawamura, Y., Diserens, A.C., and Van Meir, E.G. (1999). Frequent co-alterations of TP53, p16/CDKN2A, p14ARF, PTEN tumor suppressor genes in human glioma cell lines. Brain Pathol *9*, 469-479.

Jones, P.A., Issa, J.-P.J., and Baylin, S. (2016). Targeting the cancer epigenome for therapy. Nat Rev Genet *17*, 630-641.

Kagoya, Y., Nakatsugawa, M., Yamashita, Y., Ochi, T., Guo, T., Anczurowski, M., Saso, K., Butler, M.O., Arrowsmith, C.H., and Hirano, N. (2016). BET bromodomain inhibition enhances T cell persistence and function in adoptive immunotherapy models. J Clin Invest *126*, 3479-3494.

Korb, E., Herre, M., Zucker-Scharff, I., Darnell, R.B., and Allis, C.D. (2015). BET protein Brd4 activates transcription in neurons and BET inhibitor Jq1 blocks memory in mice. Nat Neurosci *18*, 1464-1473.

Kuilman, T., Michaloglou, C., Mooi, W.J., and Peeper, D.S. (2010). The essence of senescence. Genes Dev *24*, 2463-2479.

Kurscheid, S., Bady, P., Sciuscio, D., Samarzija, I., Shay, T., Vassallo, I., Criekinge, W.V., Daniel, R.T., van den Bent, M.J., Marosi, C.*, et al.* (2015). Chromosome 7 gain and DNA hypermethylation at the HOXA10 locus are associated with expression of a stem cell related HOX-signature in glioblastoma. Genome Biol *16*, 16.

Lamoureux, F., Baud'huin, M., Rodriguez Calleja, L., Jacques, C., Berreur, M., Redini, F., Lecanda, F., Bradner, J.E., Heymann, D., and Ory, B. (2014). Selective inhibition of BET bromodomain epigenetic signalling interferes with the bone-associated tumour vicious cycle. Nature communications *5*, 3511.

Lee, J.K., Wang, J., Sa, J.K., Ladewig, E., Lee, H.O., Lee, I.H., Kang, H.J., Rosenbloom, D.S., Camara, P.G., Liu, Z.*, et al.* (2017). Spatiotemporal genomic architecture informs precision oncology in glioblastoma. Nat Genet *6*.

Lee, S., Rellinger, E.J., Kim, K.W., Craig, B.T., Romain, C.V., Qiao, J., and Chung, D.H. (2015). Bromodomain and extraterminal inhibition blocks tumor progression and promotes differentiation in neuroblastoma. Surgery *158*, 819-826.

Lenain, C., Gusyatiner, O., Douma, S., van den Broek, B., and Peeper, D.S. (2015). Autophagy-mediated degradation of nuclear envelope proteins during oncogene-induced senescence. Carcinogenesis *36*, 1263-1274.

Liau, B.B., Sievers, C., Donohue, L.K., Gillespie, S.M., Flavahan, W.A., Miller, T.E., Venteicher, A.S., Hebert, C.H., Carey, C.D., Rodig, S.J.*, et al.* (2017). Adaptive chromatin remodeling drives glioblastoma stem cell plasticity and drug tolerance. Cell Stem Cell *20*, 233-246 e237.

Louis, D.N., Ohgaki, H., Wiestler, O.D., and Cavenee, W.K., eds. (2016a). WHO Classification of tumours of the central nervous system, Revised 4th edition edn (Lyon: IARC).

Louis, D.N., Perry, A., Reifenberger, G., von Deimling, A., Figarella-Branger, D., Cavenee, W.K., Ohgaki, H., Wiestler, O.D., Kleihues, P., and Ellison, D.W. (2016b). The 2016 World Health Organization Classification of Tumors of the Central Nervous System: a summary. Acta Neuropathol *131*, 803-820.

Loven, J., Hoke, H.A., Lin, C.Y., Lau, A., Orlando, D.A., Vakoc, C.R., Bradner, J.E., Lee, T.I., and Young, R.A. (2013). Selective inhibition of tumor oncogenes by disruption of super-enhancers. Cell *153*, 320-334.

Mack, S.C., Witt, H., Piro, R.M., Gu, L., Zuyderduyn, S., Stutz, A.M., Wang, X., Gallo, M., Garzia, L., Zayne, K.*, et al.* (2014). Epigenomic alterations define lethal CIMP-positive ependymomas of infancy. Nature *506*, 445-450.

Marcotte, R., Sayad, A., Brown, K.R., Sanchez-Garcia, F., Reimand, J., Haider, M., Virtanen, C., Bradner, J.E., Bader, G.D., Mills, G.B.*, et al.* (2016). Functional Genomic Landscape of Human Breast Cancer Drivers, Vulnerabilities, and Resistance. Cell *164*, 293-309.

Massard, C., Soria, J.C., Stathis, A., Delord, J.P., Awada, A., Peters, S., Lewin, J., Bekradda, M., Rezai, K., Zeng, Z., *et al.* (2016). A phase lb trial with MK-8628/OTX015, a small molecule inhibitor of bromodomain (BRD) and extra-terminal (BET) proteins, in patients with selected advanced solid tumors. European Journal of Cancer *69*, S2-S3.

Matzuk, M.M., McKeown, M.R., Filippakopoulos, P., Li, Q., Ma, L., Agno, J.E., Lemieux, M.E., Picaud, S., Yu, R.N., Qi, J., *et al.* (2012). Small-molecule inhibition of BRDT for male contraception. Cell *150*, 673-684.

Mazur, P.K., Herner, A., Mello, S.S., Wirth, M., Hausmann, S., Sanchez-Rivera, F.J., Lofgren, S.M., Kuschma, T., Hahn, S.A., Vangala, D., *et al.* (2015). Combined inhibition of BET family proteins and histone deacetylases as a potential epigenetics-based therapy for pancreatic ductal adenocarcinoma. Nat Med *21*, 1163-1171.

Mertz, J.A., Conery, A.R., Bryant, B.M., Sandy, P., Balasubramanian, S., Mele, D.A., Bergeron, L., and Sims, R.J., 3rd (2011). Targeting MYC dependence in cancer by inhibiting BET bromodomains. Proc Natl Acad Sci U S A *108*, 16669-16674.

Michels, A.A., Fraldi, A., Li, Q., Adamson, T.E., Bonnet, F., Nguyen, V.T., Sedore, S.C., Price, J.P., Price, D.H., Lania, L., *et al.* (2004). Binding of the 7SK snRNA turns the HEXIM1 protein into a P-TEFb (CDK9/cyclin T) inhibitor. EMBO J *23*, 2608-2619.

Murat, A., Migliavacca, E., Gorlia, T., Lambiv, W.L., Shay, T., Hamou, M.F., de Tribolet, N., Regli, L., Wick, W., Kouwenhoven, M.C., *et al.* (2008). Stem cell-related "self-renewal" signature and high epidermal growth factor receptor expression associated with resistance to concomitant chemoradiotherapy in glioblastoma. J Clin Oncol *26*, 3015-3024.

Murat, A., Migliavacca, E., Hussain, S.F., Heimberger, A.B., Desbaillets, I., Hamou, M.F., Ruegg, C., Stupp, R., Delorenzi, M., and Hegi, M.E. (2009). Modulation of angiogenic and inflammatory response in glioblastoma by hypoxia. PLoS ONE *4*, e5947.

O'Dwyer, P.J., Piha-Paul, S.A., French, C., Harward, S., Ferron-Brady, G., Wu, Y.H., Barbash, O., Wyce, A., Annan, M., Horner, T., *et al.* (2016). GSK525762, a selective bromodomain (BRD) and extra terminal protein (BET) inhibitor: results from part 1 of a phase I/II open-label single-agent study in patients with NUT midline carcinoma (N MC) and other cancers. Cancer Research *76*.

Olarerin-George, A.O., and Hogenesch, J.B. (2015). Assessing the prevalence of mycoplasma contamination in cell culture via a survey of NCBI's RNA-seq archive. Nucleic Acids Res *43*, 2535-2542.

Ott, C.J., Kopp, N., Bird, L., Paranal, R.M., Qi, J., Bowman, T., Rodig, S.J., Kung, A.L., Bradner, J.E., and Weinstock, D.M. (2012). BET bromodomain inhibition targets both c-Myc and IL7R in high-risk acute lymphoblastic leukemia. Blood *120*, 2843-2852.

Parker, B.S., Rautela, J., and Hertzog, P.J. (2016). Antitumour actions of interferons: implications for cancer therapy. Nat Rev Cancer *16*, 131-144.

Pastori, C., Daniel, M., Penas, C., Volmar, C.H., Johnstone, A.L., Brothers, S.P., Graham, R.M., Allen, B., Sarkaria, J.N., Komotar, R.J.*, et al.* (2014). BET bromodomain proteins are required for glioblastoma cell proliferation. Epigenetics *9*.

Patel, A.P., Tirosh, I., Trombetta, J.J., Shalek, A.K., Gillespie, S.M., and Wakimoto, H. (2014). Single-cell RNA-seq highlights intratumoral heterogeneity in primary glioblastoma. Science *344*.

Piunti, A., Hashizume, R., Morgan, M.A., Bartom, E.T., Horbinski, C.M., Marshall, S.A., Rendleman, E.J., Ma, Q., Takahashi, Y.H., Woodfin, A.R.*, et al.* (2017). Therapeutic targeting of polycomb and BET bromodomain proteins in diffuse intrinsic pontine gliomas. Nat Med *23*, 493-500.

Prados, M.D., Byron, S.A., Tran, N.L., Phillips, J.J., Molinaro, A.M., Ligon, K.L., Wen, P.Y., Kuhn, J.G., Mellinghoff, I.K., de Groot, J.F.*, et al.* (2015). Toward precision medicine in glioblastoma: the promise and the challenges. Neuro Oncol *17*, 1051-1063.

Puissant, A., Frumm, S.M., Alexe, G., Bassil, C.F., Qi, J., Chanthery, Y.H., Nekritz, E.A., Zeid, R., Gustafson, W.C., Greninger, P.*, et al.* (2013). Targeting MYCN in neuroblastoma by BET bromodomain inhibition. Cancer Discov *3*, 308-323.

Pyonteck, S.M., Akkari, L., Schuhmacher, A.J., Bowman, R.L., Sevenich, L., Quail, D.F., Olson, O.C., Quick, M.L., Huse, J.T., Teijeiro, V.*, et al.* (2013). CSF-1R inhibition alters macrophage polarization and blocks glioma progression. Nat Med *19*, 1264-1272.

R Core Team (2015). A language and environment for statistical computing. (R Foundation for Statistical Computing, Vienna, Austria.).

Schroder, K., Hertzog, P.J., Ravasi, T., and Hume, D.A. (2004). Interferon-gamma: an overview of signals, mechanisms and functions. Journal of leukocyte biology *75*, 163-189.

Sciuscio, D., Diserens, A.C., van Dommelen, K., Martinet, D., Jones, G., Janzer, R.C., Pollo, C., Hamou, M.F., Kaina, B., Stupp, R.*, et al.* (2011). Extent and patterns of MGMT promoter methylation in glioblastoma- and respective glioblastoma-derived spheres. Clin Cancer Res *17*, 255-266.

Shahbazi, J., Liu, P.Y., Atmadibrata, B., Bradner, J.E., Marshall, G.M., Lock, R.B., and Liu, T. (2016). The bromodomain inhibitor JQ1 and the histone deacetylase inhibitor panobinostat synergistically reduce N-Myc expression and induce anticancer effects. Clin Cancer Res.

Shang, E., Wang, X., Wen, D., Greenberg, D.A., and Wolgemuth, D.J. (2009). Double bromodomain-containing gene Brd2 is essential for embryonic development in mouse. Dev Dyn *238*, 908-917.

Shannon, M., Capes-Davis, A., Eggington, E., Georghiou, R., Huschtscha, L.I., Moy, E., Power, M., Reddel, R.R., and Arthur, J.W. (2016). Is cell culture a risky business? Risk analysis based on scientist survey data. International Journal of Cancer *138*, 664-670.

Stathis, A., and Bertoni, F. (2017). BET Proteins as Targets for Anticancer Treatment. Cancer Discov.

Stathis, A., Zucca, E., Bekradda, M., Gomez-Roca, C., Delord, J.P., Rouge, T.D., Uro-Coste, E., de Braud, F., Pelosi, G., and French, C.A. (2016). Clinical Response of Carcinomas Harboring the BRD4-NUT Oncoprotein to the Targeted Bromodomain Inhibitor OTX015/MK-8628. Cancer Discovery *6*, 492-500.

Stone, M.L., Chiappinelli, K.B., Li, H., Murphy, L.M., Travers, M.E., Topper, M.J., Mathios, D., Lim, M., Shih, I.M., Wang, T.L.*, et al.* (2017). Epigenetic therapy activates type I interferon signaling in murine ovarian cancer to reduce immunosuppression and tumor burden. Proc Natl Acad Sci U S A.

Stupp, R., Hegi, M.E., Mason, W.P., van den Bent, M.J., Taphoorn, M.J., Janzer, R.C., Ludwin, S.K., Allgeier, A., Fisher, B., Belanger, K.*, et al.* (2009). Effects of radiotherapy with concomitant and adjuvant temozolomide versus radiotherapy alone on survival in glioblastoma in a randomised phase III study: 5-year analysis of the EORTC-NCIC trial. Lancet Oncol *10*, 459-466.

Stupp, R., Taillibert, S., Kanner, A., Read, W., Steinberg, D.M., Lhermitte, B., Toms, S., Idbaih, A., Ahluwalia, M.S., Fink, K.*, et al.* (2017). Effect of Tumor-Treating Fields plus maintenance temozolomide vs maintenance temozolomide alone on survival in patients with glioblastoma: A randomized clinical trial. Jama *318*, 2306-2316.

Sullivan, J.M., Badimon, A., Schaefer, U., Ayata, P., Gray, J., Chung, C.W., von Schimmelmann, M., Zhang, F., Garton, N., Smithers, N.*, et al.* (2015). Autism-like syndrome is induced by pharmacological suppression of BET proteins in young mice. J Exp Med *212*, 1771-1781.

Suva, M.L., Rheinbay, E., Gillespie, S.M., Patel, A.P., Wakimoto, H., Rabkin, S.D., Riggi, N., Chi, A.S., Cahill, D.P., Nahed, B.V.*, et al.* (2014). Reconstructing and Reprogramming the Tumor-Propagating Potential of Glioblastoma Stem-like Cells. Cell *9*, 00229-00223.

Todaro, M., Boi, M., Vurchio, V., Ercole, E., Machiorlatti, R., Messana, K., Landra, I., Urigu, S., Aliberti, S., Riveiro, E.*, et al.* (2014). OTX015, a novel BET inhibitor is a promising anticancer agent for multiple myeloma. In: Proceedings of the 105th Annual Meeting of the American Association for Cancer Research; 2014 Apr 5-9; San Diego, CA Philadelphia (PA): AACR; 2014 Abstract nr 5531.

Tolani, B., Gopalakrishnan, R., Punj, V., Matta, H., and Chaudhary, P.M. (2014). Targeting Myc in KSHV-associated primary effusion lymphoma with BET bromodomain inhibitors. Oncogene *33*, 2928-2937.

Topper, M.J., Vaz, M., Chiappinelli, K.B., DeStefano Shields, C.E., Niknafs, N., Yen, R.C., Wenzel, A., Hicks, J., Ballew, M., Stone, M.*, et al.* (2017). Epigenetic Therapy Ties MYC Depletion to Reversing Immune Evasion and Treating Lung Cancer. Cell *171*, 1284-1300 e1221.

Uhrbom, L., Dai, C., Celestino, J.C., Rosenblum, M.K., Fuller, G.N., and Holland, E.C. (2002). Ink4a-Arf loss cooperates with KRas activation in astrocytes and neural progenitors to generate glioblastomas of various morphologies depending on activated Akt. Cancer Res *62*, 5551-5558.

Vassallo, I., Zinn, P., Lai, M., Rajakannu, P., Hamou, M.F., and Hegi, M.E. (2016). WIF1 re-expression in glioblastoma inhibits migration through attenuation of non-canonical WNT signaling by downregulating the lncRNA MALAT1. Oncogene *35*, 12-21.

Vazquez, R., Riveiro, M.E., Astorgues-Xerri, L., Odore, E., Rezai, K., Erba, E., Panini, N., Rinaldi, A., Kwee, I., Beltrame, L.*, et al.* (2017). The bromodomain inhibitor OTX015 (MK-8628) exerts anti-tumor activity in triple-negative breast cancer models as single agent and in combination with everolimus. Oncotarget *8*, 7598-7613.

Verhaak, R.G., Hoadley, K.A., Purdom, E., Wang, V., Qi, Y., Wilkerson, M.D., Miller, C.R., Ding, L., Golub, T., Mesirov, J.P.*, et al.* (2010). Integrated genomic analysis identifies clinically relevant subtypes of glioblastoma characterized by abnormalities in PDGFRA, IDH1, EGFR, and NF1. Cancer Cell *17*, 98-110.

Wang, J., Cazzato, E., Ladewig, E., Frattini, V., Rosenbloom, D.I., Zairis, S., Abate, F., Liu, Z., Elliott, O., Shin, Y.J.*, et al.* (2016). Clonal evolution of glioblastoma under therapy. Nat Genet *48*, 768-776.

Wang, Q., Hu, B., Hu, X., Kim, H., Squatrito, M., Scarpace, L., deCarvalho, A.C., Lyu, S., Li, P., Li, Y.*, et al.* (2017). Tumor evolution of glioma-intrinsic gene expression subtypes associates with immunological changes in the microenvironment. Cancer Cell *32*, 42-56 e46.

Whyte, W.A., Orlando, D.A., Hnisz, D., Abraham, B.J., Lin, C.Y., Kagey, M.H., Rahl, P.B., Lee, T.I., and Young, R.A. (2013). Master transcription factors and mediator establish super-enhancers at key cell identity genes. Cell *153*, 307-319.

Woods, D.M., Sodre, A.L., Villagra, A., Sarnaik, A., Sotomayor, E.M., and Weber, J. (2015). HDAC Inhibition Upregulates PD-1 Ligands in Melanoma and Augments Immunotherapy with PD-1 Blockade. Cancer Immunol Res *3*, 1375-1385.

Wrangle, J., Wang, W., Koch, A., Easwaran, H., Mohammad, H.P., Vendetti, F., Vancriekinge, W., Demeyer, T., Du, Z., Parsana, P.*, et al.* (2013). Alterations of immune response of Non-Small Cell Lung Cancer with Azacytidine. Oncotarget *4*, 2067-2079.

Young, L., Sung, J., Stacey, G., and Masters, J.R. (2010). Detection of Mycoplasma in cell cultures. Nature protocols *5*, 929-934.

Zhu, H., Bengsch, F., Svoronos, N., Rutkowski, Melanie R., Bitler, Benjamin G., Allegrezza, Michael J., Yokoyama, Y., Kossenkov, Andrew V., Bradner, James E., Conejo-Garcia, Jose R.*, et al.* (2016). BET Bromodomain Inhibition Promotes Anti-tumor Immunity by Suppressing PD-L1 Expression. Cell Reports *16*, 2829-2837.

Zuber, J., Shi, J., Wang, E., Rappaport, A.R., Herrmann, H., Sison, E.A., Magoon, D., Qi, J., Blatt, K., Wunderlich, M.*, et al.* (2011). RNAi screen identifies Brd4 as a therapeutic target in acute myeloid leukaemia. Nature *478*, 524-528.

Chapter 6   Supplement

Table 6:1. Molecular characterization and tumourogenecity of GS-lines used in the study.

GS-lines	LN-2207-GS	LN-2540-GS	LN-2669-GS	LN-2683-GS	LN-3704-GS	LN-3708-GS
TP53	wt	p.Arg248Trp homozygous	wt	p.Glu224Lys/ p.Pro250Leu both heterozygous	nd	nd
PTEN	p.Tyr27Cys56 homozygous	c.253+5G>A and heterozygous del of exons 1 to 9	p.Asp323ValfsX19 homozygous	*heterozygous del of exons 1 to 9	nd	nd
P16/ARF	homozygous del	hemizygous del	homozygous del	homozygous del	nd	nd
Tumour-igenicity in nude/NSG mice	Non tumour-igenic, ic, sc	Intra cerebral (Sciuscio et al., 2011) sc, nd	Intra cerebral (Sciuscio et al., 2011) sc, nd	Intra cerebral (Sciuscio et al., 2011) sc, nd	Intra cerebral(primary cells, un-published) sc, nd	Intra cerebral(primary cells, un-published) sc, nd
population doubling time	5 days	6 days	15 days	8 days	5 days	4 days

* sequencing data not usable; ic, intra cerebral; sc, sub-cutaneous; nd, not defined. LN-2683-GS was derived from recurrent glioblastoma treated by temozolomide/radiotherapy in the first line (Sciuscio et al., 2011). Population doubling times were estimated by counting cell number 3-4 times in 2 weeks and calculating according to

$$Doubling\ time = \frac{duration * \ln(2)}{\ln(\text{FinalConcentration}) - \ln(\text{InitialConcentration})}$$

Table 6:2. List of primers used for qPCR.

Gene	Forward primer (5'-3')	Reverse primer (5'-3')
GAPDH	AGGTGAAGGTCGGAGTCAACG	CGTTCTCAGCCTTGACGGTG
hGAPDH	CATGAGAAGTATGACAACAGCCT	AGTCCTTCCACGATACCAAAGT
C1orf43	TACGGGAGCCTGGACTTGAA	AGTGTTTCGCAGATCCAGCA
C-MYC	CGACTCTGAGGAGGAACAAGAA	GGATAGTCCTTCCGAGTGGA
hC-MYC	TGCTCCATGAGGAGACACC	CCTCATCTTCTTGTTCCTCCA
N-MYC	TGAGCGATTCAGATGATGAAGA	GCATCGTTTGAGGATCAGC
MX1	GAAAGAGGCGAAGCGAGAG	CCGTGACACTGGGATTCCT
OAS1	GGTGGAGTTCGATGTGCTG	AGGTTTATAGCCGCCAGTCA
TUBB3	GCGAGATGTACGAAGACGAC	TTTAGACACTGCTGGCTTCG
CD274	CCATACAGCTGAATTGGTCATC	CAGAATTACCAAGTGATCCTTTCA

Table 6:3. List of primers used for ChIP-qPCR.

GAPDH TSS	*sequence unknown, provided by Di-agenode	
Myglobin exon2	*sequence unknown, provided by Di-agenode	
CD274 TSS	AAGCCATATGGGTCTGCTC	TTATCAGAAAGGCGTCCCCC
MX1 TSS	ATACGTGCAGGCTTGGATGAC	AGGCCCGTCTGAGGATCAA
OAS1 TSS	ACGTGTTTCCGCATGCAAAT	GGCCTGGACTCACCTTTACC
CD274 TSS A	CTCGCTGGGCACTTTAGGAC	TACTGCCCCCTAGACCATCG
CD274 TSS B	TTATCAGAAAGGGGGACGCC	CCAACATCTGAACGCACCTTG

Figure 6:1. Original uncropped Western Blots for Figure 3:7.